

**DEVELOPMENT OF THERMOPLASTIC CONDUCTING POLYMER  
COMPOSITES BASED ON POLYANILINE AND POLYTHIOPHENES  
FOR MICROWAVE AND ELECTRICAL APPLICATIONS**

*Thesis submitted to the  
Cochin University of Science and Technology*

*By*

**Lakshmi. K**

*In partial fulfilment of the requirements  
for the award of the degree of*

**DOCTOR OF PHILOSOPHY**

*Under  
Faculty of Technology*



**DEPARTMENT OF POLYMER SCIENCE AND RUBBER TECHNOLOGY  
COCHIN UNIVERSITY OF SCIENCE AND TECHNOLOGY  
KOCHI-682022**


**SEPTEMBER 2007**

# Certificate

This is to certify that this thesis, entitled “Development of thermoplastic conducting polymer composites based on polyaniline and polythiophenes for microwave and electrical applications”, is a report of the original work carried out by Smt. Lakshmi. K under our supervision and guidance in the Department of Polymer science and Rubber Technology and Department of Electronics, Cochin university of Science and Technology, Kochi. No part of the work reported in this thesis has been presented for any other degree from any other institutions.

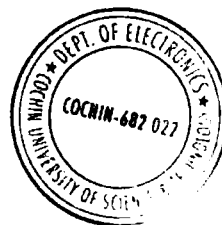
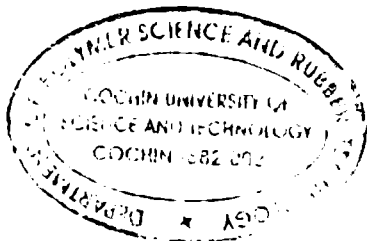


**Dr. K. E. George**  
Professor  
Dept. of Polymer Science and Rubber  
Technology  
Cochin University of Science and  
Technology



**Dr. K. T. Mathew**  
Emeritus Professor  
Department of Electronics,  
Cochin University of Science and  
Technology

Kochi - 22  
September, 2007



## *Declaration*

I hereby declare that this thesis entitled “**Development of thermoplastic conducting polymer composites based on polyaniline and polythiophenes for microwave and electrical applications**” is the original work carried out by me under the supervision and guidance of Dr. K. E. George, Professor, Dept. of Polymer Science and Rubber Technology and Dr. K. T. Mathew, Emeritus Professor, Department of Electronics, Cochin University of Science and Technology, Kochi - 22, and no part of this thesis has been presented for any other degree from any other institutions.

*Kochi - 22  
September, 2007*

  
**Lakshmi. K**

# Acknowledgements

During these years of dedication and hardworking, I have received immense support, help and strength to pursue my goal from many persons and I would like to express my sincere gratitude to all of them.

First of all, I want to thank my supervisors at Cochin University of Science and Technology, **Dr. K. E. George**, Professor, Dept. of Polymer Science and Rubber Technology (PS & RT) and **Dr. K. T. Mathew**, Emeritus Professor, Department of Electronics, for their constant support and encouragement. I would like to thank **Dr. Rani Joseph**, my subject expert, who gave a lot of insight into the area and guided me in taking challenging paths in this work.

I joined the Department of PS & RT of CUSAT in 1996 and continued to be a student here till date, completing my B.Tech, M.Tech and PhD in due course. I am very much attached and obliged to all my teachers and would like to express my gratitude to Dr. Thomas Kurian, HOD, Dr. Philip Kurian, Dr. Eby Thomas Thachil, Dr. Sunil Narayanankutty and Dr. A. P. Kuriakkose. Dr. Honey John, Dept of PS & RT, CUSAT, has helped me in and out in all possible ways and I would take this opportunity to thank her wholeheartedly. I am extremely thankful to all the office staff of the department who gave me full support and help all through these ten years.

Throughout my career at Amrita Vishwa Vidyapeetham, Prof. R. Subba Rao, Chairman, Dept. of Chemical Engineering and Material Science, Amrita School of Engineering has been helping me in many ways and I thank him for the same. I owe special thanks to Prof. S. S. Bhagawan from the same department who helped me a lot in testing, analysis, corrections and Design of Experiments.

I am grateful to my entire family members for being with me through these years of great efforts with their appreciation and encouragement which motivated me a lot. My husband, Madhu, and daughter, Revathy, compromised a lot and went through all the difficulties with immense patience and my love for them. Special mention is for my parents and brothers whose motivation and support helped me aim higher and row ahead through the difficulties.

The work leading to this thesis was carried out between June 2003 and September 2007 at Department of Polymer Science and Rubber Technology and Department of Electronics (DoE) of Cochin University of Science and Technology, Kochi and Department of Chemical Engineering and Material Science of Amrita School of Engineering, Coimbatore. I have been bestowed full support and encouragement from these three departments and I thank each and every member of these departments for their help and cooperation.

Finally, but most importantly I thank the Almighty for blessing me with health and resources for performing at my best all through these years.

**Lakshmi. K**

# Preface

Conducting polymers show some specific characteristics in microwave frequencies that make them far more interesting than traditional dielectric materials. The intrinsic conductivity of conjugated polymers leads, in the field of their microwave properties to a dynamic conductivity leading to high levels of dielectric constant. Microwave properties of conducting polymers are crucial because of their wide areas of applications such as coating in reflector antennas, coating in electronic equipments, frequency selective surfaces, EMI materials, satellite communication links, microchip antennas etc. Radar Absorbing Materials (RAM) based on conducting polymers have been developed. This study brings forth the microwave applications of conducting polymers like poly para phenylene diazomethine, polythiophene and more importantly that of Poly (3, 4-ethylenedioxythiophene), which has already found major applications in solar cells, LED's etc. Preparation of composites of conducting polymers has been considered to provide a suitable solution to the processibility problem. These composites have the ability to enhance their material properties with desirable mechanical and physical characteristics. One way of making these composites involves synthesizing the conducting polymer inside the matrices of conventional polymers using chemical or electrochemical polymerization.

The thesis consists of eight chapters

**Chapter 1** presents a review of the literatures in this field and the scope of the present investigation. This chapter explains the mechanisms of polymer conduction in DC and microwave fields and gives an insight into the microwave

properties studied in the work. The theory and equations related to the properties studied are dealt in detail. The different methods used to evaluate the microwave properties are discussed and compared to substantiate the use of cavity perturbation technique for the microwave characterization. Literature survey pertaining to the different methods of synthesis, advantages and applications of the polymers under consideration is given. The importance of following design of experiments in formulating experiments has been emphasized. The Taguchi method which was used in the preparation of PPDA is explained in detail. The scope and objectives of the work are explained. The methodology adopted to achieve these objectives is briefly explained.

**Chapter 2** deals with the materials used and the experimental procedures adopted for the study.

**Chapter 3** is divided into two parts; Part I discusses the use of Design of Experiments for optimizing the polycondensation reaction parameters for the preparation of poly paraphenylene diazomethine. The optimum monomer ratio, reaction time, temperature and the solvent to be used for the polycondensation of paraphenylene diammine and glyoxal trimeric hydrate to get maximum yield and conductivity is found by generating factor plots from standard L<sub>9</sub> experimental design. Part II deals with the characterization of the polymer thus produced by FTIR, TGA and DSC analysis. The effect of HClO<sub>4</sub> and copper acetate doping on the structure of the polymer are studied using FTIR spectra.

**Chapter 4** gives the preparation and characterization of polythiophene. Polythiophene was characterized by FTIR, TGA and DSC analysis. The effect of FeCl<sub>3</sub> doping on the structure of the polymer was studied using FTIR spectra.

**Chapter 5** gives the preparation and characterization of Poly (3, 4-Ethylene Dioxy Thiophene -PEDOT). PEDOT was characterized by FTIR, TGA and DSC analysis.

**Chapter 6** gives a comparative study of dielectric constant, dielectric loss, absorption coefficient, heating coefficient, skin depth and conductivity in the microwave frequency (S band) and DC conductivity of Polyaniline, PEDOT, Polythiophene, Polypyrrole, and Polyparaphenylene diazomethine (PPDA).

**Chapter 7** is divided into three parts. Part I deal with the optimization of  $FeCl_3$ : Thiophene ratio in preparing PTH-PVC composite. Effect of ferric chloride: Thiophene ratio on microwave properties like dielectric constant, dielectric loss and conductivity of PTH-PVC composite was analyzed and optimum ratio was determined. The effect of drying condition on microwave properties of PTH-PVC composites are discussed in Part II. Composites were prepared at room temperature drying and vacuum oven drying conditions and the microwave properties like dielectric constant, dielectric loss, absorption coefficient and conductivity of PTH-PVC composites were analyzed .Microwave properties of different conducting composites are analyzed in Part III. In this section dielectric constant, dielectric loss, conductivity, loss tangent, absorption coefficient, heating coefficient and skin depth of PEDOT-PVC, PTH-PVC, PPDA-PVC and PANI-PVC composites are compared to find the best combination.

**Chapter 8** deals with the application study of PANI-PU composite. The EMI shielding and microwave absorption property of PANI-PU composite was evaluated at S and X bands of microwave frequency and potential applications are discussed



**Chapter 9** comprises the summary and conclusions derived from these studies.

At the end of each chapter a list of references has been given. A list of abbreviations used, figures, tables, schemes and publications are also given at the end of the thesis.

## Table of Contents

No.	Titles	Page Number
	<b>Certificate</b> .....	i
	<b>Declaration</b> .....	ii
	<b>Acknowledgements</b> .....	v
	<b>Preface</b> .....	vii
	<b>Chapter.1</b>	1
	<b>Introduction</b> .....	
1.1	Intrinsically conducting polymers .....	2
1.2	Conjugated Polymers.....	3
1.3	Conduction in polymers.....	4
1.3.1	Mott's hopping conductivity model.....	4
1.3.2	Sheng model: Tunnel junctions between conducting regions.....	6
1.4	Conduction in microwave field.....	9
1.4.1	Orientation polarization.....	10
1.4.2	Electronic and atomic polarization.....	11
1.4.3	Interfacial or space charge polarization.....	11
1.5	Microwave properties.....	11
1.5.1	Relaxation time.....	11
1.5.2	Dielectric constant and dielectric loss.....	12
1.5.3	Cole-Cole diagram .....	12
1.5.4	Maxwell-Wagner effect.....	13
1.5.5	Loss tangent.....	14

1.5.6	Microwave absorption.....	15
1.6	Measurement of microwave properties.....	19
1.6.1	Coaxial probe.....	19
1.6.2	Transmission line.....	20
1.6.3	Free space.....	20
1.6.4	Parallel plate.....	21
1.6.5	Resonant cavities.....	21
1.6.6	Cavity perturbation technique.....	21
1.6.7	Comparison of methods.....	27
1.7	Microwave properties and applications of conducting composites.....	28
1.8	Polyazomethines.....	30
1.8.1	Synthesis of polyazomethines.....	30
1.8.1.1	Solution polycondensation.....	30
1.8.1.2	Chemical vapour deposition.....	30
1.8.1.3	Oxidative polymerization.....	31
1.8.2	Modifications.....	31
1.8.3	Applications.....	32
1.9	Polythiophenes.....	33
1.9.1	Synthesis of polythiophenes.....	33
1.9.1.1	Chemical synthesis of unsubstituted polythiophenes.....	33
1.9.1.2	Chemical synthesis of polyalkylthiophenes.....	34
1.9.1.3	Metal-catalyzed cross-coupling polymerizations.....	34
1.9.1.4	FeCl <sub>3</sub> method for the polymerization of PATs.....	35

1.9.1.5	Electrochemical polymerization.....	36
1.9.2	Regioregular poly alkyl thiophenes.....	37
1.9.3	Applications.....	37
1.10	Poly (3, 4-Ethylenedioxythiophene) - PEDOT.....	38
1.10.1	Synthesis of poly (3, 4-Ethylenedioxythiophene)s.....	38
1.10.1.1	Oxidative chemical polymerization of the edot based monomers.....	39
1.10.1.2	Electrochemical polymerization of EDOT derivatives.....	40
1.10.1.3	Transition metal mediated coupling of dihalo dcrivatives of EDOT.....	40
1.10.2	Applications of PEDOT.....	41
1.11	Polyaniline.....	41
1.11.1	Synthesis of polyanilines.....	42
1.11.1.1	Chemical synthesis.....	42
1.11.1.2	Electrochemical synthesis.....	42
1.11.2	Applications.....	43
1.12	Design of experiments (DOE).....	44
1.12.1	Taguchi method.....	44
1.12.2	Orthogonal array.....	45
1.13	Scope and objectives of the work.....	46
1.14	Methodology.....	49
1.15	References.....	52

## Chapter.2

<b>Experimental Methods</b> .....	67
2.1 Materials used.....	67
2.1.1 Monomers.....	67
2.1.2 Dopants.....	69
2.1.3 Solvents.....	70
2.1.4 Miscellaneous.....	71
2.2 Preparation of conducting polymers.....	72
2.2.1 Preparation of para phenylene diazomethine (PPDA).....	72
2.2.2 Preparation of polythiophene (PTH).....	72
2.2.3 Preparation of poly (3,4-Ethylenedioxythiophene) (PEDOT).....	72
2.2.4 Preparation of polyaniline (PANI).....	73
2.3 Preparation of thermoplastic conducting composites.....	73
2.3.1 Preparation of polythiophene - PVC composites.....	73
2.3.2 Preparation of PEDOT- PVC composites.....	73
2.3.3 Preparation of polyaniline- PVC composites.....	74
2.3.4 Preparation of PPDA - PVC composites.....	74
2.3.5 Preparation of PEDOT - PU composites.....	74
2.3.6 Preparation of PANI - PU composites.....	75
2.4 Characterisation of polymers.....	75
2.4.1 Fourier transform infra red spectrometer (FTIR).....	75
2.4.2 Thermo gravimetic analysis and differential thermal analysis. ....	76

2.4.3	Differential scanning calorimetry (DSC) .....	77
2.5	Testing of polymers and composites.....	78
2.5.1	Measurement of DC conductivity.....	78
2.5.2	Measurement of microwave properties- cavity perturbation technique.....	78
2.5.2.1	Rectangular waveguides.....	78
2.5.2.2	Experimental setup.....	80
2.5.2.3	Theory.....	83
2.5.3	Shielding efficiency.....	84
2.5.4	Mechanical properties.....	86
2.6	References .....	87

## **Chapter.3**

<b>Preparation and properties of PPDA (poly para phenylene diazomethine)</b> .....	89
--	----

### **Part-I**

<b>3.1 Optimization of reaction parameters for polycondensation of PPDA</b> .....	92
3.1.1 Experimental methods.....	92
3.1.2 Results and discussion.....	93
3.1.2.1 Effect of solvent on yield and conductivity of PPDA.....	93
3.1.2.2 Optimization of reaction parameters for polycondensation of PPDA using taguchi design.....	94
3.1.2.3 Validation experiment.....	98
3.1.3 Conclusions.....	98

## **Part-II**

<b>3.2 Characterisation of PPDA</b> .....	99
3.2.1 Experimental methods.....	99
3.2.2 Results and discussion .....	100
3.2.2.1 FTIR of undoped PPDA.....	100
3.2.2.2 FTIR of HClO <sub>4</sub> doped PPDA.....	102
3.2.2.3 FTIR of copper acetate doped PPDA.....	104
3.2.2.4 Thermogravimetric analysis of PPDA.....	107
3.2.2.5 Differential scanning calorimetry of PPDA.....	108
3.3 Conclusions.....	109
3.4 References.....	109

## **Chapter.4** 113

### **Preparation and properties of polythiophene**.....

4.1 Experimental methods.....	115
4.1.1 Preparation of polythiophene.....	115
4.1.2 Doping of polythiophene.....	115
4.1.3 Characterisation of polythiophene.....	115
4.2 Results and discussion.....	116
4.2.1 FTIR of undoped polythiophene.....	116
4.2.2 FTIR of FeCl <sub>3</sub> doped polythiophene.....	119
4.2.3 TGA/DTA curves of undoped polythiophene.....	121
4.2.4 DSC curve of undoped polythiophene.....	122

4.3	Conclusions.....	123
4.4	References.....	124

## **Chapter.5**

<b>Preparation and properties of PEDOT- poly(3, 4-ethylene dioxy thiophene)</b> .....	127
---	-----

5.1	Experimental methods.....	129
5.1.1	Preparation of PEDOT.....	129
5.1.2	Characterization of PEDOT .....	129
5.2	Results and discussion.....	130
5.2.1	FTIR of PEDOT .....	130
5.2.2	TGA/DTA curves of PEDOT .....	132
5.2.3	DSC curve of PEDOT .....	133
5.3	Conclusions.....	134
5.4	References.....	135

## **Chapter.6**

<b>Microwave Properties of Conducting Polymers</b> .....	137
--	-----

6.1	Experimental methods.....	138
6.2	Results and discussion.....	141
6.2.1	Microwave properties .....	141
6.2.1.1	Dielectric constant.....	141
6.2.1.2	Dielectric loss .....	143
6.2.1.3	Loss tangent.....	145



6.2.1.4	Absorption coefficient .....	146
6.2.1.5	Conductivity .....	147
6.2.1.6	Dielectric heating coefficient .....	148
6.2.1.7	Skin depth .....	149
6.2.2	DC conductivity .....	150
6.3	Conclusions.....	151
6.4	References.....	153

## **Chapter.7**

### **Microwave Properties of Selected Thermoplastic Conducting Composites.....**

155

#### **Part-I**

<b>7.1</b>	<b>Optimization of ratio of FeCl<sub>3</sub>: Thiophene in preparing PTH-PVC composites.....</b>	<b>158</b>
7.1.1	Experimental methods.....	158
7.1.2	Results and discussion.....	160
7.1.2.1	Effect of ferric chloride on dielectric constant of PTH-PVC composite .....	160
7.1.2.2	Effect of ferric chloride on dielectric loss of PTH-PVC composite...	161
7.1.2.3	Effect of ferric chloride on conductivity of PTH-PVC composite..	162
7.1.3	Conclusions.....	163

## **Part-II**

<b>7.2</b>	<b>Effect of drying condition on microwave properties of conducting polymer-PVC composites.....</b>	<b>164</b>
7.2.1	Experimental methods.....	164
7.2.2	Results and discussion.....	165
7.2.2.1	Variation of dielectric constant for vacuum dried and room temperature dried conducting polymer- PVC composites .....	165
7.2.2.2	Variation of dielectric loss for vacuum dried and room temperature dried conducting polymer- PVC composites .....	167
7.2.2.3	Variation of conductivity for vacuum dried and room temperature dried conducting polymer- PVC composites .....	168
7.2.2.4	Variation of absorption coefficient for vacuum dried and room temperature dried conducting polymer- PVC composites.....	169
7.2.3	Conclusions.....	170

## **Part-III**

<b>7.3</b>	<b>Comparison Of Microwave Properties Of Thermoplastic Conducting Composites .....</b>	<b>171</b>
7.3.1	Experimental methods.....	172
7.3.2	Results and discussion.....	173
7.3.2.1	Comparison of dielectric constant of thermoplastic conducting composites.....	173
7.3.2.2	Comparison of dielectric loss of thermoplastic conducting composites.....	174

7.3.2.3	Comparison of conductivity of thermoplastic conducting composites.....	175
7.3.2.4	Comparison of absorption coefficient of thermoplastic conducting composites.....	176
7.3.2.5	Comparison of loss tangent of thermoplastic conducting composites.....	177
7.2.3.6	Comparison of heating coefficient of thermoplastic conducting composites.....	178
7.2.3.7	Comparison of skin depth of thermoplastic conducting composites.....	180
7.4	Conclusions.....	181
7.5	References.....	181

## **Chapter.8**

### **Application Study: Microwave absorption, reflection, EMI shielding and mechanical properties of PANI-PU composite.....**

		185
8.1	Experimental methods.....	189
8.1.1	Absorption coefficient, reflection coefficient and EMI shielding.....	189
8.1.2	Mechanical properties.....	189
8.1.3	Load sensitivity.....	190
8.2	Results and discussion.....	190
8.2.1	EMI shielding.....	190
8.2.2	Absorption coefficient.....	193
8.2.3	Reflection coefficient.....	196
8.2.4	Mechanical properties.....	198
8.2.5	Load sensitivity.....	199

8.3	Conclusions.....	200
8.4	References.....	201

## **Chapter.9**

<b>Summary and Conclusions.....</b>	<b>203</b>
<b>List of Abbreviations and Symbols.....</b>	<b>211</b>
<b>List of Tables and Schemes.....</b>	<b>213</b>
<b>List of Figures.....</b>	<b>215</b>
<b>List of Publications.....</b>	<b>219</b>
<b>Curriculum vitae.....</b>	<b>220</b>

## **INTRODUCTION**

Conducting polymers have established themselves as an important class of materials with wide range of applications such as electroluminescence devices, non-linear optical materials, oscillators, amplifiers, frequency converters, sensors, EMI shielding, radar absorption etc. Conducting polymers show very interesting properties in electrical and microwave frequencies that make them far more superior to traditional dielectric materials. Non biological materials exhibiting the dielectric properties of biological tissue at microwave frequencies have been used extensively to evaluate hyperthermia applicators , assess microwave imaging systems , to determine electromagnetic absorption patterns and as phantoms.

The microwave and electrical properties and applications of conducting polymers like poly para phenylene diazomethine, polythiophene, polyaniline and Poly (3, 4-ethylenedioxythiophene) (PEDOT) is the subject of this investigation. One of the major drawbacks of conducting polymers is their poor processability, and a solution to overcome this is sought in this investigation. Conducting polymer/ thermoplastic composites were prepared by the insitu polymerization method to improve the homogeneity of the composites, probably to a semi IPN level. An important outcome of the work is the development of a processable conducting composite with very good electrical, mechanical and microwave properties and which can be easily solvent cast or coated on various surfaces.

## 1.1 INTRINSICALLY CONDUCTING POLYMERS

The intrinsically conducting polymers (ICP) have emerged as a new class of materials because of their unique electrical, optical and chemical properties. By proper doping, the conductivity of these materials can be varied from semi conducting to metallic range. Wide and diversified areas of potential applications exist for conducting polymers, such as diodes, battery anodes or cathodes, semiconductors, energy storage and conversion devices, electroluminescence devices, non-linear optical materials, EMI shielding, radar absorbers oscillators, amplifiers, frequency converters, sensors etc. have been reported [1-14] .

One of the most exciting areas of research in microelectronics is the development of bio sensing devices. The entrapment of enzymes in conducting polymer films provides a controlled method of localizing biologically active molecules in defined area on the electrodes [6-8]. Probably the most publicized and promising of the current applications are light weight rechargeable batteries. Some prototype cells are comparable to, or better than nickel-cadmium cells now on the market [11]. Microwave properties of conductive polymers finds applications such as coating in reflector antennas, coating in electronic equipments, frequency selective surfaces, EMI materials, satellite communication links, microchip antennas, radar absorbing materials etc [15-18].

## 1.2 CONJUGATED POLYMERS

Intrinsically conducting polymers are usually extensively conjugated molecules. Conjugated polymers are either insulators or wide-gap semiconductors in their pristine neutral state, and some of them turn into metallic type conductors after a process called doping. The first conjugated polymer, polythiazyl (SN)<sub>x</sub>, was discovered in 1975, which possesses metallic conductivity and becomes superconductor at 0.29 K [19].

However, the idea of using polymers for their electrical conducting properties actually emerged in 1977 with the findings of Shirakawa et al. [20], that the iodine doped trans-polyacetylene, (CH)<sub>x</sub>, exhibits conductivity of 10<sup>3</sup> S/cm. Since then, an active interest in synthesizing other organic polymers possessing this property has been initiated. As a result, other conducting polymers having pi-electron conjugated structure, such as polyaniline (PANI), polypyrrole (PPY), polythiophene (PTH), polyfuran (PFU), poly(para phenylene vinylene) and polycarbazole [1,9,20,21] have been synthesized for exploring them in many applications. Figure 1.1 shows the structural formulae of some important conjugated polymers.

It is believed that conjugated polymers possess a spatially delocalized band-like electronic structure [22, 23]. The essential structural characteristic of all conjugated polymers is their quasi-infinite  $\pi$  system extending over a large number of recurring monomer units. This feature results in materials with directional conductivity, strongest along the axis of the chain [24].

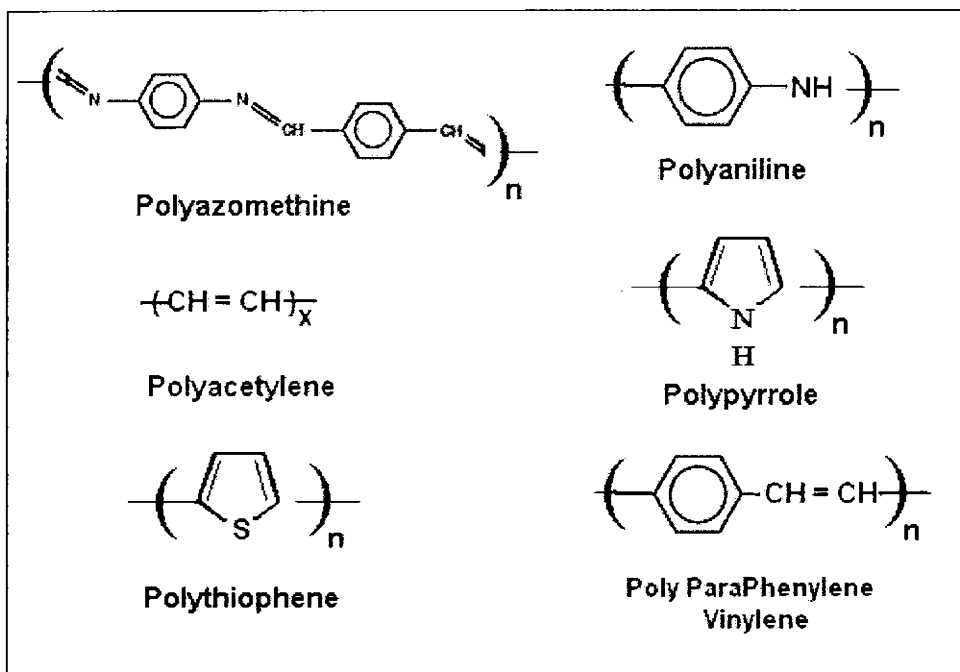


Figure 1.1 Structural formulae of various conjugated polymers.

### 1.3 CONDUCTION IN POLYMERS

For conduction to occur, electrons must be excited (e.g. via a collision with a phonon or with a photon or by an electric field) to an empty level where they can propagate through the material. Conduction in polymers has been explained by Mott and Sheng [25-27].

#### 1.3.1 Mott's hopping conductivity model

Sir Nevill Mott developed a model of electron conduction in amorphous materials using a non-periodic energy potential throughout the volume of the material and can be applied to conducting polymers [25, 26]. Mott assumes that the electron is



going to move or hop to another site less than the distance ' $R$ ' away. The number of energy states per unit energy per unit volume is given by ' $N(E)$ ', where ' $E$ ' is the energy. Near the Fermi level, the corresponding density of states per unit volume is just ' $N(E_F)$ '. Within a radius ' $R$ ' of the starting point, the numbers of energy states per unit energy near the Fermi energy is given by

$$n(R) = N(E_F) \cdot V(R) = \left( \frac{4\pi}{3} \right) R^3 N(E_F) \quad (1)$$

If there are ' $n(R)$ ' energy states per unit energy in the volume, then the average energy between the states is the inverse of ' $n(R)$ '

$$\Delta E = \left[ \left( \frac{4\pi}{3} \right) R^3 N(E_F) \right]^{-1} \quad (2)$$

The probability of an electron being thermally excited is proportional to  $\exp(-\Delta E/kT)$ . However, if an electron travels a long distance, it must tunnel through a much longer effective barrier. The likelihood of tunneling a distance ' $R$ ' decreases exponentially with ' $R$ ' as  $\exp(-2\alpha R)$ . ' $1/\alpha$ ' is the decay length of the wave function at the starting site and is related to the height of the potential barrier between sites. By combining the likelihood of gaining the energy ' $\Delta E$ ' and of tunneling through the distance ' $R$ ' we can get the likelihood of the electron moving:

$$P \propto \exp(-2\alpha R) \cdot \exp\left(-\frac{\Delta E}{kT}\right) \quad (3)$$

The probability is maximized (with respect to  $R$ ) when  $\delta P/\delta R = 0$

$$R = \left[ \left( \frac{8}{9} \right) \pi k T \alpha N(E_F) \right]^{1/2} \quad (4)$$

Substituting for 'R', we can finally write the expression for the likelihood of hopping to another site as:

$$P \propto \exp(-B/T^{1/4}) \quad (5)$$

$$B = 4 \left( \frac{2}{9\pi} \right)^{1/2} (\alpha^3 / [kN(E_F)])^{1/2} \quad (6)$$

Since the conductivity is proportional to the probability of hopping, the conductivity is given by an equation of the form:

$$\sigma = \sigma_0 \exp(-B/T^{1/4}) \quad (7)$$

which is known as Mott's  $T^{-1/4}$  Law.

### 1.3.2 Sheng Model: Tunnel junctions between conducting regions

Sheng [27] proposed a model for conduction where large (metallic) conducting regions are separated by tunneling junctions. In Sheng's model, Johnson noise induces fluctuating voltages across the junctions. The equation for conductivity is given by

$$\sigma(T) = \sigma_0 \exp[-T_1/(T + T_0)] \quad (8)$$

where ' $T_0$ ' and ' $T_1$ ' are constants. At high temperatures,  $T \gg T_0$ , the fluctuations dominate and the conductivity varies as

$$\sigma(T) = \sigma_0 \exp [-T_1/T] \quad (9)$$

In Sheng's derivation, if a parabolic potential barrier is assumed between conducting regions

$$T_1/T_0 = \left(\frac{\pi}{4}\right)\left(\frac{2}{\hbar}\right) w [2 m V_0]^{1/2} \quad (10)$$

$$\text{and } k T_1 = 8 \epsilon_0 (A/w) (V_0/e)^2 \quad (11)$$

where 'A' and 'w' are the (averaged) cross-sectional area and distance across the junction,  $V_0$  is the barrier height, 'e' is the electron charge, 'm' is the electron mass, ' $\epsilon_0$ ' is the permittivity of free space, and ' $\hbar$ ' is Planck's constant. The values of ' $V_0$ ', 'A', and 'w' are experimentally very difficult or impossible to measure. Schimmel et al [28] have offered a simpler phenomenological model with the same form, but a more intuitive definition for ' $T_0$ ' and ' $T_1$ '. At high temperatures, the thermal energy is able to overcome the potential barrier and the conductivity will be proportional to  $\exp (-\Delta E/kT)$ . Thus, when  $T \gg T_1$

$$\exp (-\Delta E / kT) = \exp (-T_1 / T) \quad (12)$$

and

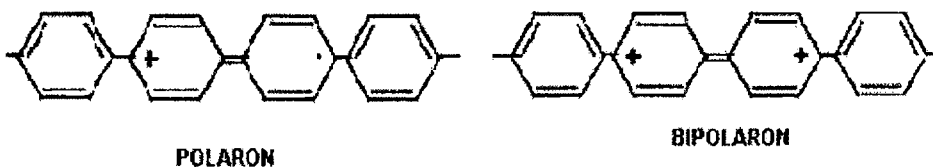
$$T_1 = \Delta E / k \quad (13)$$

where ' $\Delta E$ ' is just the barrier height ' $V_0$ '. At low temperature (as  $T$  tends to 0), if it is assumed that the conduction is due solely to tunneling, then

$$\exp (-T_1 / T_0) = \exp (- (2 / \hbar) (2mV_0)^{1/2} w) \quad (14)$$

where there are now just two parameters ' $V_0$ ' (the barrier height) and ' $w$ ' (the tunneling distance). And ' $m$ ' is the effective mass of the electron which is roughly the free electron mass.

It is generally agreed that the mechanism of conductivity in these polymers is based on the motion of charged defects within the conjugated framework [29, 30]. Oxidation of the polymer initially generates a radical cation with both spin and charge. This species is referred to as a polaron and comprises both the hole site and the structural distortion that accompanies it. This condition is depicted in Figure 2. The cation and radical form a bound species, since any increase in the distance between them would necessitate the creation of additional higher energy quinoid units. Theoretical treatments [31, 32] have demonstrated that two nearby polarons combine to form the lower energy bipolaron shown in Figure 1.2.



**Figure 1.2 Schematic representations of polaron and bipolaron.**

One bipolaron is more stable than two polarons despite the coulombic repulsion of the two ions. Since the defect is simply a boundary between two moieties of equal energy (the infinite conjugation chain on either side) it can migrate in either direction without affecting the energy of the backbone, provided that there is no significant energy barrier to the process. It is this charge carrier mobility that leads to the high conductivity of these polymers.

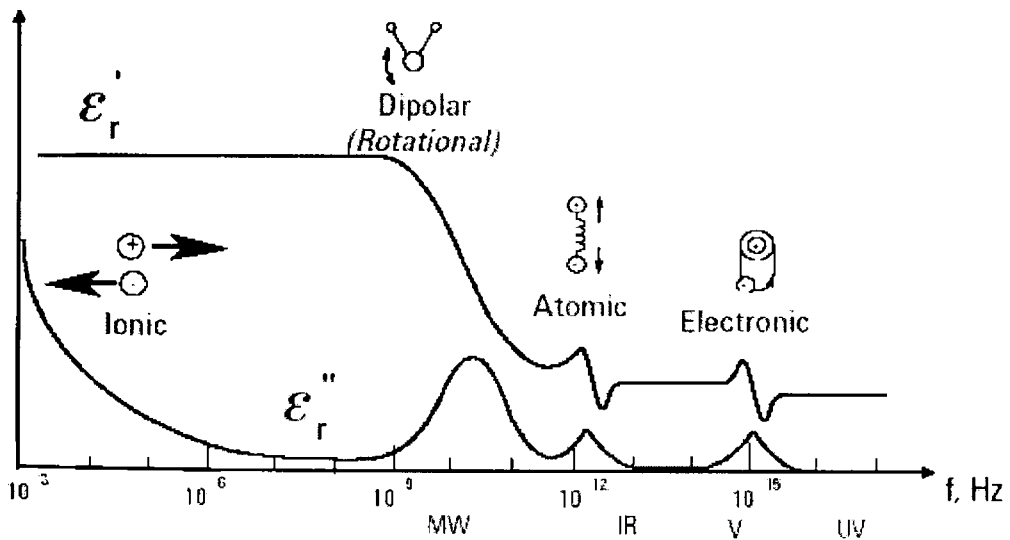
The conductivity  $\sigma$  of a conducting polymer is related to the number of charge carriers 'n' and their mobility,  $\mu$

$$\sigma \propto n \mu$$

Because the band gap of conjugated polymers is usually fairly large, 'n' is very small under ambient conditions.

#### 1.4 CONDUCTION IN MICROWAVE FIELD

At the microscopic level, a material may have several dielectric mechanisms or polarization effects that contribute to its overall permittivity (Figure 1.3) [33].



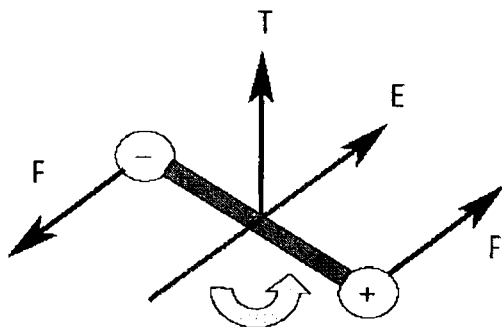
**Figure 1.3** Frequency responses of dielectric mechanisms

When an electric field is applied to a material, an induced dipole moment connected to the polarisability appears. There are several types of polarization [34]

- The electronic cloud displacement around the atom called electronic polarization.
- Electric field can modify the electron repartition and consequently the equilibrium location of the atoms in the molecule, called as the atomic polarization.
- Orientation of permanent dipoles causing dipolar polarization.

### 1.4.1 Orientation (dipolar) polarization

Permanent dipole moments are oriented in a random manner in the absence of an electric field so that no polarization exists. The electric field ' $E$ ' will exercise torque ' $T$ ' on the electric dipole, and the dipole will rotate to align with the electric field causing orientation polarization to occur (Figure 1.4).



**Figure 1.4 Dipole rotation in an electric field**

The friction accompanying the orientation of the dipole will contribute to the dielectric losses. The dipole rotation causes a variation in both ' $\epsilon'$ ' and ' $\epsilon''$ ' at the relaxation frequency which usually occurs in the microwave region.

### **1.4.2 Electronic and atomic polarization**

Electronic polarization occurs in neutral atoms when an electric field displaces the nucleus with respect to the electrons that surround it. Atomic polarization occurs when adjacent positive and negative ions “stretch” under an applied electric field. The amplitude of the oscillations will be small for any frequency other than the resonant frequency.

### **1.4.3 Interfacial or space charge polarization**

Interfacial or space charge polarization occurs when the motion of migrating charges is impeded. The charges can become trapped within the interfaces of a material. Motion may also be impeded when charges cannot be freely discharged or replaced at the electrodes. The field distortion caused by the accumulation of these charges increases the overall capacitance of a material which appears as an increase in ‘ $\epsilon'$ ’.

## **1.5 MICROWAVE PROPERTIES**

### **1.5.1 Relaxation time**

Relaxation time ‘ $\tau$ ’ is the time required for a displaced system aligned in an electric field to return to ‘ $1/e$ ’ of its random equilibrium value (or the time required for dipoles to become oriented in an electric field). Constant collisions cause internal friction so that the molecules turn slowly and exponentially approach the final state of orientation polarization with relaxation time constant ‘ $\tau$ ’. When the field is switched off, the sequence is reversed and random distribution is restored with the

same time constant. The relaxation frequency ' $f_c$ ' is inversely related to relaxation time [34, 35]:

$$\tau = \frac{1}{\omega_c} = \frac{1}{2\pi f_c} \quad (15)$$

### 1.5.2 Dielectric constant and dielectric loss

The real part of permittivity ' $\epsilon'$ ' is a measure of how much energy from an external electric field is stored in a material. The imaginary part of permittivity ' $\epsilon''$ ' is called the loss factor and is a measure of how dissipative or lossy a material is to an external electric field. At frequencies below relaxation the alternating electric field is slow enough that the dipoles are able to keep pace with the field variations. Because the polarization is able to develop fully, the loss ' $\epsilon''$ ' is directly proportional to the frequency. As the frequency increases, ' $\epsilon_r'$ ' continues to increase but the storage ' $\epsilon'$ ' begins to decrease due to the phase lag between the dipole alignment and the electric field. Above the relaxation frequency both ' $\epsilon''$ ' and ' $\epsilon'$ ' drop off as the electric field is too fast to influence the dipole rotation and the orientation polarization disappears.

### 1.5.3 Cole-Cole diagram

The complex permittivity may be shown on a Cole-Cole diagram by plotting the imaginary part ' $\epsilon''$ ' on the vertical axis and the real part ' $\epsilon'$ ' on the horizontal axis with frequency as the independent parameter. A material that has a single relaxation frequency as exhibited by the Debye relation will appear as a semicircle



with its centre lying on the horizontal ' $\epsilon'' = 0$ ' axis and the peak of the loss factor occurring at ' $1/\tau$ '. A material with multiple relaxation frequencies will be a semicircle (symmetric distribution) or an arc (nonsymmetrical distribution) with its centre lying below the horizontal ' $\epsilon'' = 0$ ' axis. The curve in Figure 1.5 is a half circle with its centre on the x-axis and its radius. The maximum imaginary part of the dielectric constant ' $\epsilon''_{\max}$ ' will be equal to the radius. The frequency moves counter clockwise on the curve.

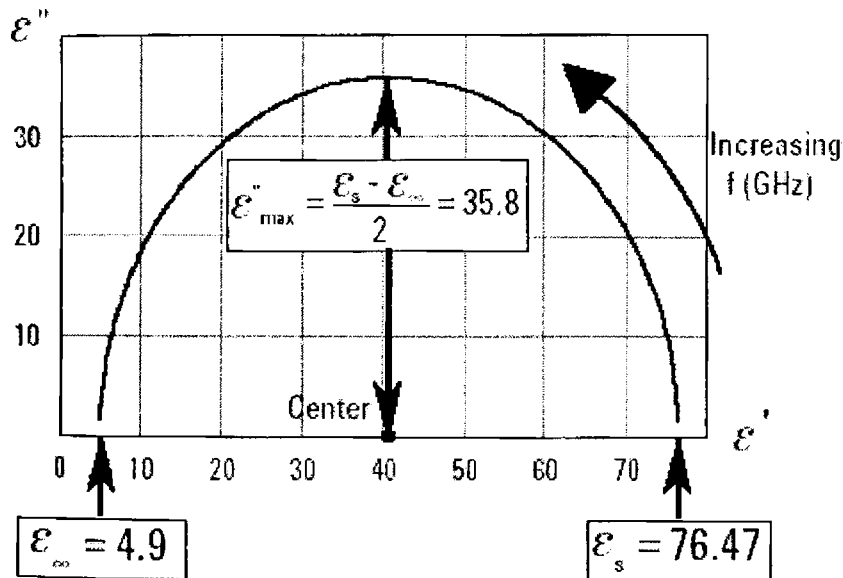


Figure 1.5 Cole-Cole diagram of water at 30 °C [33].

#### 1.5.4 Maxwell-Wagner effect

Mixtures of materials with electrically conducting regions that are not in contact with each other (separated by non-conducting regions) exhibit the Maxwell-

Wagner effect at low frequencies. If the charge layers are thin and much smaller than the particle dimensions, the charge responds independently of the charge on nearby particles. At low frequencies the charges have time to accumulate at the borders of the conducting regions causing ' $\epsilon'$ ' to increase. At higher frequencies the charges do not have time to accumulate and polarization does not occur since the charge displacement is small compared to the dimensions of the conducting region. As the frequency increases, ' $\epsilon''$ ' decreases and the losses exhibit the same ' $1/f$ ' slope as observed in normal ionic conductivity [33-37].

### 1.5.5 Loss tangent

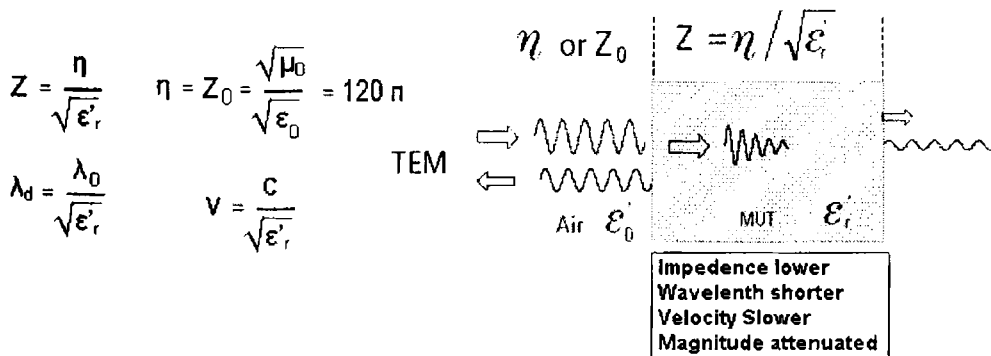
When complex permittivity is drawn as a simple vector diagram, the real and imaginary components are  $90^\circ$  out of phase. The vector sum forms an angle ' $\delta$ ' with the real axis ' $\epsilon'$ '. The relative "lossiness" of a material is the ratio of the energy lost to the energy stored.

$$\tan \delta = \frac{\epsilon''}{\epsilon'} = \frac{1}{Q} = \text{Energy Lost per Cycle} / \text{Energy Stored per cycle} \quad (17)$$

' $D$ ' denotes dissipation factor and ' $Q$ ' is quality factor. The loss tangent ' $\tan \delta$ ' is called tan delta, tangent loss or dissipation factor. The loss tangent represents a ratio of the conduction current to the displacement current in a material. The conduction current is the current due to losses in the material. The displacement current is related to the current present if the material were a perfect dielectric [38].

### 1.5.6 Microwave absorption

This electromagnetic wave can propagate through free space (at the speed of light,  $c = 3 \times 10^8$  m/s) or through materials at slower speed. Consider a flat slab of material (MUT- Material under Test) in space, with a TEM (Transverse Electro Magnetic) wave incident on its surface. There will be incident, reflected and transmitted waves. Since the impedance of the wave in the material ' $Z$ ' is different (lower) from the free space impedance ' $\eta$  (or  $Z_0$ )' there will be impedance mismatch and this will create the reflected wave. Part of the energy will penetrate the sample. Once in the slab, the wave velocity ' $v$ ', is slower than the speed of light, ' $c$ '. The wavelength ' $\lambda_d$ ' is shorter than the wavelength ' $\lambda_0$ ' in free space according to the equations below. Since the material will always have some loss, there will be attenuation or insertion loss (Figure 1.6).

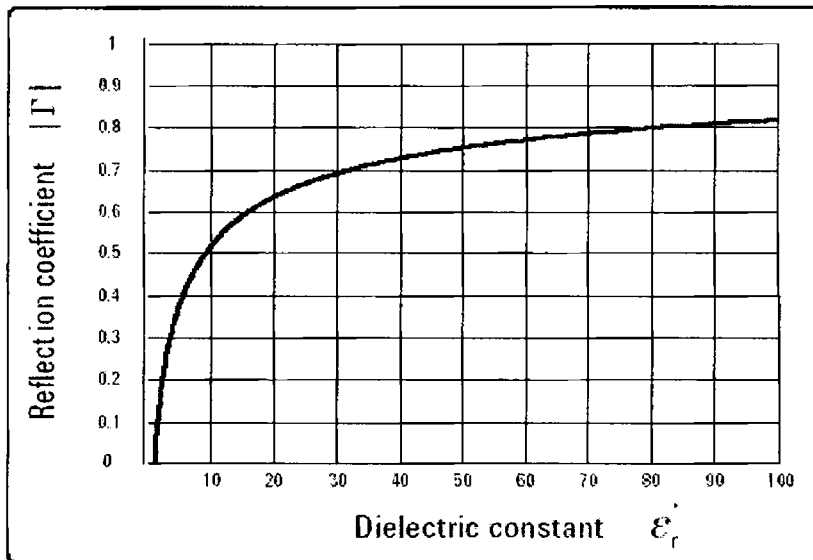


**Figure 1.6 Reflected and transmitted signals from a material under test (MUT).**

Figure 1.7 depicts the relation between the dielectric constant of the Material under Test (MUT) and the reflection coefficient  $|\Gamma|$  for an infinitely long sample (no reflection from the back of the sample is considered). For small values of the

dielectric constant (approximately less than 20), there is a lot of change of the reflection coefficient for a small change of the dielectric constant.

Microwave absorbing materials can be classified in two broad categories, either dielectric or magnetic absorbers. Dielectric absorbers depend on the ohmic loss of energy that can be achieved by loading lossy fillers like carbon, graphite, conducting polymers or metal particles/powder into a polymeric matrix. Magnetic absorbers depend on the magnetic hysteresis effect, which is obtained when particles like ferrites are filled into a polymeric matrix [39-41].



**Figure 1.7 Reflection coefficient Vs. dielectric constant [33].**

There are three conditions that result in a minimum microwave reflectivity.

The first equation of interest is that describing the reflection coefficient at an interface.

$$r = \frac{\eta_M - \eta_0}{\eta_M + \eta_0} = \frac{Z_M - Z_0}{Z_M + Z_0} \quad (18)$$

where 'r' is the reflection coefficient and 'η' the admittance of the propagating medium (subscript 0 for incident medium or air and M for the substrate). The reflection coefficient falls to zero when 'η<sub>M</sub> = η<sub>0</sub>', or in other words the material in the layer is impedance matched to the incident medium. The intrinsic impedance of free space is given by

$$Z_0 = \frac{E}{H} = \frac{\sqrt{\mu_0}}{\sqrt{\epsilon_0}} \approx 377 \text{ ohms} \quad (19)$$

where 'E' and 'H' are the electric and magnetic field vectors and 'μ<sub>0</sub>' and 'ε<sub>0</sub>' are the permeability and permittivity of free space. Thus a material with an impedance of 377 ohms will not reflect microwaves if the incident medium is free space. Perfect impedance matching can also be realised if the electric permittivity and the magnetic permeability are equal. This gives the second condition that result in a minimum in the reflection coefficient. In this case the expression for 'r' becomes [38, 39]

$$r = \frac{\frac{Z_M}{Z_0} - 1}{\frac{Z_M}{Z_0} + 1} \quad (20)$$

The normalized intrinsic impedance is

$$\frac{Z_M}{Z_0} = \frac{\sqrt{\mu_r^*}}{\sqrt{\epsilon_r^*}} \quad \text{Where } \epsilon_r^* = \frac{\epsilon' - i\epsilon''}{\epsilon_0} \quad \text{and} \quad \mu_r^* = \frac{\mu' - i\mu''}{\mu_0} \quad (21)$$

If the incident medium is free space and the reflectivity is zero, then it follows that  $\epsilon_r^* = \mu_r^*$ . The implication is if both the real and imaginary parts of the permittivity and permeability are equal, then the reflectivity coefficient is zero. The third consideration is the attenuation of the wave as it propagates into the absorbing medium. The power of the wave decays exponentially with distance,  $x$ , by the factor  $e^{-\alpha x}$  is the attenuation constant of the material and can be expressed as

$$\alpha = -\sqrt{\epsilon_0 \mu_0} \omega (a^2 + b^2)^{1/4} \sin\left(\frac{1}{2} \tan^{-1}\left[\frac{a}{b}\right]\right) \quad (22)$$

Where  $a = (\epsilon_r' \mu_r' - \epsilon_r'' \mu_r'')$  and  $b = (\epsilon_r' \mu_r' + \epsilon_r'' \mu_r'')$

To get a large amount of attenuation in a small thickness,  $\alpha$  must be large, which implies that  $\epsilon_r'$ ,  $\epsilon_r''$ ,  $\mu_r'$  and  $\mu_r''$  must be large. It is noted here that this condition must be tempered with the first condition, where large values of permittivity and permeability would result in a large reflection coefficient [39].

Microwave Absorbing Materials are used in

- Airplanes & Ships
- Camouflage Nets & Radar Camouflage
- Electromagnetic Interference Suppression- false echoes from ships own superstructure
- Antenna Performance Enhancement – Side and black lobes

The different types of microwave absorbing materials are given in Figure 1.8.

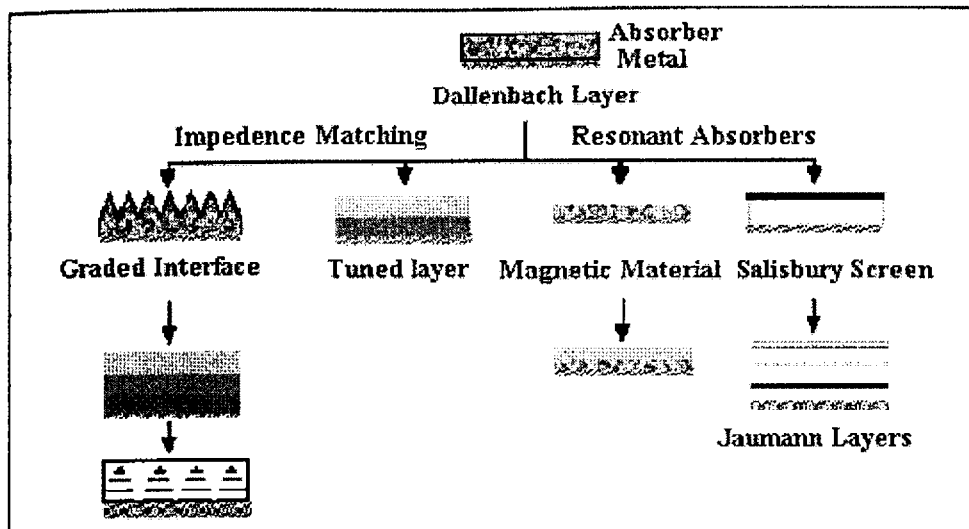


Figure 1.8 Types of Radar Absorbing Materials (RAM's).

## 1.6 MEASUREMENT OF MICROWAVE PROPERTIES

Microwave properties of materials can be evaluated with coaxial probe, transmission line, free space, parallel plate and resonant cavity methods [33, 42-48].

### 1.6.1 Coaxial probe

The open-ended coaxial probe is a cut off section of transmission line. The properties of the material is measured by immersing the probe into a liquid or touching it to the flat face of a solid (or powder) material. The fields at the probe end “fringe” into the material and change as they come into contact with the material. The reflected signal ( $S_{11}$ ) can be measured and related to  $\epsilon_r^*$  [42].

### 1.6.2 Transmission line

Transmission line methods involve placing the material inside a portion of an enclosed transmission line. The line is usually a section of rectangular waveguide or coaxial line (Figure 1.9). ' $\epsilon_r$ ' and ' $\mu_r$ ' are computed from the measurement of the reflected signal ( $S_{11}$ ) and transmitted signal ( $S_{21}$ ).

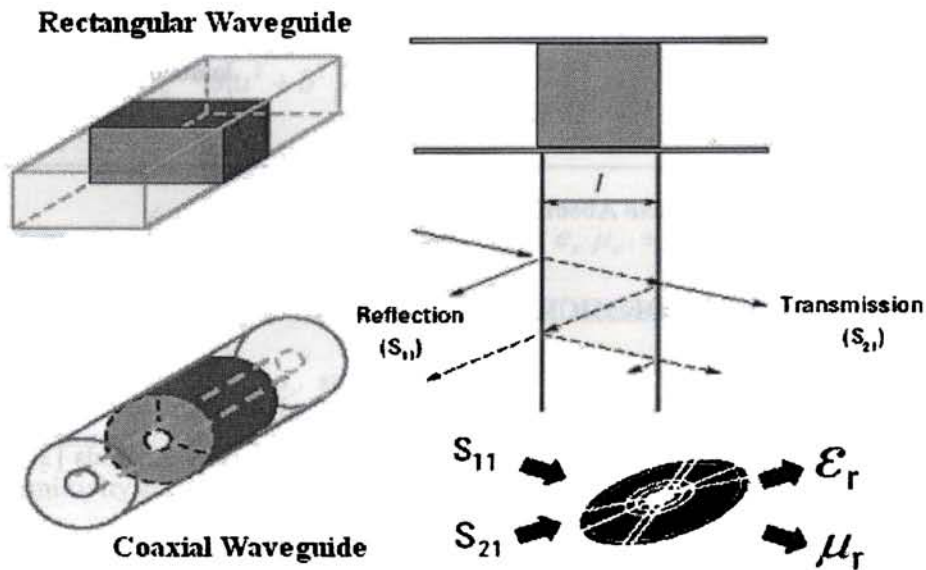


Figure 1.9 Transmission line, wave guide and coaxial line methods.

### 1.6.3 Free space

Free-space methods use antennas to focus microwave energy at or through a slab of material without the need for a test fixture. This method is non-contacting and can be applied to materials to be tested under high temperatures and hostile environments [33].



#### **1.6.4 Parallel plate**

The parallel plate capacitor method involves sandwiching a thin sheet of material between two electrodes to form a capacitor. A typical measurement system using the parallel plate method consists of an LCR meter or impedance analyzer and a fixture such as the 16451B dielectric test fixture, which operates up to 30 MHz [33].

#### **1.6.5 Resonant cavities**

Resonant cavities are high ' $Q$ ' structures that resonate at certain frequencies. A piece of sample material affects the centre frequency ' $f$ ' and quality factor ' $Q$ ' of the cavity. From these parameters, the complex permittivity ' $\epsilon_r$ ' or permeability ' $\mu_r$ ' of the material can be calculated at a single frequency. There are many different types of cavities and methods. Here, the most widely used **Cavity Perturbation Method**, as described in ASTM 252010 [43-47], is considered.

#### **1.6.6 Cavity perturbation technique**

The measurements of permittivity and permeability of the dielectric materials are performed by inserting a small and appropriately shaped sample into a cavity and determining the properties of the sample from the resultant change in the resonant frequency and loaded quality factor of the cavity. The basic idea of the cavity perturbation is the change in the overall geometric configuration of the electromagnetic fields with the insertion of a small sample [43-48].

When a small sample is inserted in a cavity which has an electric field ' $E_0$ ' and magnetic field ' $H_0$ ' in the unperturbed state and the fields in the interior of the sample is ' $E$ ' and ' $H$ ', then for loss less sample, the variation of resonance frequency is given by equation (23) as

$$\frac{f_s - f_0}{f_s} = - \frac{\int (\Delta \varepsilon E \cdot E_0^* + \Delta \mu H \cdot H_0^*) d\tau}{\int (\varepsilon E \cdot E_0^* + \mu H \cdot H_0^*) d\tau} \quad (23)$$

Where ' $\varepsilon$ ' and ' $\mu$ ' are the permittivity and permeability of the medium in the unperturbed cavity. ' $d\tau$ ' is the elementary volume and ' $\Delta \varepsilon$ ' and ' $\Delta \mu$ ' are the changes in the permittivity and permeability due to the introduction of the sample in the cavity [49-51]. Without affecting the generality of Maxwell's equations, the complex frequency shift due to lossy sample in the cavity is given as

$$\frac{-df^*}{f^*} = \frac{(\varepsilon_r - 1)\varepsilon_0 \int_{vs} E \cdot E_0^* dv + (\mu_r - 1)\mu_0 \int_{vs} H \cdot H_0^* dv}{\int_{vs} (D_0 \cdot E_0^* + B_0 \cdot H_0^*) dv} \quad (24)$$

Where ' $df^*$ ' is the complex frequency shift because the permittivity of practical materials is a complex quantity, so the resonance frequency is also complex. ' $B_0$ ', ' $H_0$ ', ' $D_0$ ' and ' $E_0$ ' are the fields in the unperturbed cavity and ' $E$ ' and ' $H$ ' is the field in the interior of the sample [43, 52].

When a dielectric sample is inserted into the cavity resonator where the maximum perturbation occurs that is at the position of maximum electric field, only the first term in the numerator is significant, since a small change in ' $\varepsilon_r$ ' at a point of zero

electric field or a small change in ' $\mu_r$ ' at a point of zero magnetic field does not change the resonance frequency. Therefore equation (24) can be reduced to

$$\frac{-df^*}{f^*} = \frac{(\epsilon_r - 1) \int_{vs} E \cdot E_0^* \max dv}{2 \int_{vs} |E|^2 dv} \quad (25)$$

A sample of complex permittivity ' $\epsilon_r$ ' is kept at the maximum electric field location of the cavity. The sample is taken, as cylinder with uniform cross sectional area ' $s$ ' and length is greater than narrow dimension ' $b$ ' so that it will occupy the entire narrow dimension of the cavity. After the introduction of the sample the empty resonant frequency and  $Q$ -factor alter, due to the change in the overall capacitance and conductance of the cavity. Quality factor ' $Q$ ' is given by,

$$Q = f/\Delta f \quad (26)$$

Where ' $f$ ' is the resonant frequency and ' $\Delta f$ ' is the corresponding 3 dB bandwidth. If ' $f_0$ ' and ' $Q_0$ ' are the resonance frequency and quality factor of the cavity without sample and ' $f_s$ ' and ' $Q_s$ ' all the corresponding parameters of the cavity loaded with the sample. The complex resonant frequency shift is related to measurable quantities [53, 54]. On equating real and imaginary parts of equations (24) and (25) we have

**For real part:**

$$-\frac{f_s - f_0}{f_s} = -\frac{(\epsilon_r' - 1) \int_{vs} E \cdot E_0^* \max dv}{2 \int_{vc} |E_0|^2 dv} \quad (27)$$

We may assume that  $E = E_0$  and the value of ' $E_0$ ' in the  $TE_{10p}$  mode is [34-36]

$$E_0 = E_{0 \max} \sin(p\pi z/l) \sin(p\pi z/l) \quad p = 1, 2, 3, \text{ etc.} \quad (28)$$

Where 'a' is the broader dimension of the wave guide and 'l' is the length of the cavity. Integrating and rearranging the equation (27), we obtain

$$\epsilon' = \frac{V_c(f_0^2 - f_s^2)}{4V_s f_s^2} \quad (29)$$

where,

$V_c = a \times b \times l$  (volume of the cavity), ' $V_s$ ' is the volume of the sample and ' $r$ ' is the radius and ' $h$ ' is the length of the sample.

**For Imaginary part:**

$$\frac{1}{2} \left( \frac{1}{Q_s} - \frac{1}{Q_0} \right) = \frac{\epsilon_r'' \int E \cdot E_0^* \max dv}{2 \int |E|^2 dv} \quad (30)$$

Integrating and rearranging the equation (30), we obtain

$$\left( \frac{1}{Q_s} - \frac{1}{Q_0} \right) \frac{V_c f_0^2}{4V_s f_s^2} = \epsilon'' \quad (31)$$

where ' $Q_s$ ' is the quality factor of cavity with sample and ' $Q_0$ ' is the quality factor without sample. Equation (29) and (31) are the standard form of the expression for dielectric parameters using the perturbation technique [34, 36].

For a dielectric material having non-zero conductivity, we have Maxwell's curl equation

$$\nabla \times H = (\sigma + j\omega\bar{\epsilon})E = (\sigma + \omega\epsilon'')E + j\omega\epsilon'E \quad (32)$$

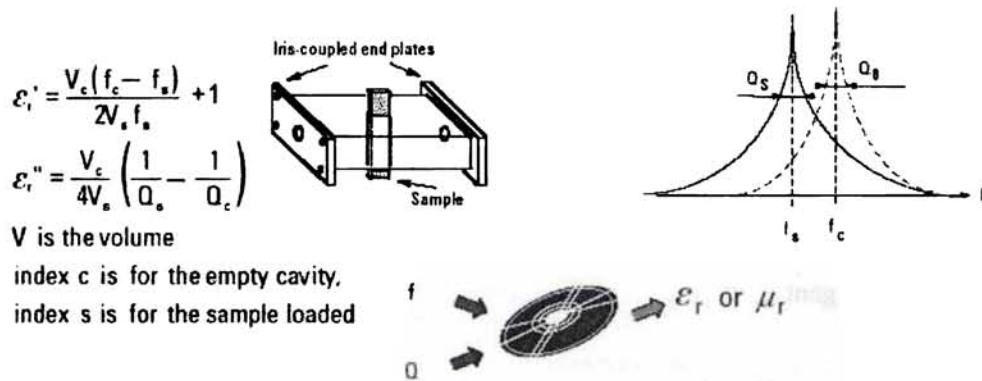
The loss tangent

$$\tan \delta = \frac{\sigma + \omega\epsilon''}{\omega\epsilon'} \quad (33)$$

When  $\sigma$  is very small, the effective conductivity is reduced to [36].

$$\sigma_e = \omega\epsilon'' = 2\pi f\epsilon_0\epsilon_r'' \quad (34)$$

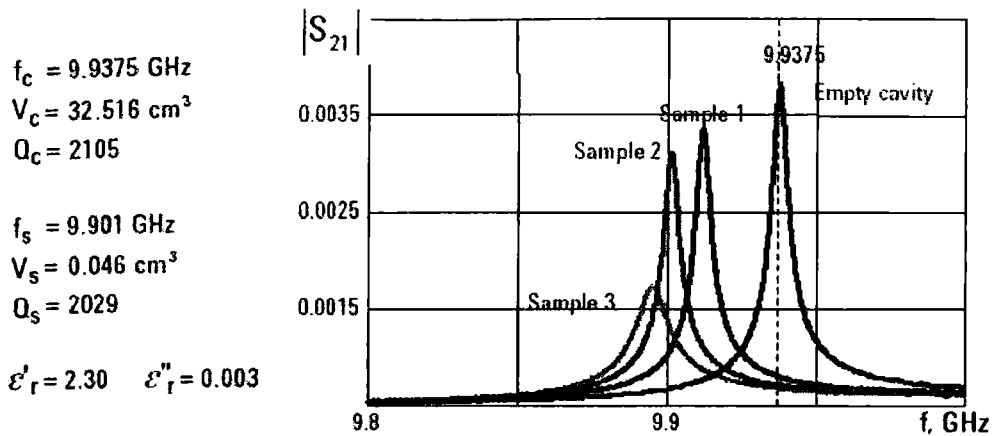
Cavity Perturbation Method uses a rectangular waveguide with iris-coupled end plates, operating in  $TE_{10n}$  mode (Figure 1.10). For a dielectric measurement the sample should be placed in a maximum electric field and for a magnetic measurement, in a maximum magnetic field. If the sample is inserted through a hole in the middle of the waveguide length, then an odd number of half wavelengths ( $n = 2k + 1$ ) will bring the maximum electric field to the sample location, so that the dielectric properties of the sample can be measured. An even number of half wavelengths ( $n = 2k$ ) will bring the maximum magnetic field to the sample location and the magnetic properties of the sample can be measured.



**Figure 1.10 Resonant cavity measurements, cavity perturbation method.**

The cavity perturbation method requires a very small sample such that the fields in the cavity are only slightly disturbed to shift the measured resonant frequency and cavity ' $Q$ '. This assumption allows simplifying the theory to use the equations above to calculate the dielectric properties of the material. Figure 1.11 shows measurements of three different samples with this cavity. The three measurements are presented on the same graph for comparison purposes.


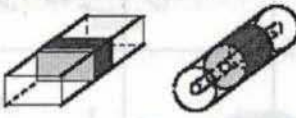

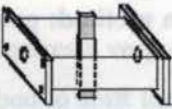

The resonant frequency of the empty cavity is  $f_c = 9.9375$  GHz (for  $TE_{107}$  mode) and it shifts to a lower frequency when the sample is inserted in the cavity. When the resonator is loaded with a sample, the resonance curve broadens, which results in a lower quality factor ' $Q$ '. On the y-axis of Figure 1.11 is the magnitude of the linear transmission coefficient  $|S_{21}|$ . The 8720ES network analyzer is used for these measurements. On the left of the figure is a calculation for the Sample 2, which has a cross section of 0.29 by 0.157 cm [33].



**Figure 1.11 Cavity perturbation method: graphs of empty cavity and samples**  
[35]

### 1.6.7 Comparison of Methods

Many factors such as accuracy, convenience, and the material shape and form are important in selecting the most appropriate measurement technique. Some of the significant factors to consider are summarized in Figure 1.12.

Coaxial Probe $\epsilon_r$		Broadband, non-destructive Best for lossy MUT's; Liquids or semi solids
Transmission Line $\epsilon_r$ and $\mu_r$		Broadband Best for lossy to low loss MUT's; Machinable solids
Free space $\epsilon_r$ and $\mu_r$		Non-contacting Best for high temperatures; Flat samples
Resonant cavity $\epsilon_r$ and $\mu_r$		Accurate Best for low loss MUT's; Small samples
Parallel Plate $\epsilon_r$		Accurate Best for low frequencies ; Thin flat sheets

**Figure 1.12 Summary of measurement techniques.**

## 1.7 MICROWAVE PROPERTIES AND APPLICATIONS OF CONDUCTING COMPOSITES

The study of microwave properties of conductive polymers is crucial because of their wide areas of applications such as coating in reflector antennas, coating in electronic equipments, frequency selective surfaces, EMI materials, satellite communication links, microchip antennas, radar absorbing materials etc. Study of the dielectric loss, conductivity, dielectric constant, and absorption coefficient of these polymers in microwave region will highlight their application in these fields [54-57].



Composite materials comprising micro particles of the environmentally stable conducting polymer poly(3,4-ethylenedioxythiophene) (PEDOT) have been prepared [58]. Rimili and coworkers have developed Polyaniline (PANI/DEHEPSA) films of high conductivity (5000-6000 S/m) and permittivity of above 6000 over X and S bands. This confirms the metallic character of PANI-films and their efficient use in micro-electronic technology such as microwave integrated circuits (MMIC) and microwave devices [59]. Microwave conductivity study of regioregular poly (3-hexyl thiophene) [60], MnZn ferrite- PVC composite [61] polyurethane, polystyrene and poly vinyl acetate has been reported [62]. Brosseau and coworkers reported the microwave response (30MHz-14GHz) of carbon black and silica particles embedded in linear low-density polyethylene, and carbon black particles and carbon fibers embedded in an epoxy resin [63].

The development of stealth technologies makes use of several types of technique, essentially the optimization of the shape of the object and the application of materials which absorb radar waves. In the latter case, the utilization of polymers has several advantages both from the point of view of matrix properties, when the materials are obtained by filler dispersion (the case of granular materials), and the possibility of giving the polymer a controlled electronic conductivity [64-72]. Electromagnetic interference behaviour of conducting polyaniline composites in the radio frequency range X, Ku, and Ka bands were studied. The conducting composites made from CSA-doped polyaniline blended with the styrene acrylonitrile host polymer exhibit high conductivities, up to  $10^4$  S/m, and therefore are compatible with an electromagnetic shielding application [69].

## **1.8 POLYAZOMETHINES**

Polymeric aldimines or poly (schiff base)s are classes of materials known as polyazomethines. It is understood that, the incorporation of nitrogen atoms into the conjugated molecular chains aids in the thermal stability of these materials [73-75]. The first polyazomethine (polyimine or poly schiff base) has been reported in 1923 as a result of polycondensation of terephthalaldehyde and benzidine [76]. Since then, conjugated aromatic polyazomethines with different moieties on both sides of CH=N group have been reported [77- 81].

### **1.8.1 Synthesis of Polyazomethines**

#### *1.8.1.1 Solution polycondensation*

Many groups have reported synthesis of polyazomethines by solution polycondensation [77-83]. A polyazomethine ether was synthesized by polycondensation reaction of a single monomer containing nitro as well as hydroxyl group in presence of excess  $K_2CO_3$  in DMAC and toluene solvent system [82].

#### *1.8.1.2 Chemical vapour deposition (CVD)*

This process involves co- sublimation of two or more reactive monomers which impinge onto a substrate surface, where they react to form a polymer film has been shown to be an effective and efficient means of producing polyazomethines with high conjugation lengths [84, 85]. Electric-field-assisted CVD (EFCVD) has also been recently used to alter the macroscopic structure of these materials. This

technique is especially applicable to fabricate polymer films for optic and electronic application [86].

### *1.8.1.3 Oxidative polymerization*

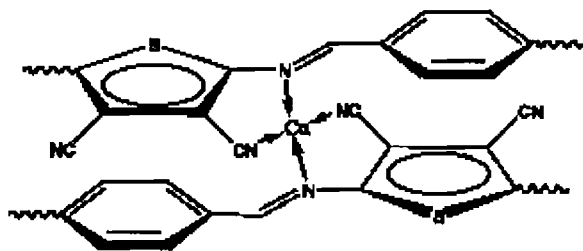
Simionescu and co-workers reports a novel method for the synthesis of wholly aromatic polyazomethines by oxidative polymerization of monomers having a preformed azomethine linkage [73]. Thiophene or furan-containing polyazomethines were synthesized by chemical oxidative polymerization with ferric (III) chloride [87].

## **1.8.2 Modifications**

Initial reports described polyazomethines as insoluble and infusible polymers, a situation that would minimize their practical applications. Three strategies were employed to produce polymers with reduced processing temperatures:

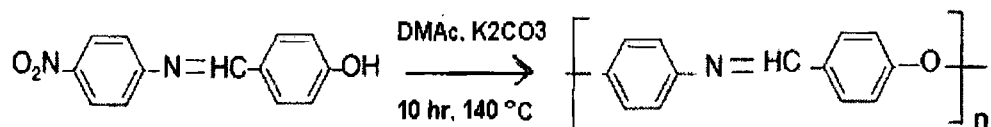
(i) modification of the length of the flexible spacer, (ii) alteration of the coaxiality in the mesogenic rigid core especially by using meta substituted monomers and (iii) copolymerisation [88-94].

Another interesting way to modify polyazomethines is by complexation with metal ions (Figure 1.13) [92, 93].



**Figure 1.13** Intermolecular complexation with copper salts in Thienylene-Phenylene polyazomethine.

Solubility could be affected by modifying polyazomethines to polyazomethine ether (Scheme 1.1) [82] or polyazomethine-urethanes [94].



**Scheme 1.1** Synthesis of polyazomethine ether [82].

### 1.8.3 Applications

Because of wide range of fascinating properties, polyazomethines attracted the attention for applications in many fields, e.g. battery anodes or cathodes, semiconductors, energy storage and conversion devices and in integrated electro-optics for switching, displays, electroluminescence (EL) devices, non linear optical materials etc. [99-102].

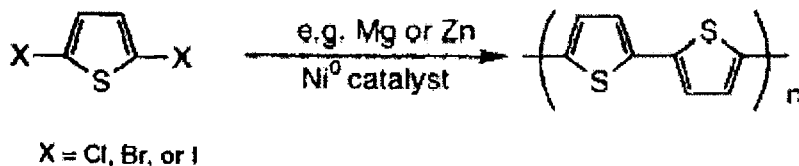
## 1.9 POLYTHIOPHENES

Polythiophenes are also an important class of conjugated polymers which are in general environmentally and thermally stable materials. Pure polythiophene without side chains is neither soluble nor fusible. However side chains which give solubility and fusibility to the polymer can be attached to the repeating unit [103-110]. Polymerization of thiophenes can be carried out in many ways and they have recently been excellently described by R. D. McCullough [107].

### 1.9.1 Synthesis of Polythiophenes

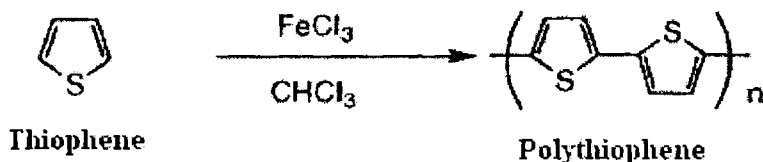
#### 1.9.1.1 Chemical synthesis of unsubstituted polythiophenes

One of the first chemical preparations of unsubstituted polythiophene (PTH) was reported in 1980 by two groups [108,109]. Both synthesized polythiophene by metal-catalyzed polycondensation of 2,5-dibromothiophene (Scheme 1.2).



**Scheme 1.2 Synthesis of polythiophene by polycondensation dehalogenation reaction.**

Sugimoto [111] described a very simple and effective synthesis of polythiophene by treating thiophene with  $\text{FeCl}_3$  (Scheme 1.3).



**Scheme 1.3** Synthesis of polythiophene by oxidative polymerization reaction.

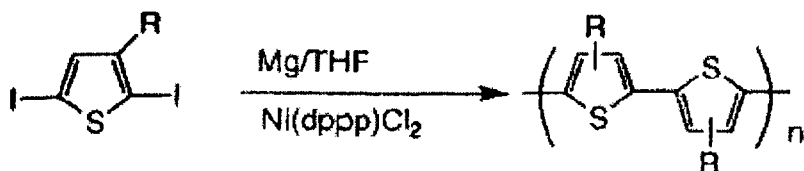
Systematic studies of the polymerization of 2, 5-dihalo thiophene have been performed by Yamamoto's group [110-114] and also by others [115-117]. Berlin and coworkers have reported the treatment of thiophene with butyl lithium to give 2, 5-dilithio thiophene that can be polymerized with  $\text{CuCl}_2$  [118] to form polythiophenes.

#### *1.9.1.2 Chemical synthesis of polyalkylthiophenes (PATs)*

The first chemical synthesis of environmentally stable and soluble poly (3-alkylthiophenes) (PATs) [119] was reported by Elsenbaumer and co-workers in 1985. Very shortly after this report, other groups [120-121] also reported both the chemical and electrochemical preparation of PATs.

#### *1.9.1.3 Metal-catalyzed cross-coupling polymerizations*

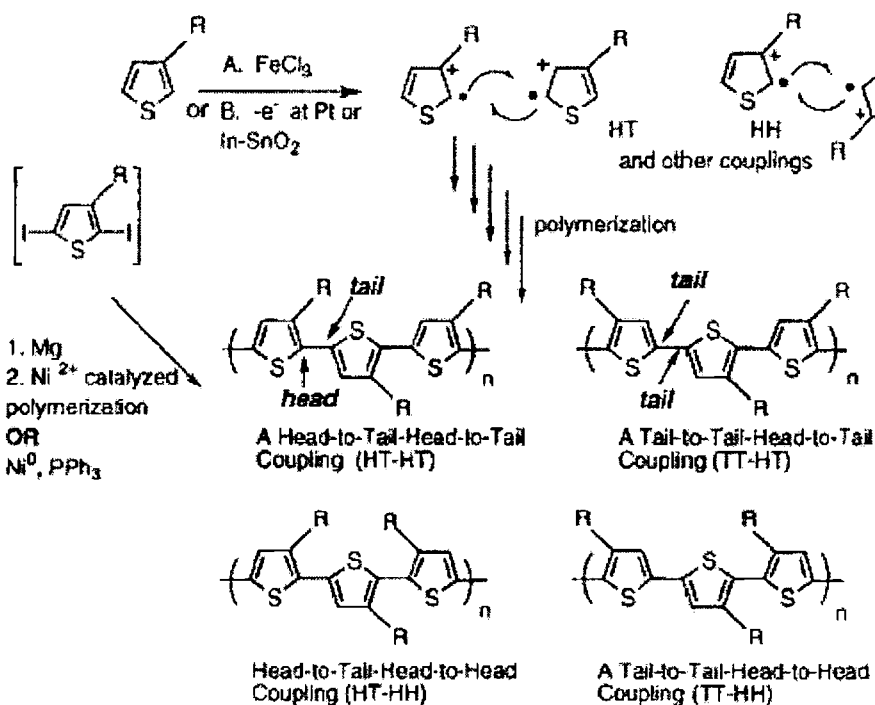
Polyalkyl thiophenes were prepared by Kumada cross coupling reaction [119] where, 5-diiodo-3-alkylthiophene is treated with one equivalent of Mg in THF, generating a mixture of Grignard species [107,123]. A catalytic amount of  $\text{Ni}(\text{dppp})\text{Cl}_2$  is then added and the polymer is generated by a halo-Grignard coupling reaction (Scheme 1.4).



**Scheme 1.4** Poly (alkyl thiophenes) from cross coupling polymerization.

#### 1.9.1.4 FeCl<sub>3</sub> method for the polymerization of PATs

Sugimoto et al. [124] reported in 1986 a very simple method to prepare PATs. The monomer, 3-alkylthiophene, is dissolved in chloroform and oxidatively polymerized with FeCl<sub>3</sub> [119,125,126], MoCl<sub>5</sub>, or RuCl<sub>3</sub> [111]. The FeCl<sub>3</sub> method does not appear to generate 2, 4-couplings in PATs [107]. The Finnish company; Neste Oy has reported a mechanism of the FeCl<sub>3</sub> synthesis of PATs [127]. The FeCl<sub>3</sub> initiates an oxidation of the alkylthiophene to produce radical centres predominantly at the 2- and 5- positions of thiophene, which propagate to form polymer (Scheme 1.5).



**Scheme 1.5 Mechanism of PAT synthesis by  $\text{FeCl}_3$  route and the possible regiochemical couplings possible in polyalkyl thiophenes.**

### 1.9.1.5 Electrochemical polymerization

The electrochemical polymerization is usually done by electrochemical oxidation of thiophene on a Pt-coated substrate to obtain a thin uniform film. Pt is selected because it is inert against the polymerization reaction at the relatively high oxidation potential of thiophene. Metallic gold (Au) and silver (Ag) nanowire arrays coated with polythiophene (PTH) films were fabricated by successive electrochemical depositions of PTH and metal into the pores of a micro porous alumina membrane [128].



### **1.9.2 Regioregular poly alkyl thiophenes (PAT)**

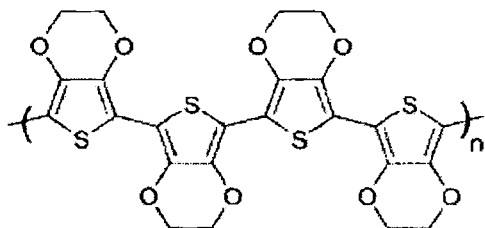
It is important to point out that the methods discussed above produce irregular PATs with no regional chemical control. Polymerisation leads to a mixture of four chemically distinct triad regioisomers when 3-substituted (asymmetric) thiophene monomers are employed [129]. Irregularly substituted polythiophenes have structures where unfavourable head-head (H-H) couplings cause a sterically driven twist of thiophene rings, resulting in a loss of conjugation. On the other hand, regioregular, head-to-tail (H-T) poly (3-substituted) thiophene can easily access a low energy planar conformation, leading to highly conjugated polymers. The first synthesis of regioregular head-to-tail coupled poly (3-alkylthiophenes) (PATs) was reported by McCullough and Lowe [130] early in 1992. The PATs synthesized by this method contain ~100% HT-HT couplings.

### **1.9.3 Applications**

Polythiophenes are potential candidates to be used as electrical conductors, nonlinear optical devices, polymer LEDs, electro chromic or smart windows, photoresists, antistatic coatings, sensors, batteries, electromagnetic shielding materials, artificial noses and muscles, solar cells, electrodes, microwave absorbing materials, new types of memory devices, nanoswitches, optical modulators and valves, imaging materials, polymer electronic interconnects, nanoelectronic and optical devices, and transistors [103-106,131-133].

## 1.10 POLY (3, 4-ETHYLENEDIOXYTHIOPHENE) - PEDOT

During the second half of the 1980s, scientists at the Bayer AG research laboratories in Germany developed a new polythiophene derivative, poly (3, 4-ethylenedioxythiophene) [134-138], having the backbone structure shown below.



PEDOT was initially found to be an insoluble polymer, yet exhibited some very interesting properties. In addition to a very high conductivity (ca. 300 S/cm), PEDOT was found to be almost transparent in thin, oxidized films and showed a very high stability in the oxidized state [134-139].

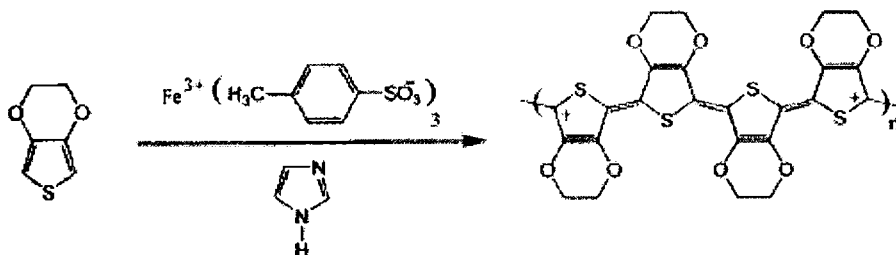
### 1.10.1 Synthesis of Poly (3, 4-Ethylenedioxythiophene)s

The synthesis of PEDOT derivatives can be divided into three different types of polymerization reactions:

- Oxidative chemical polymerization of the EDOT-based monomers.
- Electrochemical polymerization of the EDOT-based monomers.
- Transition metal mediated coupling of dihalo derivatives of EDOT.

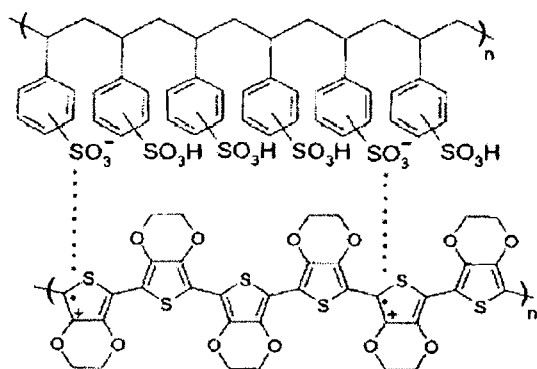
### 1.10.1.1 Oxidative chemical polymerization of the EDOT-based monomers

Chemical polymerization of EDOT derivatives can be carried out using several methods and oxidants [131,152,153]. Another polymerization method of EDOT has been reported by de Leeuw et.al [154] utilizing  $\text{Fe}_3(\text{OTs})_3$  at elevated temperature in combination with imidazole as a base (Scheme 1.6). PEDOT prepared by chemical oxidative method exhibited conductivities of up to 550 S/cm [155-156].



**Scheme 1.6** Chemical oxidative polymerization of EDOT [154].

The third, and most practically useful, polymerization method for EDOT is the so-called BAYTRON P synthesis that was developed at Bayer AG [157-160]. This method utilizes the polymerization of EDOT in an aqueous polyelectrolyte (most commonly PSS) solution using  $\text{Na}_2\text{S}_2\text{O}_8$  as the oxidizing agent. Carrying this reaction out at room temperature results in a dark blue, aqueous PEDOT/PSS dispersion, which is commercially available from Bayer AG under its trade name BAYTRON P (Figure 1.14). An interesting aspect of BAYTRON P is that, after drying, the remaining PEDOT/PSS film is highly conducting, transparent, mechanically durable, and insoluble in any common solvent [140-143] and has found several applications [121,144-151].



**Figure 1.14 PEDOT/PSS blend (BAYTRON P).**

#### *1.10.1.2 Electrochemical polymerization of EDOT derivatives*

Another especially useful polymerization method utilizes electrochemical oxidation of the electron-rich EDOT-based monomers. This method stands out as it requires only small amounts of monomer, short polymerization times, and can yield both electrode-supported and freestanding films. Electrochemical polymerization results in the formation of a highly transmissive sky-blue, doped PEDOT film at the anode [150,161]. A variety of electrolytes are compatible with EDOT-derivative polymerization, including polyelectrolytes, as was nicely demonstrated by Wernet and co-workers, or using an aqueous micellar medium [162-163].

#### *1.10.1.3 Transition metal mediated coupling of dihalo derivatives of EDOT*

Many thiophene-based polymers have been prepared over the years using transition metal catalyzed coupling of activated organometallic derivatives. Yamamoto et al.

recently applied this methodology to the direct formation of neutral PEDOT [144]. Prolonged storage (~2 years) or gentle heating (50-80°C) of crystalline 2, 5-dibromo-3, 4- ethylene dioxy thiophene affords a highly conducting, bromine-doped PEDOT. Using this approach, thin films of PEDOT with conductivity as high as 20 S/cm were fabricated on insulating flexible plastic surfaces [164].

### **1.10.2 Applications of PEDOT**

PEDOT-based polymers are applied in many applications like through-hole plating of printed circuit boards, antistatic coatings for cathode ray tubes to prevent dust attraction, primers for electrostatic spray coating of plastics, hole-injecting layers on ITO substrates for organic electroluminescent devices, transparent electrodes for inorganic electroluminescent devices, sensors, rechargeable batteries, cathode radiation tubes, photodiodes, electro-chromic windows, corrosion protection, and photovoltaic devices. Of utmost importance, these examples show that PEDOT is one of the few organic conducting polymers that have successfully found its way from a laboratory curiosity into multiple technical applications [144,169-178].

## **1.11 POLYANILINE**

Due to its ease of synthesis and processing, environmental stability, relatively high conductivity and cost economics, polyaniline is probably the most industrially important conducting polymer today [179-181]. With the extent of doping polyaniline can have four different oxidation states [182-186] like Leucomeraldine base (LEB), Emeraldine (EB), Emeraldine salt (ES) and Pernigraniline (PNB).

Polyaniline can be synthesized mainly by chemical or electrochemical oxidation of aniline under acidic conditions. The method of synthesis depends on the intended application of the polymer. For bulk production chemical method is preferred where as for thin films and better patterns, electrochemical method is preferred.

### **1.11.1 Synthesis of polyanilines**

#### *1.11.1.1 Chemical synthesis*

The conventional method of synthesis of emeraldine salt is the emulsion polymerization of aniline monomer in aqueous media in presence of a mineral acid like HCl [181, 187-190]. An oxidant like ammonium per sulphate or potassium dichromate can be used to initiate the reaction [191- 193]. The ideal molar ratio of monomer to acid to oxidizing agent is proved to be 1: 1: 1 [194, 195]. The aniline salt of protonic acid in the protonic acid medium is mixed with aqueous solution of ammonium per sulphate with a continuous stirring for 4 hrs. The precipitate obtained is then filtered and washed with distilled water so as to obtain emeraldine salt. The principle function of the oxidant is to withdraw a proton from the aniline monomer.

#### *1.11.1.2 Electrochemical synthesis*

Electrochemical polymerization is a radical combination reaction and is diffusion controlled. The anodic oxidative polymerization is the preferable method to obtain a clean and better-ordered polymer as a thin film. Electrochemical synthesis is achieved by:

1. Galvanostatic method
2. Potentiostatic method

### 3. Potential sweep method

Electrochemical reaction is carried out by dissolving 0.1 mole of protonic acid in distilled water at platinum electrode. The first step in the oxidation of aniline is the formation of a radical cation, which is independent of pH. Mohilner et.al [196] classified the oxidation of aniline as an ECE reaction (a succession of rapid electrochemical–chemical–electrochemical reactions). The colour changes observed with polyaniline are yellow ( $-0.2$  V), blue ( $0.0$  V) and green ( $0.65$  V), which are associated with different oxidation states (doping levels).

#### **1.11.2 Applications**

PANI's conductivity can be reversibly controlled either electrochemically (by oxidation–reduction) or chemically (by protonation/ deprotonation), and conductivity increases with doping from the undoped insulating base form to fully doped conducting acid form. PANI with different forms find different uses like leucoemeraldine — the completely reduced form find applications in electrochromic devices and in Li–PANI batteries; pernigraniline is used for non-linear optics while emeraldine base consisting of 50% reduced and 50% oxidised moieties is used in HCl sensors and for making thin films. Other applications of conducting PANI include electrostatic charge dissipation, electromagnetic interference, anticorrosion coating, light emitting diodes and batteries. Recently the protonation of PANI with organic sulphonic acids and macromolecules has been reported for the preparation of electrically conducting polymers with improved processability [184–187] for making conductive blends and composites for various applications. While Shacklette et al. [188] have developed a surface–core doping process in which PANI is predominately doped with one acid at the core of a particle and a second dopant predominately at the surface just to achieve increased

compatibility between the PANI particles and a second polymer matrix e.g. Nylon, polystyrene (PS), low density polyethylene (LDPE).

## **1.12 DESIGN OF EXPERIMENTS (DOE)**

DOE is a formal mathematical method for systematically planning and conducting scientific studies that change experimental variables together in order to determine their effect of a given response. It makes controlled changes to input variables in order to gain maximum amounts of information on cause and effect relationships with a minimum sample size. It generates information on the effect various factors have on a response variable and in some cases may be able to determine optimal settings for those factors. Application of Design of experiments leads to an understanding of the often complex relationship between the input parameters and the output. In the last half century, statisticians have devoted immense effort to the construction and study of layouts for experiments, with various criteria defined for improving the efficiency of designs [197,198].

Some of the important DOE methods are

- Taguchi
- Box Behnken
- Central composite circumscribed
- Central composite faced
- D-Optimal designs
- Response surface methods etc.

### **1.12.1 Taguchi method**

Dr. Genichi Taguchi of Japan modified the classical DOE approach using 'orthogonal arrays' to improve the quality of a process / product. The various steps in the Taguchi method include:



- Identification of main function, noise factors and objective function to be optimized
- Choice of control factors and their levels [199,200]
- Conduction of experiments based on orthogonal arrays
- Generation of factor effect plots and selection of optimum combination of control factors
- Conduction of a verification experiment and
- Recommendation of suitable parameter settings to produce acceptable products.

The Taguchi design is widely used in the polymer industry for optimizing polymerization conditions, tyre cord properties, composition of blends, injection molding parameters, etc. [201-203].

### **1.12.2 Orthogonal array**

Orthogonal Arrays are special experimental designs that require only a small number of trials to discover main factors. It is nothing but a fractional factorial matrix, which assures balanced comparison of levels of any factor or interaction of factors. It is a matrix of numbers arranged in rows and columns. In orthogonal array, columns are mutually orthogonal. That is, for any pair of columns all combination of factor levels occurs and they occur at equal number of times. The number of columns of an orthogonal array represents the maximum number of factors that can be studied using that array. Among the various designs, the orthogonal array introduced by C. R. Rao in the forties [200] has been studied widely and is now recognized as a fundamental component in the statistical design of experiments. It has also been popularized, in particular, by its application in Taguchi methods [204,205].

The orthogonal array specified by Taguchi has certain standard arrays. Some of the standard orthogonal arrays are

- $L_4(2^3)$  : 4 experiments, 2 levels and 3 columns
- $L_8(2^7)$  : 8 experiments, 2 levels and 7 columns
- $L_{18}(2^1 \cdot 3^7)$  : 18 experiments, 3 levels and 8 columns

A typical orthogonal array is shown in the Table 1.1

**Table 1.1 Standard  $L_4$  orthogonal array**

Experiment	Columns		
	1	2	3
1	1	1	1
2	1	2	2
3	2	1	2
4	2	2	1

### 1.13 SCOPE AND OBJECTIVES OF THE WORK

The evaluation of microwave properties of conducting polymers has not been exhaustive. Some studies have been done in polyaniline, polypyrrole and to a lesser extent on polythiophenes. So in this study the microwave properties of four important conducting polymers belonging to polyaniline polythiophene and polyazomethine families are proposed to be explored. Polyazomethines are particularly attractive because they show good mechanical strength, thermal stability, nonlinear optical properties, and photoconductivity. Polyanilines and polythiophenes have been extensively studied for a great number of applications

and are used in many commercial fields. Design of experiments technique has been used in polycondensation reaction and this has helped to reduce the number of trials required to produce an optimum product with lowest cost.

One of the major drawbacks of conducting polymers is their poor processability, and this problem is proposed to be addressed in this investigation. Preparation of composites of conducting polymers has been found to improve the processability. These composites can also improve the mechanical properties and physical characteristics. Conducting polymer/ thermoplastic composites are proposed to be prepared by the insitu polymerization method to develop it as a semi IPN and hence reduce the phase separation.

The major objective of the study is to develop a processable thermoplastic conducting composite suitable for EMI shielding and microwave absorption. To achieve this, the electrical and microwave properties of conducting polymers like poly para phenylene diazomethine, polythiophene, polyaniline and that of poly (3, 4-ethylenedioxythiophene) (PEDOT) are proposed to be evaluated and compared. The polymers showing better microwave properties will be selected for further study. To improve the processability of these conducting polymers, their composites with thermoplastics are proposed to be developed. Microwave and electrical properties of these composites have to be evaluated and the most suitable composite will be selected for application studies. The most promising composite will be considered for EMI shielding and microwave absorption applications. An important objective of the work is the development of a processable conducting composite with very good electrical, mechanical and microwave properties which can be easily cast or coated on various surfaces.

The objectives of the study are summarized as

1. To optimize the polycondensation reaction conditions to prepare polyparaphenylene diazomethane (PPDA) using Taguchi Design of Experiments.
2. To synthesize polythiophene (PTH) and Poly(3,4-ethylenedioxythiophene) (PEDOT).
3. To characterize PPDA, PTH and PEDOT using FTIR, TGA and DSC.
4. To evaluate and compare the microwave properties like dielectric constant, dielectric loss, conductivity, absorption coefficient, heating coefficient, loss tangent and skin depth of PPDA, PTH, PEDOT and Polyaniline (PANI).
5. To optimize the ratio of  $\text{FeCl}_3$  : Thiophene in preparing the insitu PTH-PVC composite.
6. To study the effect of drying condition on the microwave properties of PTH-PVC composite.
7. To prepare thermoplastic conducting polymer composites like PTH-PVC, PEDOT-PVC, PANI-PVC, PPDA-PVC, PANI-PU and PEDOT-PU.
8. To evaluate and compare the microwave properties of these thermoplastic conducting polymer composites for electrical and microwave applications. To select the most promising composite based on the electrical and microwave properties.

9. To study the EMI shielding and microwave absorption applications of the selected thermoplastic composite.

## **1.14 METHODOLOGY**

The methodology proposed to be adopted to achieve the above objectives is detailed below.

### ***Step-I Synthesis and characterization of PPDA:***

A novel polyazomethine, PPDA, is proposed to be prepared by the condensation polymerization of para phenylene diamine and glyoxal trimeric dihydrate. The optimum reaction conditions will be determined by design of experiments. The prepared polymer has to be characterized by DSC, TGA and FTIR methods.

### ***Step-II Synthesis and characterization of polythiophene:***

Polythiophene is proposed to be prepared by chemical oxidative polymerization of thiophene with  $\text{FeCl}_3$ . The prepared polymer has to be characterized by DSC, TGA and FTIR methods.

### ***Step-III Synthesis and characterization of PEDOT:***

Poly (3, 4-ethylenedioxythiophene) is proposed to be prepared in DBSA micellar solution using  $\text{FeCl}_3$  as the oxidant. This method has reported to give PEDOT nanoparticles with very high conductivity [206]. The prepared polymer will be characterized by DSC, TGA and FTIR methods.

***Step-IV Evaluation of microwave and electrical properties of the conducting polymers:***

DC conductivity of the polymers is proposed to be evaluated using Kiethley nanovoltmeter and microwave properties like dielectric constant, dielectric loss, conductivity, absorption coefficient, heating coefficient, loss tangent and skin depth of PPDA, PTH, PEDOT and Polyaniline (PANI) will be evaluated using cavity perturbation technique.

***Step-V Optimization of the preparation conditions for PVC- PTH composites:***

PVC-PTH composites will be prepared by polymerizing dispersed thiophene in PVC solution using chemical oxidative technique (in situ polymerization). The conditions for the preparation of PVC-PTH composite are to be optimized based on optimum microwave properties. The ratio of FeCl<sub>3</sub>: Thiophene ratio for the insitu polymerization and the optimum casting conditions will be determined.

***Step-VI Preparation of selected thermoplastic conducting composites:***

Thermoplastic conducting composites like PTH-PVC, PEDOT-PVC, PANI-PVC, PPDA-PVC, PANI-PU and PEDOT-PU are proposed to be prepared by in situ polymerization technique as mentioned in Step V.

***Step-VII Selection of the appropriate thermoplastic conducting composite for microwave applications:***

The microwave and electrical properties of the various conducting composites will be evaluated and compared. The most suitable composite is to be selected for microwave and electrical application study.

***Step-VIII EMI shielding and microwave absorption behavior of the selected composite:***

Due to  $\text{FeCl}_3$  content in the films, it was noted that the composites may absorb moisture on storage. To rectify this effect benzyl peroxide is proposed to be used as oxidant for the polymerization instead of  $\text{FeCl}_3$ . The EMI shielding and microwave absorption property of PU-PANI composite will be evaluated at S and X bands of microwave frequency and potential applications has to be discussed.

### 1.15 REFERENCES

1. V. Saxena, B.D. Malhotra, *Current Applied Physics*, **3**, (2003) 293–305.
2. Alan G. MacDiarmid, *Angewandte Chemie*, International Edition, **40**, Issue **14**, (2001) 2581 – 2590.
3. Chen et al, *Appl. Phys. Lett.*, **80**, No. **13**, (2002) 2308-2310.
4. V. Saxena, V. Shirodkar, *J. Appl. Polym. Sci.*, **77**, (2001) 1050.
5. Tarushee Ahuja, Irfan Ahmad Mir, Devendra Kumar, Rajesh, *Biomaterials*, **28**, (2007) 791–805.
6. Sharma, B.D Malhotra, *J Appl Polym Science*, **81**, (2001) 1460–1466.
7. Sharma, B.D Malhotra, *Appl Biochem Biotechnol*, **96**, (2001) 155–165.
8. Sharma, R.Singhal, A.Kumar, Rajesh, K.K Pande, B.D Malhotra, *J. Appl Polymer Science*, **91**, (2004) 3999–4006.
9. R. H. Friend, *Pure Appl. Chem.*, **73**, No. **3**, (2001) 425–430.
10. M. Angelopoulos, *IBM J. Res. & Dev.*, **45**, No. **1**, (2001) 57-75.
11. James Margolis, *Conductive Polymers and Plastics*, Chapman and Hall, (1989) 33.
12. W. R. Salaneck, D. T. Clark and E. J. Samuelsen, *Science and Application of Conducting Polymers*, IOP Publishing (1991) 168.
13. F. J. Touwslager, N. P. Willard, and D. M. de Leeuw, *Applied Physics Letters*, **81**, Issue **24**, (2002) 4556-4558.
14. Aleksandr Noy et al., *Nano Lett.*, **2**, No. **2**, (2002) 109-112.
15. Akif Kaynak, *Fibers and Polymers*, **2**, No.4, (2001) 171-177.
16. S.K. Dhawan, N.Singh, S. Venkatachalam, *Synthetic Metals*, **129**, Number **3**, (2002) 261-267.
17. Narayan Chandra Das, Shinichi Yamazaki, Masamichi Hikosaka, Tapan Kumar Chaki, Dipak Khastgir, Ajay Chakraborty, *Polymer International*, **54**, Number **2**, (2005) 256-259.



18. Mihaela Baibarac, Gómez-Romero, Pedro, *Journal of Nanoscience and Nanotechnology*, **6**, Number **2**, (2006) 289-302.
19. R.L. Greene, G.B. Street and L.J. Sutude, *Phys. Rev. Lett.*, **34**, 577 (1975) 577.
20. H. Shirakawa, E.J. Louis, A.G. MacDiarmid, C.K. Chiang, A.J. Heeger and J.T.A. Skotheim, *Handbook of Conducting Polymers*, 2<sup>nd</sup> Ed., Marcel Dekker, New York, **1-2**, (1986).
21. Irina Schwendeman *et al*, *Adv. Mater.*, **13**, No. **9**, (2001) 634-637.
22. J.M.Lupton, I. D. W. Samuel and P. L. Burn, *Physical Review B* **66**, **15**, (2002) 206.
23. Hongchao Li and Christoph Lambert, *J. Mater. Chem.*, **15**, (2005) 1235 – 1237.
24. N.Mott, *Conduction in Non-Crystalline Materials*, Oxford, Clarendon Press, (1987).
25. J .Aguilar Hernández *et al*, *J. Phys. D: Appl. Phys.*, **34**, (2001) 1700-1711.
26. Annette.J.Nuendorf, “High Pressure Synthesis of Conducting Polymers”, PhD Thesis, Griffith University, (2003).
27. P.Sheng, *Physical Review B*, **21**, No. **6**, (1980) 2180-2195.
28. T.Schimmel, D.Glaser, M.Schwoerer, H.Naarmann, “Properties of Highly Conducting Polyacetylene”, *Conjugated Polymers*, J.L. Bredas and R. Silbey Ed., Netherlands: Kluwer Academic Publishers (1991).
29. E. Z. Kurmaev *et al*, *J. Phys.: Condens. Matter*, **13**, (2001) 3907-3912.
30. P Dutta *et al*, *J. Phys.: Condens. Matter*, **13**, (2001) 9187-9196.
31. T.C.Chung, J.H Kaufman, A.J. Heeger, F.Wudl, *Phys. Rev. B*, **30**, (1984) 702.
32. J.Brédas, R.Chance and R.Silbey, *Phys. Rev. B*, **26**, (1982) 5843.

33. Agilent Technologies, Inc., "Basics of Measuring the Dielectric Properties of Materials", Application Note, 2006 5989-2589EN (2006).
34. Hari Singh Nalwa, Handbook of Organic Conductive Molecules & Polymers, Vol.3, (Ed), John Wiley & Sons, (1997).
35. F. Kohlrausch, *Pogg. Ann. Phy.*, **119**, ( 1863) 352.
36. K.L Nagai, *Comments Solid State Physics*, **9**, (1980) 141.
37. R.J.Meakins, *Progress in Dielectrics*, Ed J.B.Birks, 3, Heywood London (1961).
38. K.J.Vinoy and R. M. Jha, Radar Absorbing Materials from Theory to Design and Characterization, Boston, Kluwer Academic Publishers, (1996).
39. P.Saville, Review of Radar Absorbing Materials. *DRDC Atlantic TM* 2005-003, DRDC Atlantic, (2005).
40. R.A.Stonier, "Stealth aircraft & Technology, From World War II to the Gulf - Part II: Applications and Design" *SAMPE Journal*, **27**, No.5, September/October (1991).
41. J. Sheen, *Measurement*, **37**, (2005) 123–130.
42. D. V. Blackham, R. D. Pollard, "An Improved Technique for Permittivity Measurements Using a Coaxial Probe", *IEEE Trans. on Instr. Meas.*, **46**, No 5, Oct. (1997) 1093- 1099.
43. Meng, J. Booske, and R. Cooper, "Extended cavity perturbation technique to determine the complex permittivity of the dielectric materials," *IEEE Trans. Microwave Theory Tech.*, **43**, (1995) 2633–2636.
44. J.K.Vaid, A. Prakash, and A. Mansingh, "Measurement of dielectric parameters at microwave frequencies by cavity perturbation technique," *IEEE Trans. Microwave Theory Tech.*, **27**, (1979) 791–795.

45. Qian and W. B. Dou, "A new approach for measuring permittivity of dielectric materials," *Journal Electromagnetic Wave and Applications*, **19**, (2005) 795–810.
46. Bogle, M. Havrilla, D. Nyquis, L. Kempel, and E. Rothwell, "Electromagnetic material characterization using a partially filled rectangular waveguide," *Journal Electromagnetic Wave and Applications*, **19**, (2005) 1291–1306.
47. J.A.Roumeliotis, *Journal Electromagnetic Wave and Applications*, **11**, (1997) 185–195.
48. R.G. Carter, "Accuracy of microwave cavity perturbation measurements", *IEEE Trans. Microwave Theory Tech.*, **49**, (2001) 918–923.
49. Kumar and S. Sharma, *Progress In Electromagnetics Research*, PIER, **69**, (2007) 47–54.
50. K.Kupfer, A.Kraszewski, and R.Kno"chel, "RF & Microwave Sensing of Moist Materials, Food and other Dielectrics", *Sensors Update*, **7**, Wiley-VCH, Germany, (2000) 186–209.
51. S.B. Kumar et al., *Journal of the European Ceramic Society*, **21**, (2001) 2677–2680.
52. R.Coccioli, G. Pelosi, and S. Selleri, "Characterization of dielectric materials with the finite element method", *IEEE Trans. Microwave Theory Tech.*, **47**, (1999) 1106–1111.
53. R.A.Waldron, "Perturbation theory of resonant cavities," *Proc.IEEE*, **170C**, (1960) 272–274.
54. Akif Kaynak, *Fibers and Polymers*, **2**, No.4, (2001) 171-177.
55. S.K. Dhawan, N.Singh, S. Venkatachalam, *Synthetic Metals*, **129**, Number 3, (2002) 261-267.

56. Narayan Chandra Das, Shinichi Yamazaki, Masamichi Hikosaka, Tapan Kumar Chaki, Dipak Khastgir, Ajay Chakraborty, *Polymer International*, **54**, Number 2, (2005) 256-259.
57. Mihaela Baibarac, Gómez-Romero, Pedro, *Journal of Nanoscience and Nanotechnology*, **6**, Number 2, (2006) 289-302.
58. Alan Barnes, Rong Zhang, Peter V. Wright, Barry Chambers, "Smart Structures and Materials", *Proceedings of the SPIE*, **5055**, (2003) 364-375.
59. H. Rmili, J.L. Miane, H. Zangar and T.E. Olinga, *Eur. Phys. J. Appl. Phys.*, **29**, (2005) 65-72.
60. G.Dicker, M.P. de Haas, L.D.A. Siebbeles, J.M. Warman, *Physical Review B*, **70**, (2004).
61. Jozef Sláma, Mária Papánová, Anna Grusková, Rastislav Dosoudil, Marianna Ušáková, *Czechoslovak Journal of Physics*, **54**, Supplement 1, (2004) 667-670.
62. Thirumalizai Bhoopathy, Annamalai Anandavadivel, *Materials Research Innovations*, **6**, Numbers 5-6, (2002) 242-246.
63. Christian Brosseau, Patrick Quéffélec, and Philippe Talbot, *Journal of Applied Physics*, **89**, Issue 8, (2001) 4532-4540.
64. Roselena Faez, Inácio M. Martin, Marco-A De Paoli, Mirabel C. Rezende, *Journal of Applied Polymer Science*, **83**, Issue 7, (2001) 1568 – 1575.
65. Yuping Duan, Shunhua Liu, Bin Wen, Hongtao Guan and Guiqin Wang, *Journal of Composite Materials*, **40**, No. 20, (2006) 1841-1851.
66. N. C. Das, D. Khastgir, T. K. Chaki and A. Chakraborty, *Journal of Elastomers and Plastics*, **34**, No. 3, (2002) 199-223.
67. R. Kotsilkova, D. Nesheva, I. Nedkov, E. Krusteva, S. Stavrev, *Journal of Applied Polymer Science*, **92**, Issue 4, (2004) 2220 – 2227.

68. Kyung Wha Oh, Seong Hun Kim, Eun Ae Kim, *Journal of Applied Polymer Science*, **81**, Issue 3, (2001) 684 – 694.
69. Sylvain Fauveaux and Jean-Louis Miane, *Electromagnetics*, Taylor & Francis, **23**, Number 8, (2003) 617 - 627.
70. Honey John, Rinku M. Thomas, K. T. Mathew, Rani Joseph, *Journal of Applied Polymer Science*, **92**, Issue 1, (2004) 592 – 598.
71. H.John, S.Bijukumar, K.T.Mathew, Rani Joseph, *Plastics, Rubber and Composites*, **32**, No. 7, (2003) 306-312.
72. R. Kotsilkova , D. Nesheva, I. Nedkov , E. Krusteva , S. Stavrev , *J Appl Polym Sci.*, **92**, No. 4, (2004) 2220-2227.
73. C.I.Simionescu, M.Grigoras, I.Cianga and N.Olaru, *Eur. Polym. J*, Vol. **34**, No. 7, (1998) 891-898.
74. Claude Chevrot, Thierry Henri, *Synthetic Metals*, **118**, (2001) 157-166.
75. Maarib A. Khalid, Ali G.El-Shekeil, Fatma A, Al-Yusufy, *European Polymer Journal*, **37**, (2001) 1423-1431.
76. J.A.Puertolas, E.Carod, R.Diaz-Calleja, P.Cerrada, L.Oriol, M.Pinol, J.L.Serrano, *Macromolecules*, **30**, (1997) 773.
77. Haijun Niu, Yudong Huang, Xuduo Bai, Xin Li, Guiling Zhang, *Materials Chemistry and Physics*, **86**, (2004) 33–37.
78. Ali El-Shekeil, Mohammed Al-Khader, O.Abeer, Abu-Bakr, *Synthetic Metals*, **143**, (2004) 147–152.
79. Z.Hui, A.Gandini, *Eur Polym Journal*, **28**, (1992) 1461.
80. Y.Saegusa, T.Koshidawa, S.Nakamura, *Journal of Polymer Science Part A, Polymer Chemistry*, **30**, (1992) 1396.
81. P.K.Dutta, Pragya Jain, Pratima Sen, Rashmi Trivedi, P.K.Sen, Joydeep Dutta, *European Polymer Journal*, **39**, (2003) 1007–1011.
82. Sang Chul Suh, Sang Chul Shim, *Synthetic Metals*, **114**, (2000) 91–95.

83. T.Yoshimura, S.Tatsuura, W. Sotoyama, A. Matsuura, *Appl. Phys.Lett.*, **60**, (1992) 268.
84. M.S.Weaver, D.D.C.Bradley, *Synthetic Metals*, **83**, (1996) 61-66.
85. S. Tatsuura, W. Sotoyama et al., *Appl. Phys. Lett.*, **62**, (1993) 2182.
86. S. C. Ng, H. S. O. Chan, P. M. L. Wong, K. L. Tan and B. T. G. Tan, *Polymer*, **39**, No. **20**, (1998) 4963-4968.
87. J.M. Adella, M.P. Alonso, J. Barbera, L. Oriol, M. Pinola, J.L. Serrano, *Polymer*, **44**, (2003) 7829-7841.
88. G.Stoica, A.Stanciu, V.Cozan, A.Stoleriu, D.J.Timpu, *Macromol. Sci. Pure Appl. Chem .A*, **35**, (1998) 539.
89. Wang, L.Xiao, X.Han, D.Cai, Z.Mo Chin, *Chem. Lett*, **4**, (1993) 311.
90. C.J. Yang, S.A. Jenekhe, *Macromolecules*, **28**, (1995) 1180.
91. P.Cerrada, L.Oriol, M.Pinol, J.L.Serrano, P.J.Alonso, J.A. Puertolas, I. Iribarren, S.Munoz Guerra, *Macromolecules*, **32**, (1999) 3565.
92. J.Moulton, P.Smith, *Polymer*, **33**, (1992) 2340.
93. E.C. Buruiana, M. Olaru, B.C. Simionescu, *European Polymer Journal*, **38**, (2002) 1079-1086.
94. P.W. Morgan, S.L. Kwolek, C. Terry, *Macromolecules*, **20**, (1987) 729.
95. Catanescu, M. Grigoras, G. Colotin, A. Dobreanu, N. Hurduc, C.I. Simionescu, *Eur. Polym. Journal*, **37**, (2001) 2213.
96. Ribera, A. Manteco'n, A. Serra, *J. Polym. Sci., A, Polym. Chem*, **40**, (2002) 4344.
97. S.C. Suh, S.C.Shim, *Synthetic Metals*, **114**, No. **1**, (2000) 91-95.
98. Janusz Jaglarz et al, *Rev.Adv.Mate.Science*, **8**, (2004) 82-85.
99. Jarzabek et al, *Journal of Non-Crystalline Solids*, **352**, Issues **9-20**, (2006) 1660-1662.
100. Kamal I. Aly, Ali A. Khalaf, *Journal of Applied Polymer Science*, **77**, (2000) 1218-1229.

101. Mircea Grigoras, Nicoleta Cristina Antonoaia, *Polymer International*, **54**, Issue **12**, (2005) 1641-1646.
102. S. Tatsuura, W. Sotoyama T. Yoshimura, *Appl. Phys. Lett.*, **60**, (1992) 1661.
103. S. Geetha and D.C. Trivedi, *Synthetic Metals*, **155**, (2005) 232-239.
104. Binbin Xi, et al., *Polymer*, **47**, (2006) 7720-7725.
105. R.L.Patrick, Malenfant and M.J.Jean Fréchet, *Macromolecules*, **33**, No. **10**, (2000) 3634 -3640.
106. M.D.Levi et al., *Journal of the Electrochemical Society*, **147**, No.3, (2000) 1096-1104 .
107. R. D. McCullough, *Adv. Mater*, **10**, (1998) 93-116.
108. T. Yamamoto, K. Sanechika, A. Yamamoto, *J. Polym. Sci., Polym Lett. Ed.*, **18**, (1980).
109. J. W. P. Lin, L. P. Dudek, *J. Polym. Sci., Polym. Chem. Ed.*, **18**, (1980) 2869.
110. Hiromasa Goto, Xiaoman Dai, Harunori Narihiro, and Kazuo Akagi, *Macromolecules*, **37**, No.7 (2004) 2353 -2362.
111. T. Yamamoto, K. Sanechika, A. Yamamoto, *Bull. Chem. Soc. Jpn.*, **56**, (1983) 1497.
112. T. Yamamoto, K. Osakada, T. Wakabayashi, A. Yamamoto, *Makromol. Chem., Rapid Commun.*, **6**, (1985) 671.
113. T. Yamamoto, A. Morita, T. Maruyama, Z. H. Zhou, T. Kanbara, K. Saneckika, *Polym. J. (Tokyo)*, **22**, (1990) 187.
114. T. Yamamoto, T. Maruyama, Z. H. Zhou, Y. Miyazaki, T. Kanbara, K. Saneckika, *Synth. Metals*, **41**, (1991) 345.
115. C. Z. Hotz, P. Kovacic, I. A. Khoury, *J. Polym. Sci., Polym. Chem.*, **21**, (1983) 2617.

116. M. Kobayashi, J. Chen, T. C. Chung, F. Moraes, A. J. Heeger, F. Wudl, *Synth. Met.*, **9**, (1984) 77.
117. G.T.Colon, Kwiatkowski, *J. Polym. Sci., Polym. Chem.*, **28**, (1990) 367.
118. G.A.Berlin, F. Pagani, Sannicolo, *J. Chem. Soc., Chem. Commun.*, (1986) 1663.
119. K. Y. Jen, R. Oboodi, R. L. Elsenbaumer, *Polym. Mater. Sci. Eng.*, **53**, (1985) 79.
120. R. Sugimoto, S. Takeda, H. B. Gu, K. Yoshino, *Chem. Express*, **1**, (1986) 635.
121. M. Sato, S. Tanaka, K. Kaeriyama, *J. Chem. Soc., Chem. Commun.* (1986) 873.
122. S.Hotta, S.D.D.V. Rughooputh, A. J. Heeger, F. Wudl, *Macromolecules*, **20**, (1987) 212.
123. S. A. Chen, C. C. Tsai, *Macromolecules*, **26**, (1993) 2234.
124. K. Yoshino, S. Hayashi, R. Sugimoto, *Jpn. J. Appl. Phys.*, **23**, (1984) 899.
125. M. Leclerc, F. M. Diaz, G. Wegner, *Makromol. Chem.*, **190**, (1989) 3105.
126. M. Pomerantz, J. J. Tseng, H. Zhu, S. J. Sproull, J. R. Reynolds, R. Uitz, H. J. Arnott, H. I. Haider, *Synth. Met.*, **41-43**, (1991) 825.
127. V. M. Niemi, P. Knuutila, E. Osterholm, J. Korvola, *Polymer*, **33**, (1992) 1559.
128. Ballarin et al., *Synthetic Metals*, **114**, No.3, (2000) 279-285.
129. Jiaxin Zhang et al., *Journal of Material science*, **38**, No. 11, (2003) 2423-2427.
130. R. D. McCullough, R. D. Lowe, *J. Chem. Soc., Chem. Commun.*, **70**, (1992).
131. Zhipan Zhang, Fan Wang, Feng'en Chen, Gaoquan Shi, *Materials Letters*, **60**, (2006) 1039-1042.



132. C.Y. Wang, A.M. Ballantyne, S.B. Hall, C.O. Too, D.L. Officer and G.G. Wallace, *Journal of Power Sources*, **156**, Short communication, (2006) 610–614.
133. Cristina Pozo-Gonzalo et al., *J. Mater. Chem.*, **12**, (2002) 500–510.
134. X. Crispin et al., *Journal of Polymer Science: Part B: Polymer Physics*, **41**, (2003) 2561–2583.
135. J. Hwang and D. B. Tanner, *Physical Review B*, **67**, (2003) 115205.
136. Alexander Kros, A.J.M.Nico, Sommerdijk, J.M.Roeland, Nolte, *Sensors and Actuators B*, **106**, (2005) 289–295.
137. Dolores Caras-Quintero and Peter Bäuerle, *Chemical Communication, Communication* (2002) 2690-2691.
138. S. Moller, C. Perlov, W. Jackson, C. Taussig & St. R. Forrest, *Nature*, **426**, (2003) 166.
139. M. P. de Jong, L. J. Van IJzendoorn, and M. J. A. de Voigt, *Appl. Phys. Lett.*, Vol. **77**, No. **14**, (2000).
140. Ballarin et al., *Synthetic Metals*, **146**, (2004) 201–205.
141. Greczynski et al., *Journal of Electron spectroscopy and related Phenomena*, Vol.**121**, No.**1**, (2001) 1-17.
142. Dirk Hohnholz, Alan G. MacDiarmid, David M. Sarno and Wayne E. Jones, *Jr.Chem.Commun.*, (2001) 2444–2445.
143. Jonas, W. Krafft, B. Muys, *Macromol. Symp.*, **100**, (1995) 169.
144. L. Bert Groenendaal, Friedrich Jonas, Dieter Freitag, Harald Pielartzik, and John R. Reynolds, *Adv. Mater.*, **12**, No. **7**, (2000) 481-494.
145. DeLongchamp and P. T. Hammond, *Advanced Materials*, **13**, Issue **19**, (2001) 1455-1459.
146. S.K.M. Johnsson, *Synthetic Metals*, 10361, (2003) 1–10.
147. Bayer AG, *US Patent* 5792558, (1996).

148. Kros, S. W. F. M. van Hövell, N. A. J. M. Sommerdijk, R. J. M. Nolte, *Advanced Materials*, **13** No. **20**, (2001) 1555-1557.
149. J. Hupe, G. D. Wolf, F. Jonas, *Galvanotechnik*, **86**, (1995) 3404.
150. Jonas, J. T. Morrison, *Synth. Met.*, **85**, (1997) 1397.
151. K. Lerch, F. Jonas, M. Linke, *J. Chem. Phys.*, **95**, (1997) 1506.
152. Y.S. Jeong, H. Goto, J.R. Reynolds and K. Akagi, *Current Applied Physics*, **6**, Issue **5**, (2006) 956-959.
153. Vadivel Murugan, C.W. Kwon, G. Campet, B. B. Kale, *Active and Passive Electronic Components*, **26**, Number **2**, (2003) 81-86.
154. Q. Pei, G. Zuccarello, M. Ahlskog, O. Ingan, *Polymer*, **35**, (1994) 1347.
155. D. M. de Leeuw, P. A. Kraakman, P. F. G. Bongaerts, C. M. J. Mutsaers, D. B. M. Klaassen, *Synth. Met.*, **66**, (1994) 263.
156. L. A. A. Pettersson, F. Carlsson, O. Ingan, H. Arwin, *Thin Solid Films*, **356**, (1998) 313-314.
157. L. A. A. Pettersson, T. Johansson, F. Carlsson, H. Arwin, O. Ingans, *Synth. Met.*, **101**, (1999) 198.
158. Bayer AG, *Eur. Patent* 440 957, (1991).
159. Bayer AG, *Eur. Patent* 686 662, (1995).
160. Bayer AG, *US Patent* 5 792 558, (1996).
161. Jonas, J. T. Morrison, *Synth. Met.*, **85**, (1997) 1397.
162. Q. Pei et al., *Polymer*, **35**, (1994) 1347.
163. X. Chen, K. Z. Xing, O. Ingans, *Chem. Mater.*, **8**, (1996) 2439.
164. Yamato, K. Kai, M. Ohwa, T. Asakura, T. Koshiba, W. Wernet, *Synth. Met.*, **83**, (1996) 125.
165. Hong Meng et al., *J. Am. Chem. Soc.*, **125**, Number **49**, (2003) 15151 - 15162.
166. Y. Kudoh, K. Akami, Y. Matsuya, *Synth. Met.*, **98**, (1998) 65.
167. Bayer AG, *Eur. Patent* 821025472, (1999) 103.

168. Y. Kudoh, K. Akami, Y. Matsuya, *Synth. Met.*, **102**, (1999) 973.
169. S. Ghosh, O. Ingans, *Adv. Mater.*, **11**, (1999) 1214.
170. F. Larmat, J. R. Reynolds, Y. J. Qiu, *Synth. Met.*, **79**, (1996) 229.
171. Matsushita Electric Ind. Co., *Japanese Patent* JP 10 308 116, (1998).
172. Bayer AG, *Eur. Patent* 553 671, (1993).
173. D.M. de Leeuw, P. A. Kraakman, P. F. G. Bongaerts, C. M. J. Mutsaers, *Synthetic Metals*, **66**, (1994) 263.
174. C. Liederbaum, Y. Croonen, P. van de Weijer, J. Vleggaar, H. Schoo, *Synthetic Metals*, **91** (1997) 109.
175. J. S. Kim, M. Granström, R. H. Friend, N. Johansson, W. R. Salaneck, R. Daik, W. J. Feast, F. Cacialli, *J. Appl. Phys.*, **84**, (1998) 6859.
176. J. S. Kim, F. Cacialli, M. Granström, R. H. Friend, N. Johansson, R. Salaneck, R. Daik, W. J. Feast, *Synth. Met.*, **101**, (1999) 111.
177. J. S. Kim, F. Cacialli, R. H. Friend, R. Daik, W. J. Feast, *Synth. Met.*, **102**, (1999) 1065.
178. Bayer AG, *Eur. Patent* 686662 (1995).
179. J.Y. Shimano and A.G. MacDiarmid, *Synth. Met.*, **123**, (2001), 251.
180. E.M. Genies, A. Boyd, M. Lapkowski and C. Trintavis, *Synth. Met.*, **36**, (1990), 139.
181. Y. Cao, A. Andretta, A.J. Heeger, P. Smith, *Polymer*, **30**, (1989), 2305.
182. J.-C. Chiang and A.G. MacDiarmid, *Synth. Met.*, **13**, (1986), 193.
183. J.L. Cadenas and H. Hu, *Solar Energy Mate. Sol. Cells*, **55**, (1998), 105.
184. A.G. MacDiarmid, J.C. Chiang and A.F. Richter, *Synth. Met.*, **18**, (1987), 317.
185. A.G. Green and A.E. Woodhead, *J. Chem. Soc.*, (1910) 1117.
186. A.G. Green and A.E. Woodhead, *J. Chem. Soc.*, (1910) 2388.
187. Y. Cao, A. Andretta and A.J. Heeger, *Polymer*, **67**, (1998) 1863.

188. H.R. Kricheldorf, Handbook of Polymer Synthesis, Marcel Dekker, New York, (1992) 1390
189. H.Q. Xie and Q. Xiang, *Euro. Polym. J.*, **36**, (2000) 507
190. I.Mau, M. Ziong and A. Sebenik, *Synth. Met.*, **101**, (1999), 717.
191. A.G. MacDiarmid, J.C. Chiang, M. Halpern, W.S. Huang, S.L. Mu, N.L. Somasiri, W. Wu and S.I. Yangier, *Mole. Cryst. Liq. Cryst*, **121**, (1985), 173.
192. G.E. Austrias, A.G. MacDiarmid and A.J. Epstein, *Synth. Met.*, **29**, (1989), E157.
193. S.P. Armes and J.F. Miller, *Synth. Met.*, **12**, (1985), 385.
194. M. Vijayan and D.C. Trivedi, *Synth. Met.*, **107**, (1999), 57.
195. E.T. Kang, K.G. Neoh and K.L. Tan, *Synth. Met.*, **68**, (1995), 142.
196. D.M. Mohilner, R.N. Adams and W.J. Angersinger, *J. Ame. Chem. Soc.*, **84**, (1962), 3618.
197. Ling-Yau Chan, Chang-Xing Ma and T. N. Goh, *Journal of Quality Technology*, **35**, No. **2** (2003) 123-139.
198. C.R.Rao, "Some Combinatorial Problems of Arrays and Applications to Design of Experiments", A Survey of Combinatorial Theory, Edited by J.N.Srivastava, Chapter 29, (1973) 349-359.
199. Gardiner & G. Gettingby, *Experimental Design Techniques in Statistical Practice*, Horwood, England, (1998).
200. R.F.Gunst, R.L.Mason and L.H.James, "Statistical Design and Analysis of Experiments with applications to Engineering and Science", John Wiley, New York, (1989).
201. V.Sridhar, S.S. Bhagawan, R.Muraleekrishnan and S.S.Rao, "Statistical design of Experiments: Modelling rubber formulations for low temperature applications", Chemcon 98, *IChE Meet*, Visakhapatnam, Dec (1998).

202. K. Jayanarayanan, H.S. Karthick, V. Suganya, A.L. Sivasankari and S. S. Bhagawan, "Optimization of process parameters of an injection moulded nylon gear using Taguchi Methodology", *SPE ANTEC* , (2006) 1088-1092.
203. Tao C.Chang and Earnest Faison, "Shrinkage behavior and Optimization of Injection Moulded Parts Studied by Taguchi Method", *Polymer Engineering and Science*, **41** (5), (2001) 703-710.
204. R.N.Kacker, "Offline Quality Control, Parameter Design, and the Taguchi Method", *Journal of Quality Technology*, **17**, (1985) 176–209.
205. T.N.Goh, "Taguchi Methods: Some Technical, Cultural and Pedagogical Perspectives", *Quality and Reliability Engineering International*, **9**, (1993) 185–202.
206. Jeong Wan Choi, Moon Gyu Han, Sook Young Kim, Seong Geun Oh, Seung Soon Im., *Synthetic Metals*, **141**, (2004) 293–299.

### **EXPERIMENTAL METHODS**

The methods adopted for synthesis of conducting polymers like Poly para phenylenediazomethine, polythiophene, poly (3, 4-ethylene dioxy thiophene) and polyaniline are described in this chapter. The methods and equipments used for characterisation of these polymers like, Fourier Transform Infrared spectroscopy (FTIR), Thermo Gravimetric Analysis (TGA) and Differential Scanning Calorimetry (DSC) are explained. The preparation of blends of these conducting polymers with PVC and PU are also discussed. The theory, equations and experimental set up used for the evaluation of microwave properties and EMI shielding are also dealt in detail.

#### **2.1 MATERIALS USED**

The suppliers and specifications for the various chemicals, reagents and solvents used for the study are detailed below.

##### **2.1.1 Monomers**

**P-phenylene diamine:** Para phenylene diamine was obtained from S.D Fine-Chem Ltd. The specifications are given below.

Minimum Assay	98%
Melting Point	139-143 °C
Sulphated Ash	NMT 0.05%

**Glyoxal trimer dihydrate:** Glyoxal Trimer Dihydrate having the following specifications was supplied by Fluka.

Minimum Assay	98%
Molar Mass	210.14 g/mol
pH value	4 - 5 (100 g/l)
Form	White powder
Vapour Pressure	378 hPa (26 °C)
Bulk Density	500 - 700 kg/m <sup>3</sup>

**Thiophene:** Thiophene having the following specifications was obtained from Sigma –Aldrich Chemic GmbH.

Melting point	- 38 °C
Boiling point	84 °C
Refractive Index	1.527
Sp. Gravity	1.051

**3, 4-Ethylenedioxythiophene (EDOT):** EDOT having the following specifications was supplied by Sigma –Aldrich Chemic GmbH.

Freezing Point	104 °C
Boiling Point	> 200°C
Melting Point	10.5 °C
Sp. Gravity	1.334

**Aniline:** Aniline having the following specifications was supplied by Merck.

Minimum Assay	99%
Sp. Gravity	1.020 - 1.022

### 2.1.2 Dopants

**Ferric chloride** (Also used as an oxidising agent): Anhydrous Ferric Chloride (96%) was supplied by Sd Fine Chemicals Ltd. The specifications are,

Minimum Assay	96%
Ferrous Chloride	1.0%

**DBSA (Dodecyl benzene sulfonic acid):** DBSA (Dodecyl benzene sulfonic acid-Mixture of C10 - C 13 isomers) with a density of 1.2 was supplied by Acros Organics.

**10-Camphor sulfonic acid (CSA):** CSA (98%) was supplied by Sigma –Aldrich Chemic GmbH.

**Perchloric acid:** Perchloric Acid (60%) was supplied by Nice Chemicals Pvt. Ltd. The specifications are,

Chlorate	0.0012%
Chloride	0.003%
Free Chlorine	0.0005%
Nitrate	0.001%
Sulphates	0.001%



**Hydrochloric acid:** Hydrochloric acid (35%) was supplied by Chemspure.

**Cupric acetate:** Cupric acetate was supplied by Fischer Chemic. Ltd.

### 2.1.3 Solvents

**N,N Dimethyl formamide (DMF):** DMF having the following specifications was supplied by Qualigens.

Minimum Assay	99%
Sp. Gravity	1.4295

**Dimethyl sulfoxide (DMSO):** DMSO having the following specifications was supplied by Nice Chemicals Pvt. Ltd.

Minimum Assay	99%
NVM (max.)	0.005 %
Boiling Range	189-192 °C
Water (max.)	0.2%
Wt per ml at 20 °C	1.099-1.101 g

**Nitromethane:** Nitromethane (98%) GR was supplied by Loba Chemie. Ltd

**Tetrahydrofuran (THF):** THF having the following specifications was supplied by Finar Reagents. Ltd

Minimum Assay	99%
Boiling Range	65-67 °C
Flash Point	-20 °C
Wt per ml at 20 °C	0.886-0.888 g
Refractive Index	1.4072-1.4085
Water (max.)	0.1%

#### **2.1.4 Miscellaneous**

**Methanol:** Methanol having the following specifications was supplied by Fischer Chemic. Ltd.

Minimum Assay	99%
Boiling Range	64-65 °C
Wt per ml at 20 °C	0.790-0.793 g
Refractive Index	1.328-1.331

**Acetone:** Acetone having the following specifications was supplied by Merck.

Minimum Assay	99.5%
Free Acid (max.)	0.002%
Free Alkali (max.)	0.001%
Methanol (max.)	0.05%

**PVC:** Polyvinyl chloride used in the study was a high-medium molecular weight Dispersion Resin grade 120 supplied by Chemplast Sanmar Limited, Chennai.

**Polyurethane:** Polyurethane used in this study is a polyether based TPU of grade KU2-8600 E supplied by Bayer Material Science Pvt. Ltd.

## **2.2 PREPARATION OF CONDUCTING POLYMERS**

### **2.2.1 Preparation of para phenylene diazomethine (PPDA)**

Glyoxal trimer dihydrate was dissolved in any of the suitable solvents like DMSO, DMF or para cresol. PPD was also dissolved in the same solvent and transferred to glyoxal solution. Gradually the temperature of reaction was raised and the solution polycondensation reaction was carried out for the required time. Precipitate was filtered, washed and dried. Soxhlet extraction was done with methanol and acetone for 12 hrs to remove the impurities.

### **2.2.2 Preparation of polythiophene (PTH)**

Anhydrous  $\text{FeCl}_3$  was dissolved in nitrobenzene and thiophene was added to the solution, drop wise under continuous stirring over 15 minutes. The reaction was allowed to occur in nitrogen atmosphere at room temperature over a period of 24 hrs. Precipitate was filtered, washed and dried. Soxhlet extraction was done with methanol and acetone for 12 hrs.

### **2.2.3 Preparation of poly (3,4-ethylenedioxythiophene) (PEDOT)**

DBSA was dissolved in deionised water and stirred for 1 hr at room temperature. EDOT was added to the DBSA micellar solution and solubilised with stirring for 1 hr. Then anhydrous  $\text{FeCl}_3$  dissolved in 10 ml deionised water was syringed quickly and the mixture was stirred for 20 hrs at room temperature. Precipitate was filtered and washed. Soxhlet extraction was done with acetone for 12 hrs.

#### **2.2.4 Preparation of polyaniline (PANI)**

Ferric chloride was dissolved in distilled water and stirred for 10 minutes. Aniline was added dropwise and the reaction was carried out for 24 hrs at room temperature. The PANI powder was precipitated by dumping the reaction mixture in distilled water, followed by filtration and drying by conventional methods. The PANI powder was dedoped with ammonium hydroxide and then doped with camphor sulfonic acid.

### **2.3 PREPARATION OF THERMOPLASTIC CONDUCTING COMPOSITES**

#### **2.3.1 Preparation of polythiophene - PVC composites**

PVC was dissolved in THF and thiophene was added dropwise to the solution. Calculated quantity of  $\text{FeCl}_3$  was dissolved in THF to get a  $\text{FeCl}_3$ : thiophene ratio of 1.5, 2, 2.5 and 3. The solution was added drop wise to the PVC solution and the reaction was carried out for 24 hrs. Solution was cast in a petri dish and allowed to dry at room temperature and in vacuum oven at  $40^\circ\text{C}$  for 2 hrs.

#### **2.3.2 Preparation of PEDOT- PVC composites**

PVC was dissolved in THF and EDOT was added dropwise to the solution. Calculated quantity of  $\text{FeCl}_3$  was dissolved in THF to get a  $\text{FeCl}_3$ : EDOT ratio of 2.5. The solution was added drop wise to the PVC solution and the reaction was carried out for 24 hrs. The solution was cast in petri dish and allowed to dry at room temperature and in vacuum oven at  $40^\circ\text{C}$  for 2 hrs.

### **2.3.3 Preparation of polyaniline- PVC composites**

PVC was dissolved in THF. Aniline was added dropwise and stirred for another 2 hrs. Calculated quantity of  $\text{FeCl}_3$  was dissolved in THF to get a  $\text{FeCl}_3$ : Aniline ratio of 2.5. The solution was added drop wise to the PVC solution and the reaction was carried out for 24 hrs. Camphor sulfonic acid was added and stirred for another 2 hrs. Solution was cast in petri dish and allowed to dry ant room temperature and in vacuum oven at  $40\text{ }^\circ\text{C}$  for 2 hrs.

### **2.3.4 Preparation of PPDA - PVC composites**

PPDA-PVC composite was prepared by mixing PPDA powder in PVC solution to get a 10% solution. The mixture was cast in petri dish and allowed to dry at room temperature and in vacuum oven at  $40\text{ }^\circ\text{C}$  for 2 hrs.

### **2.3.5 Preparation of PEDOT - PU composites**

PU was dissolved in THF and EDOT was added dropwise to the solution. Calculated quantity of  $\text{FeCl}_3$  was dissolved in THF to get a  $\text{FeCl}_3$ : EDOT ratio of 2.5. The solution was added drop wise to the PU solution and the reaction was carried out for 24 hrs. The solution was cast in petri dish and allowed to dry at room temperature and in vacuum oven at  $40\text{ }^\circ\text{C}$  for 2 hrs.

### **2.3.6 Preparation of PANI - PU composites**

PU was dissolved in THF. Aniline was added dropwise and stirred for another 2 hrs. Calculated quantity of  $\text{FeCl}_3$  was dissolved in THF to get a  $\text{FeCl}_3$ : Aniline ratio of 2.5. The solution was added drop wise to the PU solution and the reaction was carried out for 24 hrs. Camphor sulfonic acid was added and stirred for another 2 hrs. Solution was cast in petri dish and allowed to dry at room temperature and in vacuum oven at  $40^\circ\text{C}$  for 2 hrs.

## **2.4 CHARACTERISATION OF POLYMERS**

### **2.4.1 Fourier transform infrared spectrometer (FTIR)**

Infrared radiation of frequencies less than about  $100\text{ cm}^{-1}$  is absorbed and converted by an organic molecule into energy of molecular rotation and that in the range of  $10,000 - 100\text{ cm}^{-1}$  into energy of molecular vibration. These absorptions are quantized. Molecular rotation spectrum consists of discrete lines but vibrational spectra appear as bands. The frequency or wavelength of absorption depends on the relative masses of atoms, the force constants of the bonds and the geometry of atoms. In FTIR, radiation containing all IR wavelengths is split into two beams. One beam is of fixed length and the other of variable length. The varying distances between two path lengths result in a sequence of constructive and destructive interference and hence variations in intensities giving an interferogram. Fourier transformation converts this interferogram from the time domain into one spectral point on the more familiar form of frequency domain. FTIR of the samples are taken using Thermo Nicolet, Avatar 370 having spectral range of  $4000 - 400\text{ cm}^{-1}$  and a resolution of  $0.9\text{ cm}^{-1}$ . It is equipped with KBr beam splitter and DTGS Detector ( $7800 - 350\text{ cm}^{-1}$ ).

### 2.4.2 Thermogravimetric analysis and differential thermal analysis

The basic principle in thermogravimetric analysis (TGA) is to measure the mass of a sample as a function of temperature. The ability to analyse the volatile products during a weight loss is of great value. In this technique (TG or TGA), changes in the mass of a sample are studied while the sample is subjected to a controlled temperature programme. The temperature programme is most often a linear increase in temperature, but isothermal studies can also be carried out, when the changes in sample mass with time are followed. Many thermal changes in materials (e.g. phase transitions) do not involve a change of mass. In DTA (Differential Thermal Analysis), one instead measures the temperature difference between an inert reference and the sample as a function of temperature. When the sample undergoes a physical or chemical change the temperature increase differs between the inert reference and the sample, and a peak or a dip is detected in the DTA signal. The technique is routinely applied in a wide range of studies such as identification, quantitative composition analysis, phase diagrams, hydration-dehydration, thermal stability, polymerisation, purity, and reactivity.

TGA and DTA of the samples were taken using Perkin Elmer, Diamond TG/DTA with operating temperature range from ambient to 1200°C. The TG sensitivity is of 0.2 mg and a heating rate of 0.01 – 100°C / min and gas flow rate of 0-1000 ml/min. The different stages of degradation can be studied by noting the onset temperatures of each degradation steps, the percentage of degradation at a particular temperature, etc. The onset of degradation temperature, the temperature at which the rate of weight loss is maximum ( $T_{max}$ ), and the residual weight in percentage are evaluated. Sample size is between 5 and 10 mg.

### **2.4.3 Differential scanning calorimetry (DSC)**

DSC measures the temperatures and heat flow associated with transitions in materials as a function of time and temperature. The technique provides qualitative and quantitative information about physical and chemical changes that involve endothermic or exothermic processes or changes in heat capacity using minimal amounts of sample. It has many advantages including fast analysis time, typically thirty minutes, easy sample preparation, applicability to both liquids and solids, a wide range of temperature applicability and excellent quantitative capability. DSC can be most useful in studying glass transitions, melting and boiling points, crystallization time and temperature, percent crystallinity, heats of fusion and reactions, specific heat and heat capacity, oxidative stability, rate and degree of cure, reaction kinetics, percent purity, thermal stability etc. DSC has been used in the evaluation of small transitions such as multiple phase transitions in liquid crystals and those due to side chains in polymers which can not be resolved by most other techniques.

DSC curves of the samples are taken in Mettler Toledo DSC 822e operating at a temperature range of -150 °C to max. 700°C. The measurement resolution is 0.04 mW at RT, the heating rate is RT to 700°C in 7 min and cooling rate is + 100°C to - 100°C in 15 min. DSC gives an idea about the primary and secondary transition with change in temperature. It gives the exothermic and endothermic changes occurring over a particular temperature range. DSC was recorded from 0°C to 200°C for the samples.



## 2.5 TESTING OF POLYMERS AND COMPOSITES

### 2.5.1 Measurement of DC conductivity

The conductivity measurements were carried out using Keithley 2400 Sourcemeater and a Keithley 2182 Nanovoltmeter having a very low noise of 15 nV at 1s response time. Conductivity measurements were done using pellets for the powder samples and on cast films. The specific resistivity was calculated as:

$$\rho = (R * A) / t$$

Where,  $\rho$  is the resistivity, R is the resistance measured, A is the area of the electrode used and t is the thickness of the sample and,

$$\sigma = 1 / \rho$$

where,  $\sigma$  is the conductivity of the material.

### 2.5.2 Measurement of microwave properties - cavity perturbation technique

When a dielectric material is introduced into a rectangular cavity resonator at the position of maximum electric field, the resonant frequencies of the cavity are perturbed. The contribution of magnetic field for the perturbation is minimum at this position. So from the measurement of the perturbation due to the sample, the dielectric parameters can be determined. The availability of sweep oscillators and network analyser makes it possible to measure the dielectric parameters at a number of frequencies in single band.

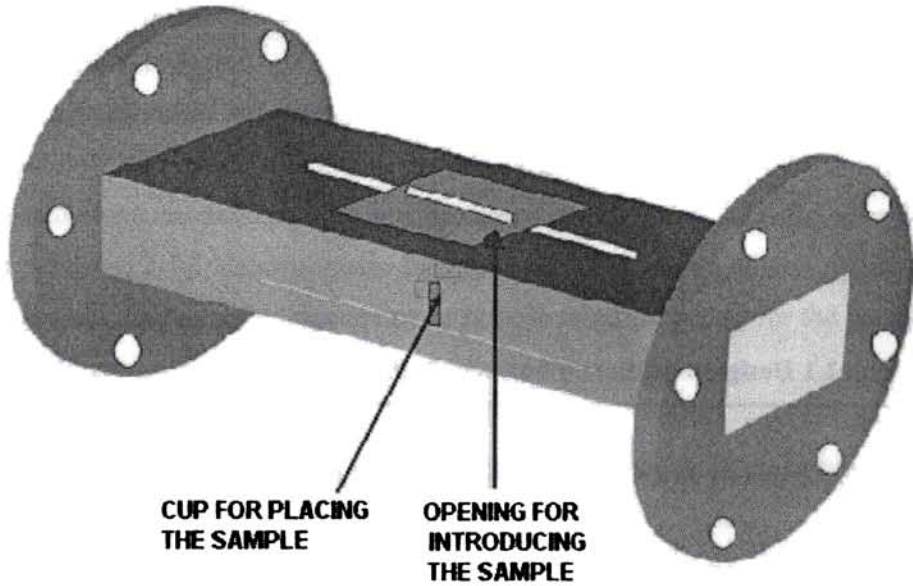
#### 2.5.2.1 Rectangular waveguides

Rectangular cavity resonator is made of brass or copper wave guide. The S-band rectangular wave guide cavity resonator is constructed from a section of standard

WR-284 wave guide. For C band cavity; a section of WR-159 wave guide is used. A section of WR-90 wave guide is selected for the fabrication of X band resonator. Table 2.1 shows the design details of S and X band rectangular wave guide cavities. The inner walls of each cavity are silvered to reduce the wall losses. All the three resonators are of transmission type, since power is coupled into or out through separate irises.

**Table 2.1 Design parameters of S and X band rectangular wave guide cavities.**

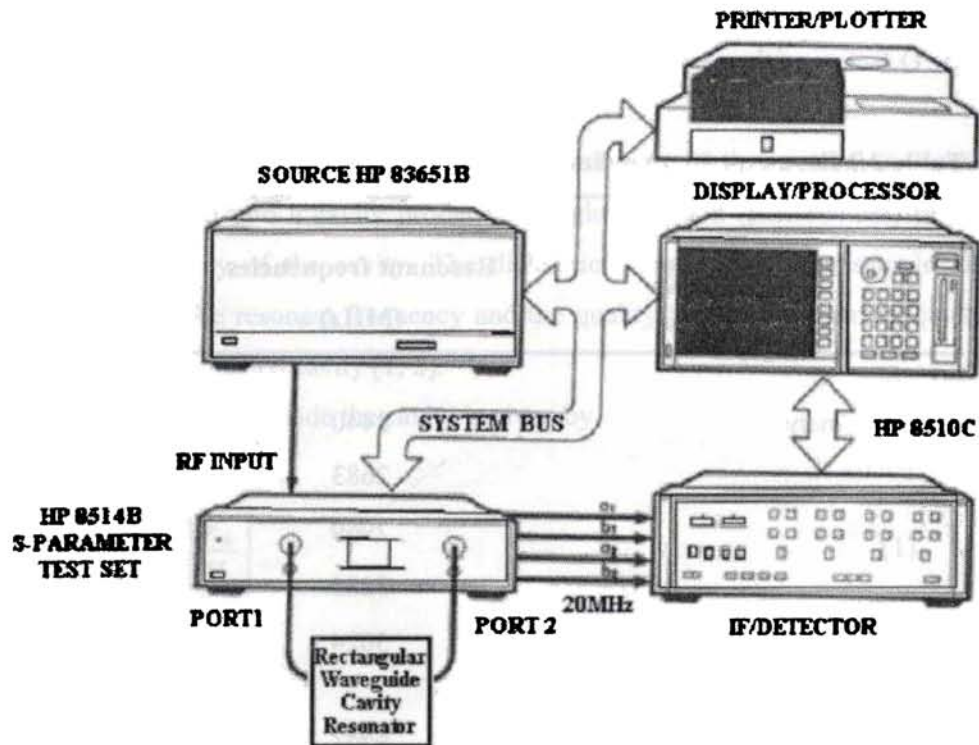
<b>Dimensions of the cavity</b>	<b>S band (mm)</b>	<b>X Band (mm)</b>
<i>Length, d</i>	353	120
<i>Breadth, a</i>	72	22.9
<i>Height, b</i>	33.5	10
<i>Diameter of the coupling hole</i>	12.8	5.5
<i>Length of the slot on the broad wall</i>	225	43
<i>Width of the slot</i>	4	1



**Figure 2.1 Schematic diagram of the rectangular cavity resonator.**

#### *2.5.2.2 Experimental setup*

The experimental set up for S band measurements consists of an HP8510 vector network analyser, sweep oscillator and the rectangular cavity resonator. The block diagram of the experimental set up is provided in the Figure 2.2. The experimental set up for X band measurements consists of an Agilent E8362B PNA series network analyzer, sweep oscillator and the rectangular cavity resonator. The measurements were done at 25 °C in S band (2GHz-4GHz) and X Band (8GHz-12GHz).



**Figure 2.2** Block diagram of the experimental set up.

The cavity resonator is constructed with a portion of a transmission line (waveguide or coaxial line) with both ends closed. There is a coupling device (iris) to couple the microwave power to the resonator. The transmission type resonator used in this experiment is excited with  $TE_{10P}$  mode by connecting it to an HP8510 C Network Analyzer. The resonant frequency ' $f_0$ ' and the corresponding quality factor ' $Q_0$ ' of each resonant peak of the empty cavity are first determined. Now after selecting a particular resonant frequency, the dielectric sample is introduced into the cavity and the position is adjusted for maximum perturbation (i.e. maximum shift of resonant frequency towards the low frequency region, with minimum amplitude for the peak) and the corresponding change in the frequency

of the resonant peak is observed. The Table 2.2 shows the resonant frequencies and the Q factors of the cavities used.

**Table 2.2 Resonant frequencies and Q factors of the cavities used.**

---

<b>Type of cavity</b>	<b>Resonant frequencies (MHz)</b>	<b>Q Factor</b>
<i>S Band cavity</i>	2440	4879
	2683	5366
	2969	3711
	3285	2986
	3624	2001
<i>X Band Cavity</i>	8726	2900
	9472	1635
	10285	921
	11149	917
	12053	993

---

The new resonant frequency ' $f_s$ ' the corresponding 3 dB bandwidth and the quality factor ' $Q$ ' are determined. The procedure is repeated for other resonant frequencies and the measurements are carried out for all the samples. Knowing the volumes of the sample and the cavity resonator the dielectric parameters can be evaluated. A very precise determination of the volume of the sample is to be ensured, to get accurate values for the parameters.

### 2.5.2.3 Theory

The basic principle of the cavity perturbation technique is that a small dielectric sample introduced into a cavity produces a slight variation (perturbation) of the resonant frequency of the cavity. The dielectric parameters of the sample are evaluated from the resonant frequency and the quality factor of the empty cavity resonator and the loaded cavity [1, 2].

The field perturbation inside the cavity is given by

$$\epsilon' = \frac{f_0 - f_s}{2f_s} \left[ \frac{V_c}{V_s} \right] \quad (1)$$

and

$$\epsilon'' = \frac{V_c}{4V_s} \left[ \frac{Q_0 - Q_s}{Q_0 \cdot Q_s} \right] \quad (2)$$

The effective conductivity ( $\sigma_e$ ) is given by:

$$\sigma_e = \omega \epsilon'' = 2\pi f \epsilon_0 \epsilon'' \quad (3)$$

Here  $\epsilon = \epsilon' - j\epsilon''$  where ' $\epsilon$ ' is the relative complex permittivity of the sample, ' $\epsilon'$ ' is the real part of the relative complex permittivity, which is usually known as dielectric constant and ' $\epsilon''$ ' is the imaginary part of the relative complex permittivity, which is associated with the dielectric loss of the material. ' $V_s$ ' and

' $V_c$ ' are the volumes of the sample and the cavity resonator, respectively. The parameters are calculated using the following formulae (4-10) [3-5]

$$\epsilon' = 1 + \frac{f_0 - f_s}{2f_s} \left[ \frac{V_c}{V_s} \right] \quad (4)$$

$$\epsilon'' = \frac{V_c}{4V_s} \left[ \frac{Q_0 - Q_s}{Q_0 \cdot Q_s} \right] \quad (5)$$

$$J = \frac{1}{\epsilon \tan \delta} \quad (6)$$

$$\alpha = \frac{\epsilon'' f}{n \cdot c} \quad (7)$$

$$\sigma = 2\pi f \epsilon_0 \epsilon'' \quad (8)$$

$$\tan \delta = \frac{\epsilon''}{\epsilon'} \quad (9)$$

$$d = \frac{1}{\alpha} \quad (10)$$

where,

$\epsilon'$  = Dielectric constant

$\epsilon''$  = Loss factor

$\epsilon_0$  = Permittivity of free space

$\alpha$  = Absorption Coefficient

$d$  = Penetration depth

$\sigma$  = conductivity

$J$  = Efficiency of heating

$c$  = velocity of light

$V_c$  = Volume of cavity

$V_s$  = Volume of sample

### 2.5.3 Shielding efficiency

The electromagnetic wave upon incidence on a shielding material resolves into four parts (see Figure 2.3)

- a) direct reflected wave (R)
- b) an absorbed wave (A)
- c) an internally reflected wave (B) and
- d) a transmitted wave (T)

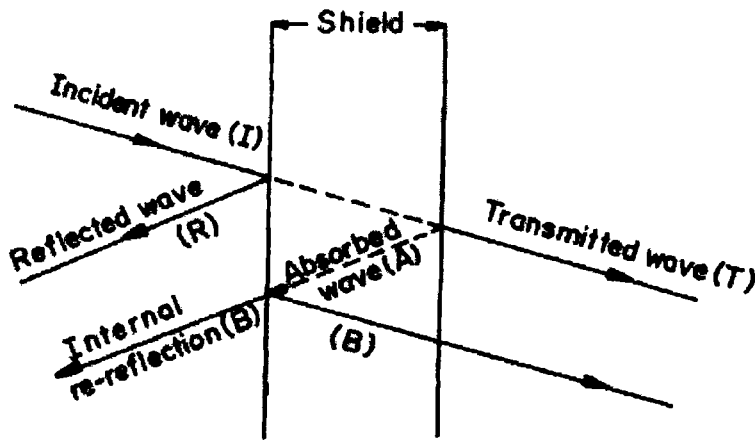


Figure 2.3 Splitting of electromagnetic wave on passing through a shield

The shielding effectiveness is defined as the insertion loss due to the shielding material and is given by

$$SE = R + A + B$$

The Shielding Effectiveness (SE) is the attenuation of an electromagnetic wave produced by its passage through a conducting shield. It is measured experimentally by comparing the field strength of a wave transmitted from a controlled source through a standard aperture to an otherwise shielded receiver, to the field strength of the same wave transmitted through the material to be tested covering the aperture. Near field, far field electric and magnetic field variations are achieved by changing the configuration of the transmitter and the receiver and the geometry of the aperture (ASTM ES 7-83).



From the measurement of S-parameters, absorption coefficient and the shielding efficiency of the material could be calculated. The sample sheet was kept between two coaxial to wave guide adapters and tightened (Figure 2.4). Using the vector network analyzer, the S-parameters ' $S_{11}$ ' and ' $S_{21}$ ' were measured. Reflection coefficient ' $R$ ' and transmission coefficient ' $T$ ' are given as  $R = |S_{11}|^2$  and  $T = |S_{21}|^2$ . The absorption coefficient ' $A$ ' can be obtained from the simple relation  $A + R + T = 1$ . The EMI shielding efficiency ' $SE$ ' [6] is defined as the ratio of the power of the incident wave ' $P_i$ ' to that of the transmitted wave ' $P_T$ '.

$$SE = 10 \log (P_i/P_T) \text{ dB} \quad (11)$$



Figure 2.4 Coaxial to wave guide adapters to measure the S parameters.

#### 2.5.4 Mechanical properties

The mechanical properties of the composites were evaluated in Shimadzu Autograph AG-1 series UTM of 10 kN load capacity. Dumbbell specimens are cut from cast films from different area and they are subjected to tensile tests at a rate of 15 mm/sec.

## 2.6 REFERENCES

1. K.Kupfer, A.Kraszewski, and R.Kno"chel, "RF & Microwave Sensing of Moist Materials, Food and other Dielectrics", *Sensors Update*, **7**, (2000) 186–209.
2. S.B. Kumar et al., *Journal of the European Ceramic Society*, **21**, (2001) 2677–2680.
3. K.T. Mathew et al, *Materials Chemistry and Physics*, **79**, (2003) 187–190.
4. Honey John, Rinku M. Thomas, K. T. Mathew, Rani Joseph, *Journal of Applied Polymer Science*, **92**, Issue 1, (2004) 592 – 598.
5. H.John, S.Bijukumar, K.T.Mathew, Rani Joseph, *Plastics, Rubber and Composites*, **32**, No. 7, (2003) 306-312.
6. K.T. Mathew, A.V. Praveen Kumar and Honey John, "Polyaniline and Polypyrrole with PVC content for effective EMI shielding", *IEEE*, (2006) 443-445.

---

### **PREPARATION AND PROPERTIES OF PPDA- POLY PARA PHENYLENE DIAZOMETHINE**

***Abstract:** Polyazomethines are a special class of conjugated polymers that have potential applications in many fields like battery, semiconductors, energy storage devices, integrated electro-optics for switching, displays, electroluminescence devices etc. A novel polyazomethine namely, poly paraphenylene diazomethine was prepared by polycondensation of para phenylene diammine (PPD) and glyoxal trimer dihydrate (GTD). Design of Experiments (DOE) approach was used for optimizing the reaction conditions for the polycondensation. The monomer ratio, temperature and time for the polycondensation reaction have been optimised based on good yield and conductivity of the polymer obtained. Taguchi design based on  $L_9$  orthogonal array was used for optimizing the reaction parameters. PPDA prepared by the validation experiment was characterized by FTIR, TGA and DSC. FTIR confirmed the structure of polyazomethine. The polymer is stable up to 250°C.*

Polymeric aldimines or Poly(Schiff base)s are classes of materials known as polyazomethines. These conjugated polymers are particularly attractive because they show good mechanical strength [1], attractive thermal stability [2], nonlinear optical properties, photoconductivity [3] and optical properties [4]. Because of this

wide range of fascinating properties, polyazomethines have potential applications in many fields, e.g. battery anodes or cathodes, semiconductors, advanced technology materials, energy storage and conversion devices, integrated electro-optics for switching, displays [5-7], electroluminescence (EL) devices [8], etc. The first polyazomethine was reported in 1923 as a result of polycondensation of terephthaldehyde and benzidine [9]. Since then, conjugated aromatic polyazomethines with different moieties on both sides of CH=N group have been reported [10-12]. Polyazomethines can be prepared by solution polycondensation [13], chemical vapour deposition [14-16] and oxidative polymerisations [17].

Most of synthesized polyazomethines have major difficulties in processing due to their insolubility/ intractability problems. To overcome these drawbacks, the preparation of soluble polyazomethines by a complexation with Lewis acids ( $\text{GaCl}_3$ ,  $\text{AlCl}_3$ ) [18] or by attachment of side chains [19] to yield more soluble polymers was performed. Another interesting way to modify polyazomethines is by complexation with metal ions. Such metal complexed schiff base polymers exhibit a wide variation in their luminescence as well as their electrical properties. Polyazomethines containing heterocyclic nuclei such as thiophene [20], furan [21], and 1, 3, 4, thiadiazole [22] show outstanding thermal and thermo-oxidative stability comparable to those of totally aromatic polyazomethines. The insertion of the naphthalene group within the main chain of polyazomethines is expected to improve polymer solubility and thermal stability [23].

DuPont showed that melting temperatures can be effectively reduced either by incorporating lateral substituents or flexible spacers into the polymeric chain, thus favouring the formation of mesophases. This work by DuPont proved that fibers of wholly aromatic polyazomethines extruded from the anisotropic melt have better tensile properties than those of semiflexible polyazomethines, but that the

incorporation of flexible spacers provides processing advantages. In any case, the tensile properties of the fibres can be substantially improved by thermal annealing [24-27].

The goal in any experimentation process is to characterize the relationship between a response and a set of factors that influence the response. This can be achieved by conducting experiments and analyzing the data. A variety of techniques have been used for providing quantitative understanding of the effect of various parameters on the properties of interest. They include one variable at a time [OVAT] approach, design of experiments (DoE), artificial neural networks, etc.

In this study the use of design of experiments for optimising the reaction conditions for polycondensation reaction is presented. The ratio of para phenylene diammine (PPD) and glyoxal trimer dehydrate (GTD), the temperature, and time for the polycondensation reaction have been selected based on good yield and conductivity of the polyazomethine obtained. The polymer prepared by the validation experiment is characterized by FTIR, TGA, DTA and DSC analysis.

## ***PART-I***

### **3.1 OPTIMISATION OF REACTION PARAMETERS FOR POLY - CONDENSATION OF PPDA**

#### **3.1.1 Experimental methods**

Glyoxal trimer dihydrate (GTD) was dissolved in a suitable solvent and nitrogen was passed through the solution for 30 minutes with continuous stirring. Para phenylene diammine was dissolved in the solvent separately and transferred to glyoxal solution. The temperature of the reaction was gradually increased to the set value and the solution polycondensation reaction was carried out for the required time. The polymer was precipitated in methanol, filtered, washed and dried. Soxhlet extraction was done with methanol and acetone successively for 48 hrs. Polymer was dried in vacuum oven at 65 °C for 5 hrs. Brownish black polymer was obtained and the yield was calculated. The dried polymer was doped with 1N HCl for 24 hrs. The polymer was pressed to pellets and conductivity of the samples was measured using Keithley 2400 Sourcemeter and a Keithley 2182 Nanovoltmeter having a very low noise of 15 nV at 1s response time .The specific resistivity was calculated as:

$$\rho = (R * A) / t$$

Where,  $\rho$  is the resistivity, R is the resistance measured, A is the area of the electrode used and t is the thickness of the sample and,

$$\sigma = 1 / \rho$$

where,  $\sigma$  is the conductivity of the material.

An  $L_9$  Orthogonal array based design for three variables was used for conducting various experiments. The factor plots were generated using MS Excel 2003 package.

### 3.1.2 Results and discussion

Poly para phenylene diazomethine (PPDA) was prepared by polycondensation of paraphenylene diammine (PPD) and glyoxal trimer dihydrate (GTD) under various conditions to get a polymer of optimum yield and conductivity.

#### 3.1.2.1 Effect of solvent on yield and conductivity of PPDA

PPDA was prepared by polycondensation of PPD and GTD in the ratio 1:1 at reflux temperature for 10 hrs using p-cresol, DMSO and DMF as solvents. Yield and conductivity are shown in Table.3.1

**Table.3.1 Yield and conductivity of PPDA prepared in various solvents.**

Experiment	Solvent	Temperature ( $^{\circ}$ c)	Yield (%)	Conductivity (S/m)	
				Undoped $\times 10^{-8}$	HCl Doped $\times 10^{-6}$
1	p-Cresol	180	36.4	1.67	2.75
2	DMSO	150	57.1	3.78	5.87
3	DMF	100	63.3	56	76.4

Samples prepared in DMF showed highest yield and conductivity and hence further studies were carried out using DMF as the solvent for polycondensation.

### *3.1.2.2 Optimization of reaction parameters for polycondensation of PPDA using Taguchi design*

Genichi Taguchi's approach of finding factors that affect a product in a Design of Experiments can dramatically reduce the number of trials required to generate necessary data [28, 29]. In Taguchi method, orthogonal array based experiments are conducted; factor effect plots are generated from which the optimum combination of control factors are selected. Finally, a verification experiment is conducted and suitable parameter settings are recommended to produce acceptable products. The Taguchi design is widely used in the polymer industry for optimizing polymerisation conditions, tyre cord properties, composition of blends, injection moulding parameters, etc. [30-34].

It is assumed that parameters like monomer ratio, temperature and polymerisation time affects the molecular weight and yield of the PPDA prepared by the polycondensation of PPD and GTD. In the present study three parameters at three levels are of relevance and hence the L<sub>9</sub> Orthogonal Array was selected for the study [35, 36]. The standard array is shown in Table.3.2 in coded levels. The codes 1, 2 and 3 refer to the lowest, middle and highest responding levels chosen for each of the parameters. The parameters and levels in uncoded form are given in Table.3.3.



**Table 3.2 Standard L<sub>9</sub> orthogonal array**

Experiment No.	P1 Monomer Ratio	P 2 Temperature (°C)	P 3 Time (Hrs)
1	1	1	1
2	1	2	2
3	1	3	3
4	2	1	2
5	2	2	3
6	2	3	1
7	3	1	3
8	3	2	1
9	3	3	2

**Table 3.3 Parameters and levels of parameters affecting the polycondensation.**

Levels	Parameters		
	P1 Monomer Ratio PPD: Glyoxal	P2 Temperature (°C)	P3 Time (Hrs)
L1	0.9:1	80	1
L2	1: 1	100	3
L3	1.1:1	120	5

Nine experiments were conducted as per the combinations mentioned in Table 3.4. Yield and conductivity of the polymer formed for each trial is also given. Factor plots were generated with respect to yield (Figure 3.1) and conductivity (Figure 3.2). It may be noted that the yield ranges from 55% to 65 % and conductivity of the polymer extends over four orders. From the figures the optimum reaction conditions for maximum yield and maximum conductivity were identified.

**Table 3.4 Properties of polymers as prepared from various trials (Taguchi Design)**

No.	Monomer Ratio	Temperature (°C)	Time (Hrs)	Yield (%)	Conductivity X 10 <sup>-6</sup> (S/m)
1	0.9:1	80	1	51	.321
2	0.9:1	100	3	52	64.3
3	0.9:1	120	5	54	74.4
4	1: 1	80	3	59	34.8
5	1: 1	100	5	63	112.4
6	1: 1	120	1	65	87
7	1.1:1	80	5	54	5.67
8	1.1:1	100	1	59	6.13
9	1.1:1	120	3	58	46.7

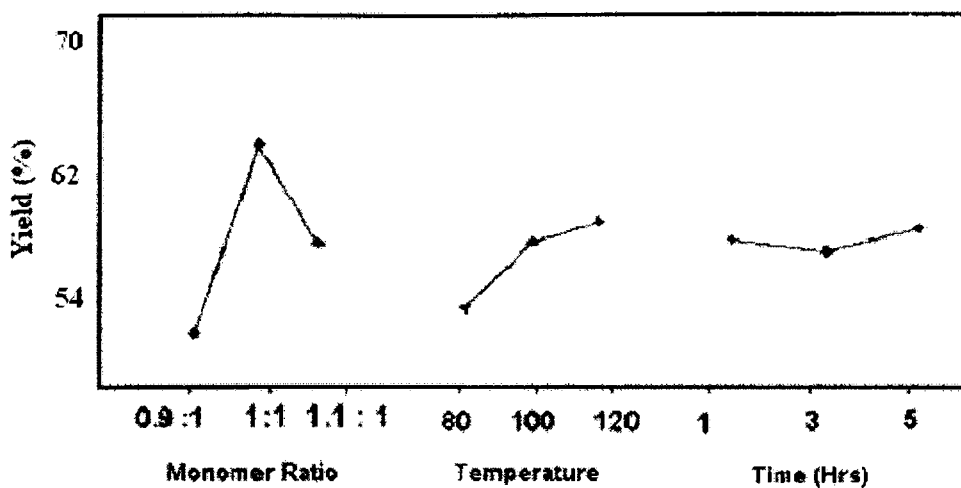


Figure 3.1 Factor plot for yield.

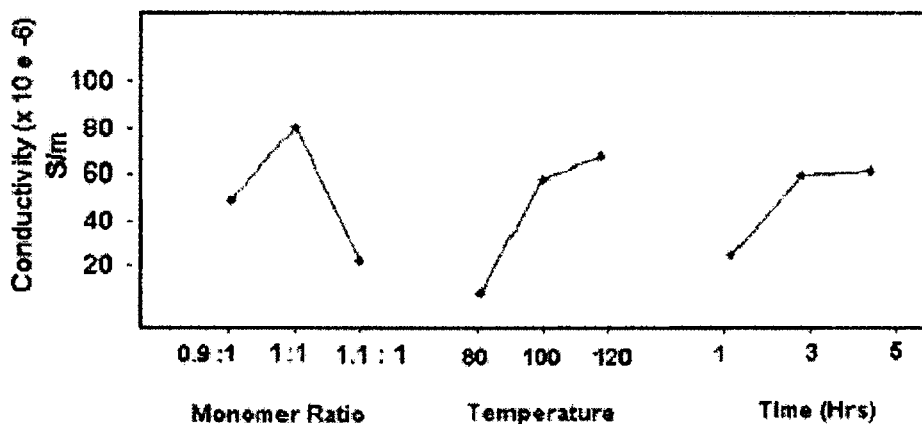


Figure 3.2 Factor plot for conductivity

From Figure 3.1 and 3.2, it is observed that maximum yield was obtained by doing the reaction at a temperature of 120 °C and a monomer ratio of 1:1 for 5 hrs. And maximum conductivity is obtained by doing the reaction at a temperature of 120 °C and a monomer ratio of 1:1 for 5 hrs. Therefore the optimum conditions for

polycondensation reaction are at a temperature of 120°C and a monomer ratio of 1:1 for 5 hrs.

### *3.1.2.3 Validation experiment*

0.1 mole of GTD was dissolved in DMF by heating to 80 °C. 0.1 mole PPD was dissolved in DMF and added to glyoxal solution. The polycondensation reaction was carried out at 120 °C for 5 hrs. Polymer was obtained at 60% yield and a conductivity of  $136 \times 10^{-6}$  (S/m). The experiment shows that the predicted levels of reaction conditions do give an optimum yield and conductivity for the polymer.

### **3.1.3 Conclusions**

Design of Experiments was effectively used in the polycondensation of para phenylene diammine and glyoxal trimeric hydrate to give polyparaphenylene diazomethane. It was predicted that optimum yield and conductivity would be obtained by condensation polymerization of PPD and GTD at 1:1 monomer ratio at 120 °C for 5 hrs. It was shown that the predicted levels of reaction conditions do give an optimum yield and conductivity for the polymer.

## ***PART-II***

### **3.2 CHARACTERISATION OF PPDA**

The polyazomethine, PPDA obtained by the validation experiment was characterised by FTIR, TGA and DSC to confirm the structure. An interesting way to modify polyazomethines is by complexation with metal ions. Such metal complexed schiff base polymers exhibit a wide variation in their luminescence as well as their electrical properties. These polymers may be considered as hybrid materials, which combine the processing properties of polymer, and the physical properties of metal atoms such as colour, electric and magnetic properties [37, 38]. PPDA was doped with HClO<sub>4</sub> and copper acetate to analyze the effect of doping.

#### **3.2.1 Experimental methods**

0.1 mole of GTD was dissolved in DMF by heating to 80 °C. 0.1 mole PPD was dissolved in DMF and added to glyoxal solution. The polycondensation reaction was carried out at 120 °C for 5 hrs. Precipitate was extracted with acetone and methanol and dried in vacuum oven. PPDA was doped in 1 N HClO<sub>4</sub> for 24 hrs. Doping/ complexation in copper acetate was done by stirring PPDA in 1 N copper acetate solution at 70 °C for 24 hrs.

The FTIR of PPDA was taken in FTIR of the samples are taken using Thermo Nicolet, Avatar 370 having spectral range of 4000-400 cm<sup>-1</sup> and a resolution of 0.9 cm<sup>-1</sup>. It is equipped with KBr beam splitter and DTGS Detector (7800 – 350 cm<sup>-1</sup>). TGA of the samples were taken using Perkin Elmer, Diamond TG/DTA with operating temperature range from ambient to 1200 °C.

The TG Sensitivity is of 0.2 mg and a heating rate of 0.01 – 100 °C / min and gas flow rate of 0-1000 ml/min. DSC curves of the samples are taken in Mettler Toledo DSC 822e operating at a temperature range of -150 °C to maximum 700°C. The samples were heated to about 300 °C and then cooled at a rate of 10.00 °C/ min under a nitrogen flow rate of 80.0 ml/min. The samples were heated and cooled for a second cycle. The two cooling DSC curves of the samples were studied to analyze the transitions.

### **3.2.2 Results and discussion**

In this section the FTIR, TGA and DSC curves of the PPDA prepared by the validation experiment are analyzed.

#### *3.2.2.1 FTIR of undoped PPDA*

The FTIR spectra of the polypara phenylene diazomethine prepared by validation experiment is shown in Figure 3.3

The absorption peaks of PPDA are assigned to various vibrations and are summarized in Table 3.5

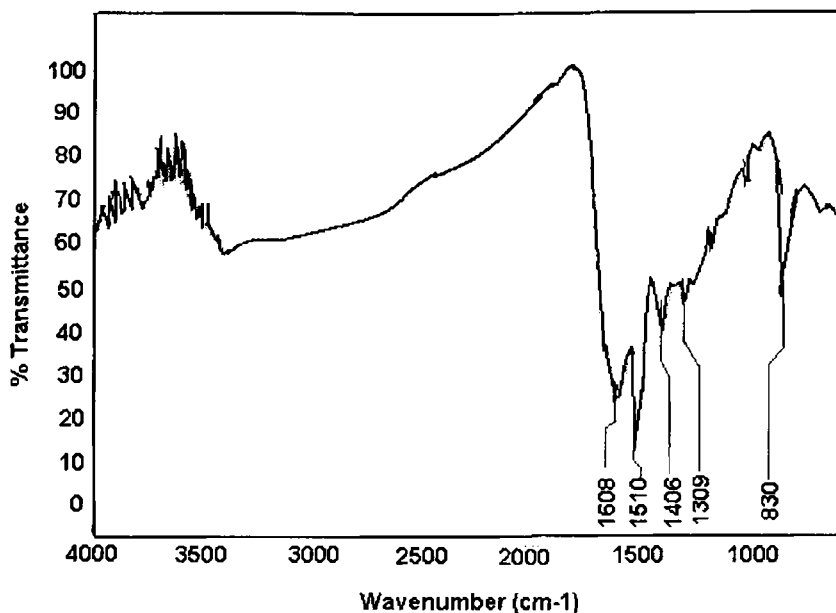
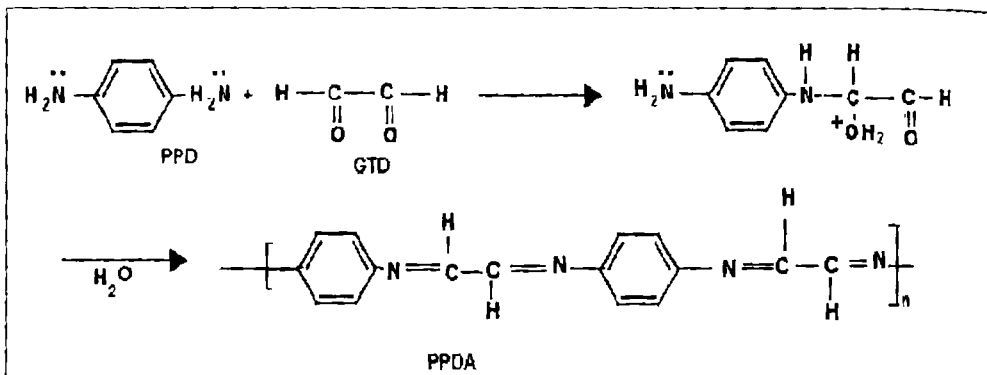


Figure 3.3 FTIR of undoped PPDA.

Table 3.5 Absorption peaks and the assigned vibrations for undoped PPDA

Peak (cm <sup>-1</sup> )	Assigned to
1608	<i>-C = N stretching mode absorption</i> <i>Characteristic peak of Polyazomethine[39]</i>
1510	<i>Aromatic C= C stretching absorption</i>
1406	<i>Aryl -C- N stretching absorption</i>
1309	<i>C-H bending vibrations</i>
830	<i>Very characteristic of para substitution</i> <i>-C-H Out of plane vibration of the aromatic ring</i>

From the Table 3.5 it can be assumed that the structure of the PPDA formed is as shown in Scheme 3.1



**Scheme 3.1 Polycondensation of paraphenylenediamine and glyoxal to form PPDA**

#### 3.2.2.2 FTIR of $\text{HClO}_4$ doped PPDA

Effect of doping on the structure of the polymer was clear from the FTIR spectrum of the polymer doped with  $\text{HClO}_4$ . The FTIR spectrum is shown in Figure 3.4. Comparing Figures 3.3 and 3.4 it could be seen that the polymer shows charge delocalization due to doping.

The absorption peaks of  $\text{HClO}_4$  doped PPDA are assigned to various vibrations and are summarized in Table 3.6.



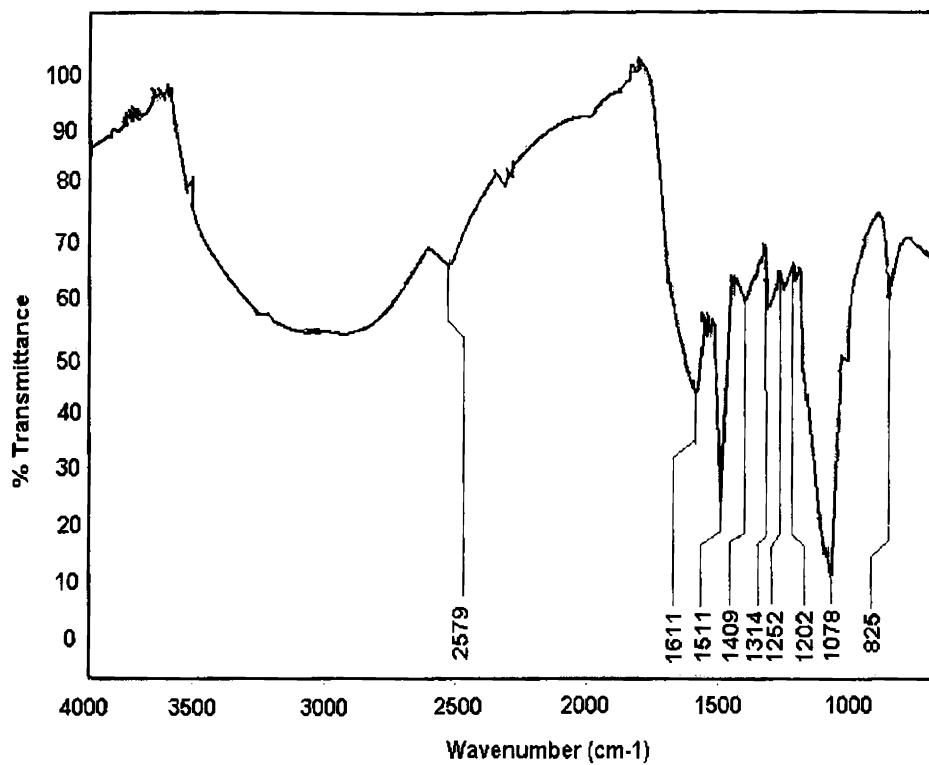


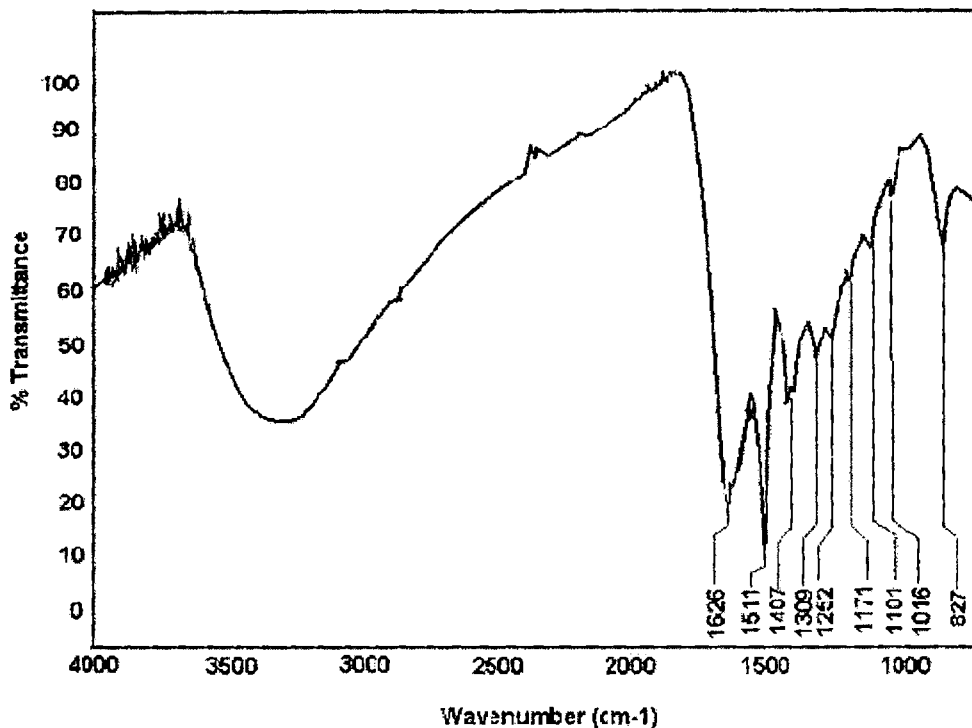
Figure 3.4 FTIR of HClO<sub>4</sub> doped PPDA.

**Table 3.6 Absorption peaks and the assigned vibrations for HClO<sub>4</sub> doped PPDA.**

Peak (cm <sup>-1</sup> )	Assigned to
2579	<i>Broad peak around 2579 is due to the protonation of the polymer chain [40]</i>
1611	<i>-C = N stretching absorption Characteristic peak of Polyazomethine[39]</i>
1511	<i>Aromatic C= C stretching absorption</i>
1409	<i>Aryl -C- N stretching absorption</i>
1314	<i>C-H bending vibrations</i>
1252,1202 & 1078	<i>Charge delocalisation on the polymer backbone [41]</i>
825	<i>Characteristic of para substitution -C-H out of plane vibration of the aromatic ring</i>

### 3.2.2.3 FTIR of copper acetate doped PPDA

Effect of metal acetate doping on the structure of the polymer was clear from the FTIR spectrum of the polymer doped with copper acetate. The FTIR spectrum is shown in Figure 3.5. The absorption peaks are assigned to various vibrations and are summarized in Table 3.7



**Figure.3.5 FTIR of copper acetate doped PPDA.**

Comparing the Figure 3.4 and 3.5, it can be seen that the charge delocalization and hence the extent of doping is less in copper acetate doped sample. So it can be inferred that metal complexation has not been so effective in this type of polyazomethine though these type of complexations have given good results with other types of polyazomethines [37, 38]. This is further confirmed from the DC conductivity measurements shown in Table 3.8. HClO<sub>4</sub> doped PPDA samples show higher conductivity than copper acetate doped samples.

**Table 3.7 Absorption peaks and the assigned vibrations for copper acetate doped PPDA**

<b>Peak (cm<sup>-1</sup>)</b>	<b>Assigned to</b>
1626	<i>-C = N stretching mode absorption Characteristic peak of polyazomethine[39]</i>
1511	<i>Aromatic C= C stretching absorption</i>
1407	<i>Aryl -C- N stretching absorption</i>
1309	<i>C-H bending vibrations</i>
1252,1171	<i>Charge delocalization on the polymer backbone [41]</i>
1101 & 1016	
827	<i>Characteristic of para substitution -C-H out of plane vibration of the aromatic ring</i>

**Table 3.8 DC conductivity of doped PPDA samples**

<b>Dopant</b>	<b>Conductivity (S/m)</b>
Nil	$136 \times 10^{-6}$
HClO <sub>4</sub>	$1.5 \times 10^{-2}$
Copper Acetate	$1.4 \times 10^{-4}$

### 3.2.2.4 Thermogravimetric analysis of PPDA

The TGA and DTA curves of the PPDA sample prepared by validation experiment are shown in Figure.3.6. From the Figure 3.6, it can be understood that the polymer is stable well up to 250 °C. Maximum degradation occurs between 300 – 400 °C. Thermal analysis of the samples show that the polyazomethine prepared has very good thermal stability as expected. It is understood that, the incorporation of nitrogen atoms into the conjugated molecular chains aids in the thermal stability of these materials [42, 43].

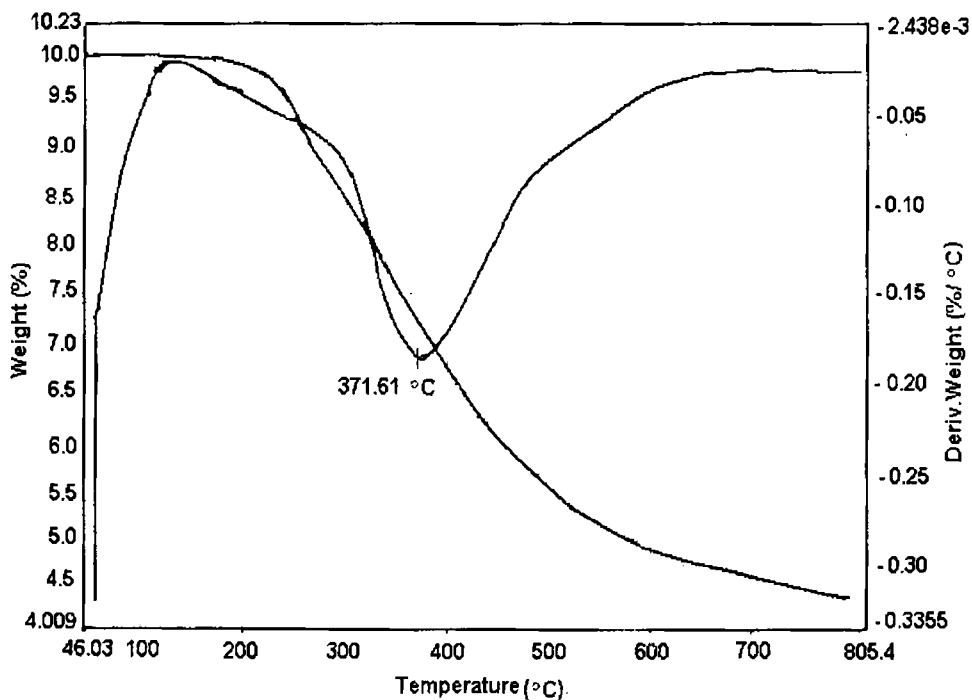


Figure 3.6 TGA and DTA curves for PPDA.

### 3.2.2.5 Differential scanning calorimetry of PPDA

DSC curve of undoped PPDA is shown in Figure.3.7. PPDA was heated to about 300 °C and then cooled to 0 °C. The cooling curve (a) shows an endothermic peak at 86 °C. This may be due to the vaporization of low molecular weight compounds in the sample. The sample was again heated to about 300 °C and then cooled to 0 °C .This cooling curve is shown in curve (b). In this curve there is no transition substantiating that the peak in curve (a) was due to vaporization of low molecular weight compounds. From the curve (b) we can infer that the Tg of the polymer is well beyond 300 °C and the polymer does not show degradation upto 300 °C.

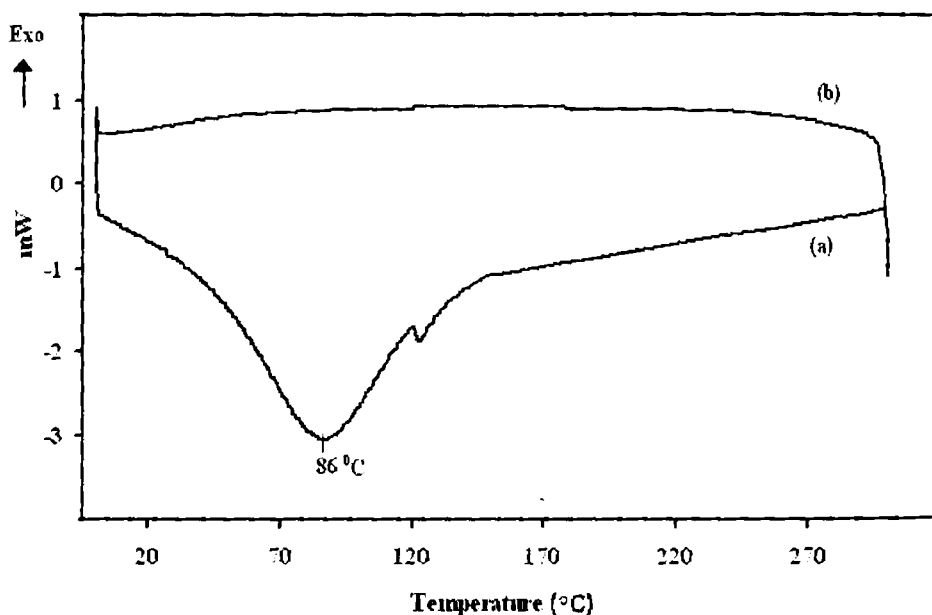


Figure 3.7 DSC curve for PPDA.

### 3.3 CONCLUSIONS

Design of experiments was effectively used in the polycondensation of para phenylene diammine and glyoxal trimeric hydrate to give a novel conducting polymer polyparaphenylene diazomethine. From the analysis of experiments, it was predicted that optimum yield and conductivity would be obtained by condensation polymerization of PPD and GTD at 1:1 molar ratio at 120 °C for 5 hrs. Validation experiment proved that the predicted levels of reaction conditions do give an optimum yield and conductivity for the polymer. PPDA prepared by the validation experiment was characterized by FTIR, TGA and DSC. FTIR shows that the prepared polymer is a polyazomethine with the expected structure. Metal complexation has not been so effective in this type of polyazomethine for enhancing conductivity though these types of complexations have given good results with other types of polyazomethines [37, 38]. HClO<sub>4</sub> doped PPDA samples show higher conductivity than copper acetate doped samples. The polymer is stable up to 250 °C.

### 3.4 REFERENCES

1. O. Catanescu, M. Grigoras, G. Colotin, A. Dobreanu, N. Hurduc, C.I. Simionescu, *Eur. Polym. Journal*, **37**, (2001) 2213.
2. D. Ribera, A. Manteco'n, A. Serra, *J. Polym. Sci., A, Polym. Chem.*, **40**, (2002) 4344.
3. Sang Chul Suh, Sang Chul Shim, *Synthetic Metals*, **114**, No.1, (2000) 91–95.
4. Janusz Jaglarz et al, *Rev. Adv. Mate. Science*, **8**, (2004) 82-85.

5. B.Jarzabek et al, *Journal of Non-Crystalline Solids*, **352**, Issues **9-20**, (2006) 1660-1662.
6. Kamal I. Aly, Ali A. Khalaf, *Journal of Applied Polymer Science*, **77**, (2000) 1218-1229.
7. Mircea Grigoras, Nicoleta Cristina Antonoaia, *Polymer International*, **54**, Issue **12**, (2005) 1641-1646.
8. Ali El-Shekeil, Mohammed Al-Khader, O.Abeer, Abu-Bakr, *Synthetic Metals*, **43**, (2004) 147-152.
9. J.A.Puertolas, E.Carod, R.Diaz-Calleja, P.Cerrada, L.Oriol, M.Pinol, J.L.Serrano, *Macromolecules*, **30**, (1997) 773.
10. Haijun Niu, Yudong Huang, Xuduo Bai, Xin Li, Guiling Zhang, *Materials Chemistry and Physics*, **86**, (2004) 33-37.
11. Z.Hui, A.Gandini, *Eur Polym Journal*, **28**, (1992) 1461.
12. P.K.Dutta, Pragma Jain, Pratima Sen, Rashmi Trivedi, P.K.Sen, Joydeep Dutta, *European Polymer Journal*, **39**, (2003) 1007-1011.
13. Sang Chul Suh, Sang Chul Shim, *Synthetic Metals*, **114**, (2000) 91-95.
14. M.S.Weaver, D.D.C.Bradley, *Synth.Metals*, **83**, (1996) 61-66.
15. S. Tatsuura, W. Sotoyama et al., *Appl. Phys. Lett.*, **62**, (1993) 2182.
16. S. C. Ng, H. S. O. Chan, P. M. L. Wong, K. L. Tan and B. T. G. Tan, *Polymer*, **39**, No. **20**, (1998) 4963-4968 .
17. Claude Chevrot, Thierry Henri, *Synthetic Metals*, **118**, (2001) 157-166.
18. T.Hattori, Wako-shi, Saltama, Eur Patent 963045604, 1996.
19. E.I.M.Jefries, D.Brian, M.Benneyworth, R.Tarkka, *Polym Prepr*, **41**, (2000)174.
20. Z.Hui, A.Gandini, *Eur Polym Journal*, **28**, (1992) 1461.
21. Y.Saegusa, T.Koshidawa, S.Nakamura, *Journal of Polymer Science Part A, Polymer Chemistry*,**30**, (1992) 1396.



22. Maarib A. Khalid, Ali G.El-Shekeil, Fatma A.Al-Yusufy, "A Study of a Thenylene- Phenylene Polyazomethine and its copper Complex", *European Polymer Journal*, **37**, (2001) 1423-1431
23. C. I. Simionescu, M. Grigoras, I. Cianga and N. Olaru , "Synthesis of new conjugated polymers with Schiff base structure containing pyrrolyl and naphthalene moieties and HMO study of the monomers reactivity", *Eur. Polym. J.*, **34**, No. 7, (1998) 891-898.
24. Morgan PW, US Patent 4122070, 1978.
25. Morgan PW, Pletcher TC, Kwolek SL., *Polym Prepr.*, **24**, (1983) 470.
26. Morgan PW, Kwolek SL, Pletcher TC., *Macromolecules*, **20**, (1987) 729.
27. Wojtkowski P.W, *Macromolecules*, **20**, (1987) 740.
28. Alexander Chandra, Shaoqin Gong, Lih-Sheng Turng and Paul Gramann, *Journal of Cellular Plastics*, **40**, (2004) 371.
29. R.A.Roy, Primer on Taguchi Method, Competitive Manufacturing Series, New York, NY: Van Nostrand Reinhold Publications, (1990).
30. V.Sridhar, S.S. Bhagawan, R.Muraleekrishnan and S.S.Rao, "Statistical design of Experiments: Modelling rubber formulations for low temperature applications", *Chemcon 98, IChE Meet*, Visakhapatnam, Dec (1998).
31. K. Jayanarayanan, H.S. Karthick, V. Suganya, A.L. Sivasankari and S. S. Bhagawan, "Optimization of process parameters of an injection moulded nylon gear using Taguchi Methodology", *SPE ANTEC*, (2006) 1088-1092.
32. Tao.C.Chang and Earnest Faison, "Shrinkage behavior and optimization of injection moulded parts studied by Taguchi method", *Polymer Engineering and Science*, **41**, No. 5, (2001) 703-710.

33. L. M. Galantucci and R. Spina, *Journal of Materials Processing Technology*, **141**, Issue 2- 20, (2003) 266-275.
34. Kwang. J. Kim *et al*, *Smart Mater. Struct.*, **12**, (2003) 65-79.
35. Hamdi H. Demirci and John P. Coulter, *Journal of Intelligent Manufacturing*, **7**, Number **1**, (1996) 23-38.
36. Mahshid Hafezi, Saied Nouri Khorasani, *Journal of Applied Polymer Science*, **102**, Issue **6**, (2006) 5358 – 5362.
37. J.Moulton, P.Smith, *Polymer*, **33**, (1992) 2340.
38. E.C. Buruiana, M. Olaru, B.C. Simionescu, *European Polymer Journal*, **38**, (2002) 1079–1086.
39. Lee YK, Jang SM Lee YK, Jang SM, *Polymer(Korea)*, **10**, No.**2**, (1986) 125-133.
40. K.G. Princy, Studies on Conducting Polymers and Conductive Elastomer Composites, PhD Thesis, CUSAT (2002) 140.
41. S.K.Dhawan and S.Chandra, Macro '98, *Macromolecules-New Frontiers*, Allied Publishers Ltd., **1**, (1998) 320.
42. A.Dhathathreyan, N.L.Mary, G.S. Radhakrishnan, J.Collins, *Macromolecules*, **29**, (1996) 1827.
43. G. Greber, H.Gruber, A.Hassanein, US Patent 453515, 1995.

### **PREPARATION AND PROPERTIES OF POLYTHIOPHENE**

***Abstract:** Polythiophenes are important class of conjugated polymers which are in general environmentally and thermally stable materials with potential applications in EMI shielding, memory devices, transistors, NLO devices etc. Chemical oxidative polymerization is reported to be a rather simple method for the synthesis of polythiophene. The  $\text{FeCl}_3$  method does not appear to generate 2, 4-couplings in polythiophenes. The  $\text{FeCl}_3$  initiates an oxidation of the alkylthiophene to produce radical centres predominantly at the 2- and 5- positions of thiophene, which propagate to form the polymer [1]r. This chapter gives the preparation of polythiophene by chemical oxidative polymerisation of thiophene using  $\text{FeCl}_3$  as the oxidising agent in nitrobenzene solvent. The polymer was characterised by FTIR, TGA, and DSC. DC conductivity and FTIR studies show that  $\text{FeCl}_3$  acts as a good dopant for polythiophene. The prepared polythiophene was thermally stable up to  $280^\circ\text{C}$ .*

Polythiophenes are an important class of conjugated polymers which are in general environmentally and thermally stable materials. Polythiophenes are potential candidates to be used as electrical conductors, nonlinear optical devices, polymer LEDs, electro chromic or smart windows, photoresists, antistatic coatings, sensors, batteries, electromagnetic shielding materials, artificial noses and muscles, solar

cells, electrodes, microwave absorbing materials, new types of memory devices, nanoswitches, optical modulators and valves, imaging materials, polymer electronic interconnects, nanoelectronic and optical devices, and transistors[1-3]. Pure polythiophene without side chains is neither soluble nor fusible. However side chains which give solubility and fusibility to the polymer can be attached to the repeating units [1]. Polythiophenes have been prepared by chemical oxidative methods [4, 5], metal catalysed cross-coupling reactions [6-11] and electrochemical methods [12-14]. The electrochemical polymerization is usually done by electrochemical oxidation of thiophene on a Pt-coated substrate to obtain a thin uniform film. Pt is selected because it is inert against the polymerization reaction at the relatively high oxidation potential of thiophene. Metallic gold (Au) and silver (Ag) nanowire arrays coated with polythiophene (PTH) films were fabricated by successive electrochemical depositions of PTH and metal into the pores of a micro porous alumina membrane [13].

In the present work it is proposed to prepare polythiophene by chemical oxidative method using  $\text{FeCl}_3$  as the oxidising agent. The  $\text{FeCl}_3$  method does not appear to generate 2, 4-couplings in polythiophenes. The  $\text{FeCl}_3$  initiates an oxidation of the alkylthiophene to produce radical centres predominantly at the 2- and 5- positions of thiophene, which propagate to form the polymer [1].

## **4.1 EXPERIMENTAL METHODS**

### **4.1.1 Preparation of polythiophene**

0.6 M anhydrous FeCl<sub>3</sub> was added to 100 ml nitrobenzene in a RB flask. The flask was purged with nitrogen gas and 0.2 M thiophene is added to the solution drop wise under continuous stirring over 15 minutes. The RB flask is closed and the reaction is allowed to occur in nitrogen atmosphere at room temperature over a period of 24 hrs. The precipitate obtained is black in colour due to doping. Precipitate was filtered, washed and dried. Soxhlet extraction was done with methanol and acetone successively for 48 hrs. Polymer was dried in vacuum oven at 65 °C for 5 hrs. Polythiophene of dark red colour was obtained at an average yield of 90%.

### **4.1.2 Doping of polythiophene**

1g polythiophene was added to 1M solution of FeCl<sub>3</sub> in nitromethane and stirred for 24 hrs. Filtered, washed with acetone and dried in vacuum oven at 45 °C for 2 hrs.

### **4.1.3 Characterisation of polythiophene**

The FTIR of polythiophene was taken in Thermo Nicolet, Avatar 370 having spectral range of 4000-400 cm<sup>-1</sup> and a resolution of 0.9 cm<sup>-1</sup>. It is equipped with KBr beam splitter and DTGS Detector (7800 – 350 cm<sup>-1</sup>).

TGA of the samples were taken using Perkin Elmer, Diamond TG/DTA with operating temperature range from ambient to 1200°C. The TG Sensitivity is of 0.2

mg and a heating rate of 0.01 – 100°C / min and gas flow rate of 0-1000 ml/min. The different stages of degradation can be studied by noting the on set temperatures of each degradation steps, the percentage of degradation at a particular temperature, etc. Sample size is between 5 and 10 mg.

DSC curves of the samples are taken in Mettler Toledo DSC 822e operating at a temperature range of -150 °C to maximum 700 °C. The measurement resolution is 0.04 mW at RT, the heating rate is RT to 700°C in 7 min and cooling rate is + 100°C to - 100°C in 15 min. It gives the exothermic and endothermic changes occurring over a particular temperature range. DSC was recorded from 0°C to 300°C for the samples. The DC conductivity measurements were carried out on pellet samples using Keithley 2400 Sourcemeter and a Keithley 2182 Nanovoltmeter having a very low noise of 15 nV at 1s response time.

## **4.2 RESULTS AND DISCUSSION**

In this section the FTIR, TGA and DSC curves of the prepared polythiophene samples are explained.

### **4.2.1 FTIR of undoped polythiophene**

The FTIR spectrum gives an idea of the structure of the polymer formed. The comparison of FTIR spectra of the undoped and doped samples gives an idea of the extent of doping. The FTIR spectrum of undoped polythiophene is given in Figure 4.1.

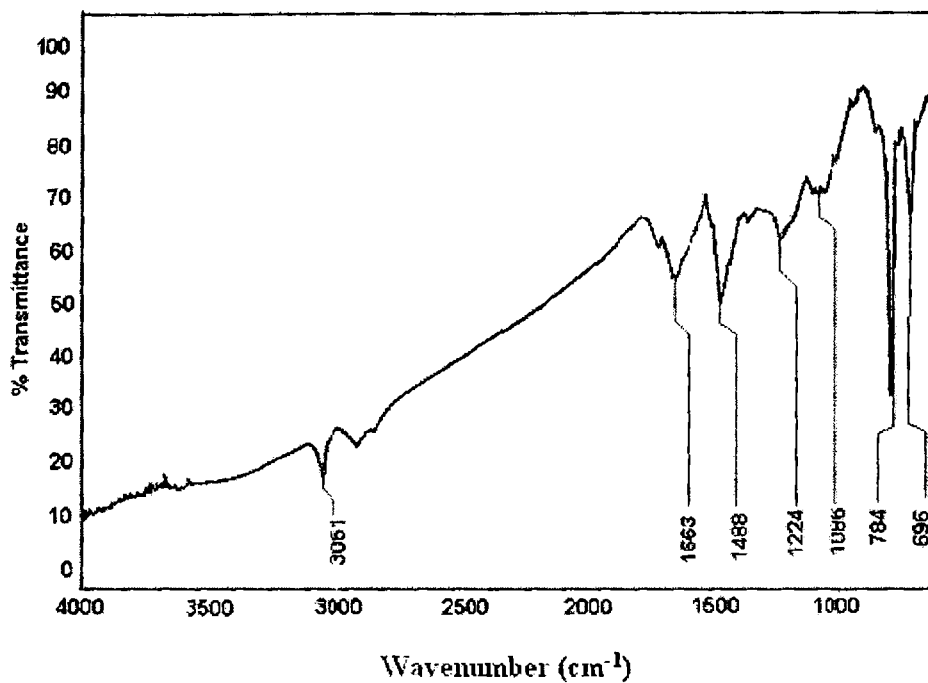


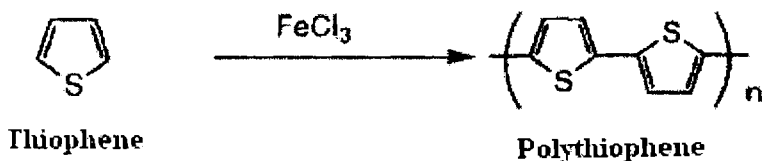
Figure 4.1 FTIR of undoped polythiophene.

The strong intensity of the  $784\text{ cm}^{-1}$  band which is characteristic of 2,5-disubstituted thiophene rings indicates that the coupling of thiophene ring occurs preferentially at 2,5 positions. Two medium bands at  $1488$  and  $1436\text{ cm}^{-1}$  are assigned to stretching vibrational modes of the thiophene ring [19]. The various peaks and the assigned vibrations are given in Table 4.1.

**Table 4.1** Absorption peaks and the assigned vibrations for undoped polythiophene.

Peak (cm <sup>-1</sup> )	Assigned to
3061	<i>C-H stretching absorption involving sp<sup>2</sup> hybridised carbon atom. Characteristic of heteroaromatics</i>
1663	<i>-C=C stretching in aromatic nuclei</i>
1488	<i>C = C asymmetric absorption. Characteristic of polythiophene</i>
1224	<i>-C-S Stretching absorption</i>
1086	<i>Aromatic C=S stretching absorption</i>
784	<i>Characteristic of 2,5-disubstituted thiophene</i>
696	<i>C-H out of plane bending, Characteristic of polynuclear aromatics</i>

From Figure 4.1 and Table 4.1 we can infer that the polymer of expected structure was formed (Scheme 4.1).

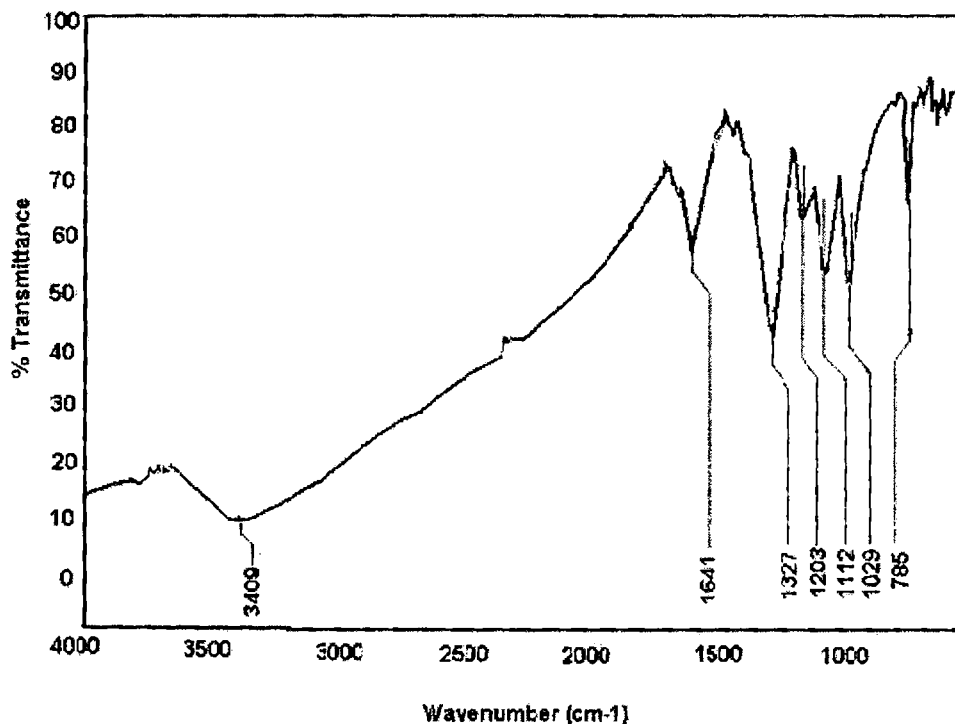


**Scheme 4.1** Polymerisation of thiophene



#### 4.2.2 FTIR of $\text{FeCl}_3$ doped polythiophene

The FTIR spectrum of  $\text{FeCl}_3$  doped polythiophene is given in Figure 4.2 and the various peaks and the assigned vibrations are given in Table 4.2.



**Figure 4.2 FTIR of  $\text{FeCl}_3$  doped polythiophene.**

From the figure 4.2 and Table 4.2 we can see that good charge delocalization has occurred and hence we can infer that  $\text{FeCl}_3$  is a good dopant for polythiophene. This is further confirmed from the DC conductivity values of the doped and undoped samples given in Table 4.3.

**Table 4.2 Absorption peaks and the assigned vibrations for doped polythiophene.**

Peak ( $\text{cm}^{-1}$ )	Assigned to
3409	<i>C-H stretching absorption involving <math>sp^2</math> hybridized carbon atom. Characteristic of heteroaromatics</i>
1641	<i>-C=C stretching in aromatic nuclei</i>
1327	<i>C = C asymmetric absorption. Characteristic of polythiophene</i>
1112	<i>Literature reports S-Cl absorption peaks at 1204- 1177 <math>\text{cm}^{-1}</math> [20]. Here this peak may be due to weak S..Cl bonds due to doping with <math>\text{FeCl}_3</math></i>
1203	<i>-C-S Stretching absorption</i>
1029	<i>Aromatic C=S stretching absorption</i>
785	<i>Characteristic of 2,5-disubstituted thiophene</i>

The DC conductivity of undoped and doped polythiophene shows that the conductivity increases by an order of 5 by doping with  $\text{FeCl}_3$ .

**Table 4.3. DC conductivity of polythiophene samples**

---

<i>Dopant</i>	<i>Conductivity (S/m)</i>
<i>Nil</i>	$6.89 \times 10^{-6}$
<i>FeCl<sub>3</sub></i>	$4.76 \times 10^{-1}$

---

#### 4.2.3 TGA/DTA curves of undoped polythiophene

The TGA and DTA curves of undoped polythiophene are given in Figure 4.3. From the TGA curve it can be seen that polythiophene is thermally stable up to 280°C. The results of differential thermal analysis show that the polymer shows an exothermic peak at 300 °C which implies the breakdown of the polymer backbone. These results matches with the reported observations [15-18]. The initial slope in the TGA curve may be due to the volatilization of low molecular weight species in the sample. This is substantiated by the DSC curve in Figure 4.4 which shows volatilization around 50-60 °C.

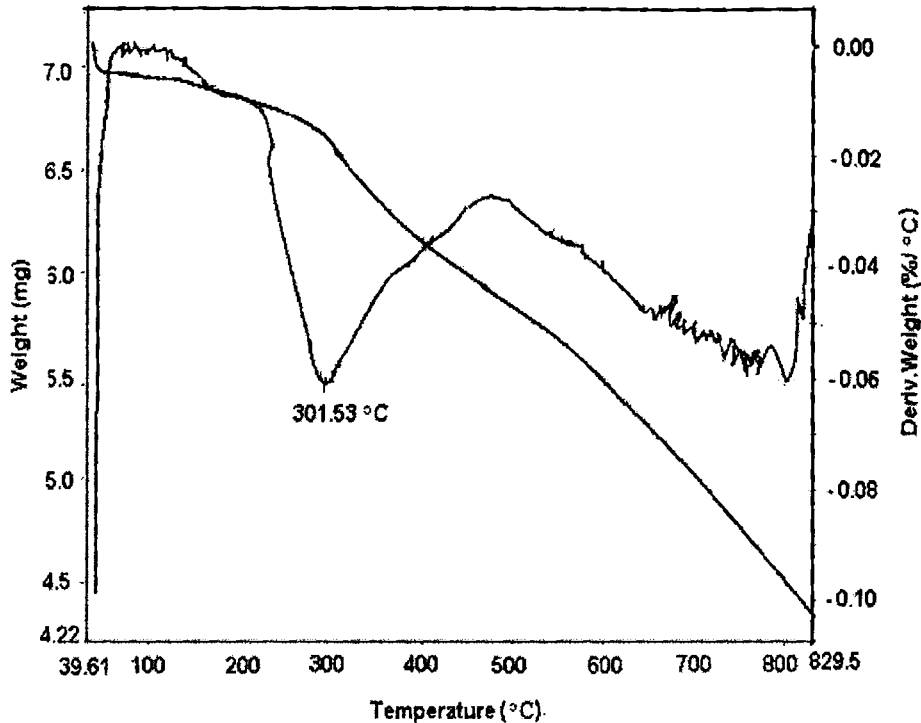


Figure.4.3 TGA/DTA curves of undoped polythiophene.

#### 4.2.4 DSC curve of undoped polythiophene

The DSC curve of the polythiophene sample is shown in Figure 4.4. PTH was heated to about 300°C and the DSC curve obtained in heating cycle is shown as curve (a). The curve shows an endothermic peak at 56 °C. This may be due to the vaporization of low molecular weight compounds in the sample. It can be seen that the degradation of the polymer starts around 100 °C. The sample is then cooled to 0 °C and again heated to about 300 °C. This heating DSC curve is shown as curve (b). In this curve there is no transition, substantiating that the peak in curve (a) was

due to vaporization of low molecular weight compounds. The curve (b) shows continuous degradation of polythiophene.

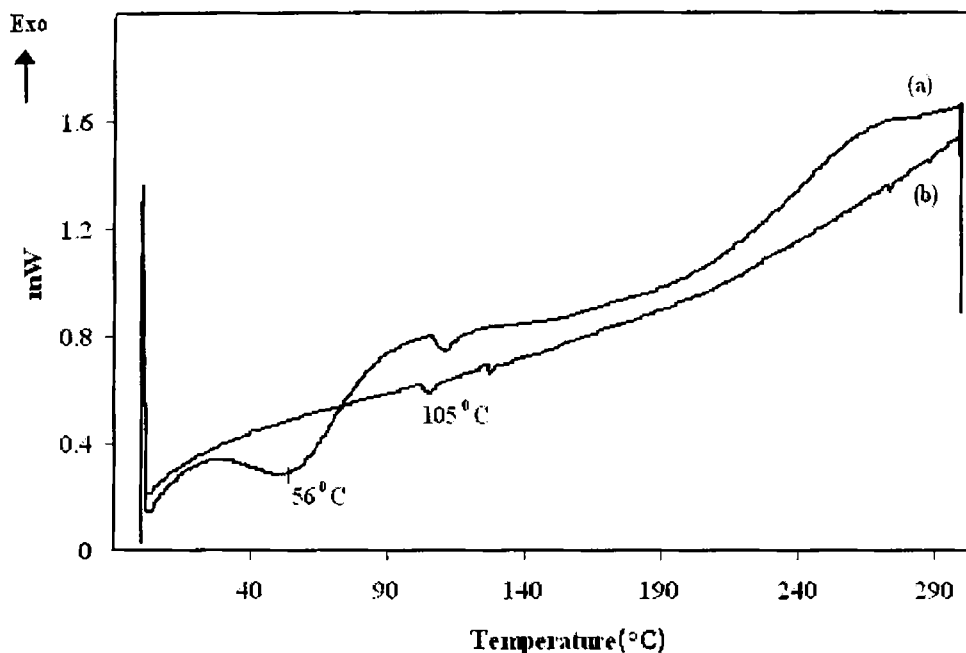


Figure 4.4 DSC curves of undoped polythiophene.

### 4.3 CONCLUSIONS

Polythiophene was prepared by chemical oxidative polymerization of thiophene using  $\text{FeCl}_3$  as oxidant in nitrobenzene solvent. FTIR spectrum of the sample proved that the polymer of expected structure was formed. The DC conductivity of undoped and doped polythiophene shows that the conductivity increases by an order of 5 by doping with  $\text{FeCl}_3$ . From the IR studies and DC conductivity values it can be seen that  $\text{FeCl}_3$  is a good dopant for polythiophene. From the TGA curve it

can be seen that polythiophene is thermally stable up to 280 °C. Break down of the polymer backbone occurs at around 300 °C.

#### 4.4 REFERENCES

1. R. D. McCullough, *Adv. Mater*, **10**, (1998) 93-116.
2. S. Geetha and D.C. Trivedi, *Synthetic Metals*, **155**, (2005) 232–239.
3. Binbin Xi, et al, *Polymer*, **47**, (2006) 7720-7725.
4. R. Sugimoto, S. Takeda, H. B. Gu, K. Yoshino, *Chem. Express*, **1**, (1986) 635.
5. K. Yoshino, S. Hayashi, R. Sugimoto, *Jpn. J. Appl. Phys.*, **23**, (1984) 899.
6. T. Yamamoto, K. Osakada, T. Wakabayashi, A. Yamamoto, *Makromol. Chem., Rapid Commun*, **6**, (1985) 671.
7. T. Yamamoto, A. Morita, T. Maruyama, Z. H. Zhou, T. Kanbara, K. Saneckika, *Polym. J. (Tokyo)*, **22**, (1990) 187.
8. T. Yamamoto, T. Maruyama, Z. H. Zhou, Y. Miyazaki, T. Kanbara, K. Saneckika, *Synth. Met.*, **41**, (1991) 345.
9. C. Z. Hotz, P. Kovacic, I. A. Khoury, *J. Polym. Sci., Polym. Chem.*, Ed., **21**, (1983) 2617.
10. M. Kobayashi, J. Chen, T. C. Chung, F. Moraes, A. J. Heeger, F. Wudl, *Synth. Met*, **9**, (1984) 77.
11. I. Colon, G. T. Kwiatkowski, *J. Polym. Sci., Polym. Chem.*, Ed., **28**, (1990) 367.
12. M. Leclerc, F. M. Diaz, G. Wegner, *Makromol. Chem.*, **190**, (1989) 3105.
13. B. Ballarin et al., *Synthetic Metals*, **114**, No.3, (2000) 279-285.

14. Jiaxin Zhang et al., *Journal of Material Science*, **38**, No. **11**, (2003) 2423-2427.
15. S. Geetha, D.C. Trivedi, *Synthetic Metals*, **155**, (2005) 232–239.
16. M.M. Nasef, *Polym. Degrad. Stabil.*, **70**, (2000) 497.
17. K.R. Benak, L. Dominguez, J. Economy, C.L. Mangun, *Carbon*, **40**, (2002) 2323.
18. M.J. Ariza, D.J. Jones, J. Rozière, *Desalination*, **147**, (2002) 183.
19. O. Ingnas, B. Liedberg, W. Chang-Ru, H. Wynberg, *Synth. Methods*, **11**, (1985) 239.
20. Robert M. Silverstein, Francis. X. Webster, *Spectrometric Identification of Organic compounds*, Sixth Edition, Wiley India Pvt. Ltd, (2006)107.

### ***PREPARATION AND PROPERTIES OF PEDOT-POLY (3, 4-ETHYLENE DIOXYTHIOPHENE)***

*Abstract:* PEDOT is one of the few organic conducting polymers that have successfully found its way from a laboratory curiosity into multiple technical applications. PEDOT was found to be almost transparent in thin, oxidized films and showed a very high stability in the oxidized state. Suspension and emulsion polymerization in the presence of long alkyl chain organic acids as dopants are expected to give high conductivity and offer a solution for the poor processability of conducting polymers. Poly (3, 4-Ethylene Dioxy thiophene) was prepared by chemical oxidative polymerization of EDOT in DBSA micellar solution using  $FeCl_3$  as the oxidising agent. The polymer was characterised by FTIR, TGA, and DSC. DC conductivity and FTIR study shows that  $FeCl_3$  and DBSA both acts as a good dopants for PEDOT and the conductivity of the order of  $10^1$  is obtained. The glass transition temperature,  $T_g$  of PEDOT was found to be  $102^0C$ .

During the second half of the 1980's, scientists at the Bayer AG research laboratories in Germany developed a new polythiophene derivative, poly (3, 4-ethylenedioxythiophene), having interesting properties. In addition to a very high conductivity (appr. 300 S/cm), PEDOT was found to be almost transparent in thin, oxidized films and showed a very high stability in the oxidized state [1-6]. The synthesis of PEDOT is carried out by chemical oxidative polymerization [7-13] electrochemical polymerization [14] and transition metal mediated coupling of dihalo



derivatives of EDOT [7, 14, 15]. The third, and most practically useful, polymerization method for EDOT is the so-called BAYTRON P synthesis that was developed at Bayer AG. This method utilizes the polymerization of EDOT in an aqueous polyelectrolyte (most commonly PSS) solution using  $\text{Na}_2\text{S}_2\text{O}_8$  as the oxidizing agent. Carrying this reaction out at room temperature results in a dark blue, aqueous PEDOT/PSS dispersion, which is commercially available from Bayer AG under its trade name BAYTRON P. An interesting aspect of BAYTRON P is that, after drying, the remaining PEDOT/PSS film is highly conducting, transparent, mechanically durable, and insoluble in any common solvent and has found several applications [11-13]. PEDOT-based polymers are applied in many applications like through-hole plating of printed circuit boards, antistatic coatings for cathode ray tubes to prevent dust attraction, primers for electrostatic spray coating of plastics, hole-injecting layers on ITO substrates for organic electroluminescent devices, transparent electrodes for inorganic electroluminescent devices, sensors, rechargeable batteries, cathode radiation tubes, photodiodes, electrochromic windows, corrosion protection, and photovoltaic devices. Of utmost importance, these examples show that PEDOT is one of the few organic conducting polymers that have successfully found its way from a laboratory curiosity into multiple technical applications [16-24].

In this study, it is proposed to prepare PEDOT by chemical oxidative polymerisation of EDOT in DBSA micellar solution. The polymer is proposed to be characterized by FTIR, TGA, DTA and DSC methods.

## **5.1 EXPERIMENTAL METHODS**

### **5.1.1 Preparation of PEDOT**

0.05M DBSA (1.6325g) was added to 90 ml of deionised water in a 250 ml RB flask and stirred for 1 hr at room temperature. Then 0.05M EDOT was added to the DBSA micellar solution and solubilised with stirring for 1 hr. Then anhydrous  $\text{FeCl}_3$  (0.05M) dissolved in 10 ml deionised water was syringed quickly and the mixture was stirred for 20 hrs at room temperature [25]. The suspension was centrifuged to get the precipitate. Precipitate was stirred with deionised water and centrifuged several times till the filtrate became colourless. Soxhlet extraction was done with acetone for 12 hrs. Bluish black polymer was obtained at an average yield of 50 %.

### **5.1.2 Characterization of PEDOT**

The FTIR of polythiophene was taken in Thermo Nicolet, Avatar 370 having spectral range of  $4000 - 400 \text{ cm}^{-1}$  and a resolution of  $0.9 \text{ cm}^{-1}$ . It was equipped with KBr beam splitter and DTGS Detector ( $7800 - 350 \text{ cm}^{-1}$ ). TGA of the samples were taken using Perkin Elmer, Diamond TG/DTA with operating temperature range from ambient to  $1200^\circ\text{C}$ . The TG Sensitivity is of 0.2 mg and a heating rate of  $0.01 - 100^\circ\text{C} / \text{min}$  and gas flow rate of 0-1000 ml/min was used. DSC curves of the samples were taken in Mettler Toledo DSC 822e operating at a temperature range of  $-150^\circ\text{C}$  to maximum  $700^\circ\text{C}$ .

## 5.2 RESULTS AND DISCUSSION

In this section the FTIR, TGA and DSC curves of the prepared PEDOT samples are explained.

### 5.2.1 FTIR of PEDOT

The FTIR spectrum of PEDOT is given in Figure 5.1. The various peaks and the assigned vibrations are given in Table 5.1.

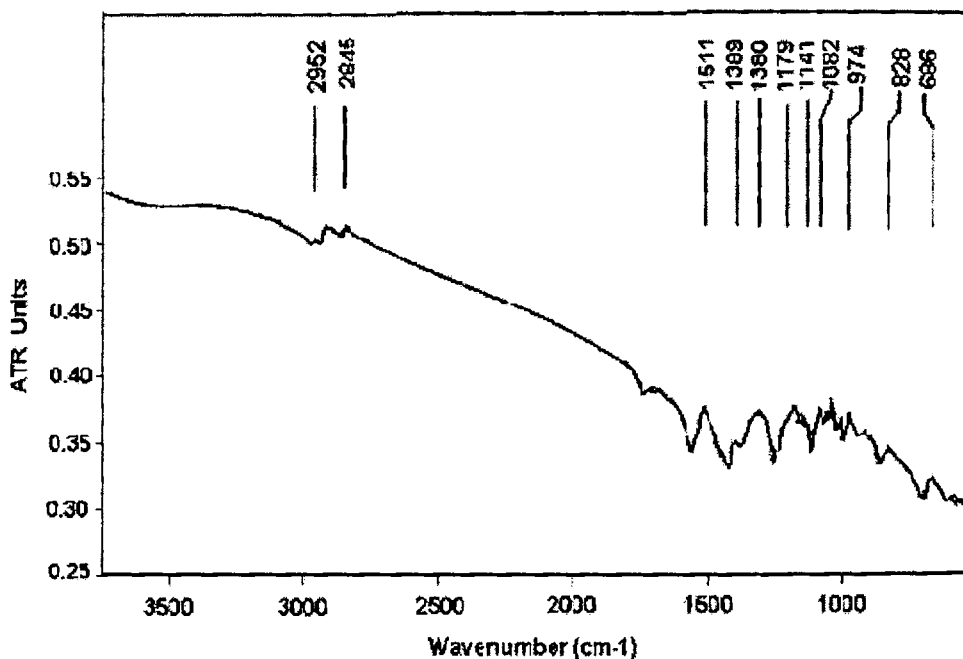


Figure 5.1 FTIR of doped PEDOT.

The vibrations at around 1389 and 1511  $\text{cm}^{-1}$  are due to C–C or C=C stretching of quinoidal structure of thiophene ring and due to ring stretching of thiophene ring,

respectively. Vibrations at 1179, 1141, and 1082  $\text{cm}^{-1}$  are originated from C–O–C bond stretching in the ethylene dioxy group. C–S bond in the thiophene ring are also seen at 974, 828, and 686  $\text{cm}^{-1}$  [26, 27]. The band at around 1380  $\text{cm}^{-1}$ , which is due to quinoidal structure, indicates the spectra of well-doped PEDOT. The small peaks ranging from 2800 to 3000  $\text{cm}^{-1}$ , which is assigned to aliphatic C–H stretching mode depending on long alkyl tail of DBSA [28], are observed in both samples. Therefore, we can surely confirm that the polymer chain is doped by DBSA.

**Table 5.1** Absorption peaks and assigned vibrations for doped PEDOT.

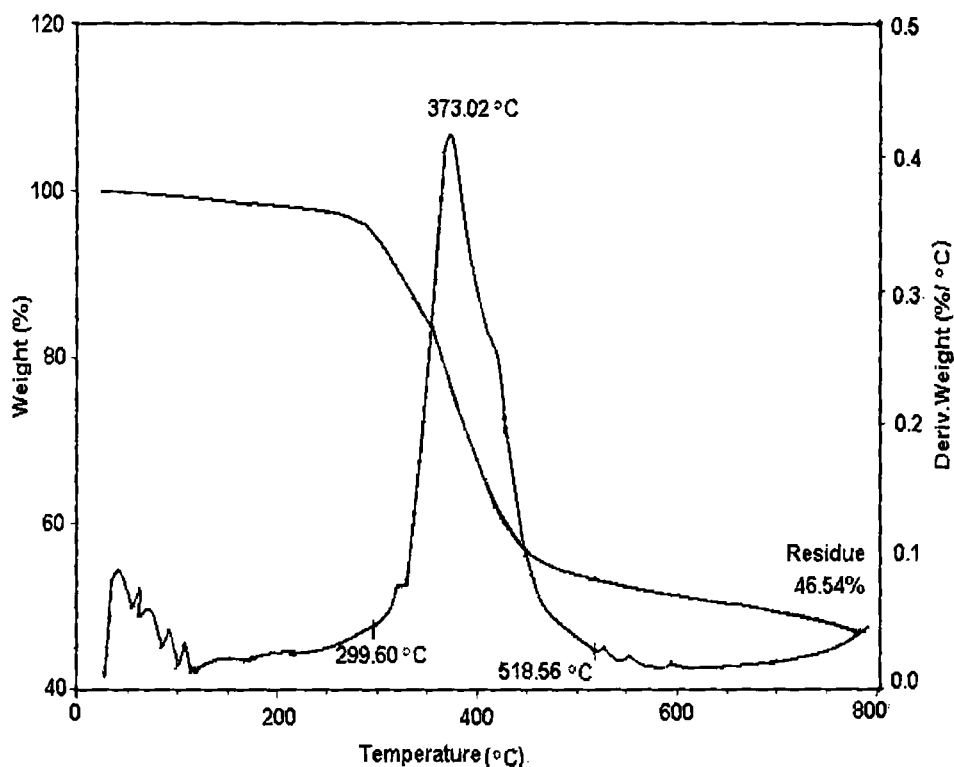
---

<b>Peak (<math>\text{cm}^{-1}</math>)</b>	<b>Assigned to</b>
2952-2845	<i>Aliphatic C–H stretching mode depending on long alkyl tail of DBSA</i>
1511	<i>Ring stretching of thiophene ring</i>
1389	<i>C–C or C=C stretching of quinoidal structure of thiophene ring</i>
1380	<i>Due to quinoidal structure, indicates good doping</i>
1179 -1141	<i>C–O–C bond stretching in the ethylene dioxy group</i>
1082	<i>Aromatic C=S stretching absorption</i>
974	<i>C–S bond in the thiophene ring</i>
686	<i>C–H out of plane bending, Characteristic of polynuclear aromatics</i>

---

### 5.2.2 TGA/DTA curves of PEDOT

The TGA and DTA curves for the prepared PEDOT are shown in Figure 5.2.



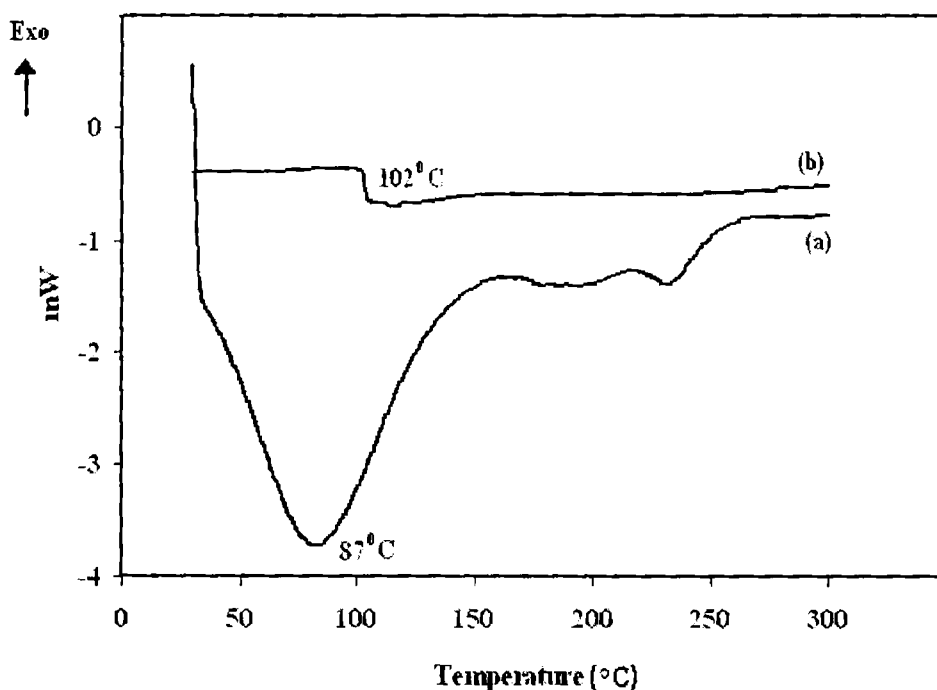
**Figure 5.2** TGA/DTA curves of PEDOT

TGA in the above figure shows that prepared PEDOT is rather stable up to the temperature of 300 °C. From 300 °C a continuous degradation occurs until major decomposition occurs in the region between 300 and 500 °C. The similar TGA analysis which was combined with DSC data on PEDOT was previously reported [24, 29]. In the study of PEDOT doped with PF<sub>6</sub> anion [29], the continuous degradation occurred from 150 °C and major decomposition occurred from 373 °C.

Compared to these results, this sample seemed to be more thermally stable up to 300 °C due to the bulky anionic surfactant which generally give conducting polymers better thermal stability.

### 5.2.3 DSC curve of PEDOT

DSC curves of the prepared PEDOT are shown in Figure 5.3.



**Figure 5.3** DSC curve of PEDOT

PEDOT was heated to about 300 °C and the recorded DSC curve (a) shows an endothermic peak at 87 °C. This may be due to the vaporization of low molecular weight compounds in the sample. The sample was then cooled from 300°C to 0°C.

This cooling curve is shown in curve (b). In this curve there is no exothermic peak showing vaporization. But the transition due to glass transition which was masked in curve (a) becomes clear. The curve shows that the  $T_g$  of PEDOT is 102 °C. We can infer that the polymer does not show degradation upto 300 °C.

### **5.3 CONCLUSIONS**

PEDOT doped with  $FeCl_3$  and DBSA was successfully prepared. The polymer is stable up to the temperature of 300°C. From 300°C a continuous degradation occurs until major decomposition occurs in the region between 300 and 500 °C. The  $T_g$  of PEDOT is found to be 102°C.

## 5.4 REFERENCES

1. X. Crispin et al, *Journal of Polymer Science: Part B: Polymer Physics*, **41**, (2003) 2561–2583.
2. J. Hwang and D. B. Tanner, *Physical Review B*, **67**, (2003) 115205.
3. Alexander Kros, Nico A.J.M. Sommerdijk, Roeland J.M. Nolte, *Sensors and Actuators B*, **106**, (2005) 289–295.
4. Dolores Caras-Quintero and Peter Bäuerle, *Chemical Communication, Communication* (2002) 2690-2691.
5. S. Moller, C. Perlov, W. Jackson, C. Taussig & St. R. Forrest, *Nature*, **426**, (2003) 166.
6. M. P. de Jong, L. J. van IJzendoorn, and M. J. A. de Voigt, *Appl. Phys. Lett.*, **77**, No. **14** (2000).
7. L. Bert Groenendaal, Friedrich Jonas, Dieter Freitag, Harald Pielartzik, and John R. Reynolds, *Adv. Mater.*, **12**, No. **7**, (2000) 481-494.
8. Y.S. Jeong, H. Goto, J.R. Reynolds and K. Akagi, *Current Applied Physics* **6**, Issue **5**, (2006) 956-959.
9. Vadivel Murugan, C.W. Kwon, G. Campet, B. B. Kale, *Active and Passive Electronic Components*, **26**, Number **2**, (2003) 81-86.
10. L. A. A. Pettersson, T. Johansson, F. Carlsson, H. Arwin, O. Ingans, *Synth. Met.*, **101**, (1999) 198.
11. Bayer AG, *Eur. Patent* 440 957, (1991).
12. Bayer AG, *Eur. Patent* 686 662, (1995).
13. Bayer AG, *US Patent* 5 792 558, (1996).
14. H. Yamato, K. Kai, M. Ohwa, T. Asakura, T. Koshiha, W. Wernet, *Synth. Met.*, **83**, (1996) 125.
15. Hong Meng et al., *J. Am. Chem. Soc.*, **125**, No. **49**, (2003) 15151 -15162.



16. S. Ghosh, O. Ingans, *Adv. Mater.*, **11**, (1999) 1214.
17. F. Larmat, J. R. Reynolds, Y. J. Qiu, *Synth. Met.*, **79**, (1996) 229.
18. Matsushita Electric Ind. Co., *Japanese Patent* JP 10 308 116, (1998).
19. Bayer AG, Eur. Patent 553 671, (1993).
20. D.M. de Leeuw, P. A. Kraakman, P. F. G. Bongaerts, C. M. J. Mutsaers, *Synthetic Metals*, **66**, (1994) 263.
21. C. Liederbaum, Y. Croonen, P. van de Weijer, J. Vleggaar, H. Schoo, *Synthetic Metals*, **91**, (1997) 109.
22. J. S. Kim, M. Granström, R. H. Friend, N. Johansson, W. R. Salaneck, R. Daik, W. J. Feast, F. Cacialli, *J. Appl. Phys.*, **84**, (1998) 6859.
23. J. S. Kim, F. Cacialli, M. Granström, R. H. Friend, N. Johansson, R. Salaneck, R. Daik, W. J. Feast, *Synth. Met.*, **101**, (1999) 111.
24. J. S. Kim, F. Cacialli, R. H. Friend, R. Daik, W. J. Feast, *Synth. Met.*, **102**, (1999) 1065.
25. Jeong Wan Choi, Moon Gyu Han, Sook Young Kim, Seong Geun Oh, Seung Soon Im., *Synthetic Metals*, **141**, (2004) 293–299.
26. K.I. Seo, I.J. Chung, *Polymer*, **41**, (2000) 4491.
27. C. Kcarnström, H. Neugebauer, S. Blomquist, H.J. Abonene, J. Kankare, A. Ivaska, *Electrochim. Acta*, **44**, (1999) 2739.
28. M.G. Han, S.K. Cho, S.G. Oh, S.S. Im, *Synth. Met.*, **126**, (2002) 53.
29. R. Kiebooms, A. Aleshin, K. Hutchison, F. Wudl, A.J. Heeger, *Synth. Met.*, **101**, (1999) 436.

---

### **MICROWAVE AND ELECTRICAL PROPERTIES OF SELECTED CONDUCTING POLYMERS**

***Abstract:** Microwave properties of conductive polymers is crucial because of their wide areas of applications such as coating in reflector antennas, coating in electronic equipments, frequency selective surfaces, EMI materials, satellite communication links, microchip antennas, medical applications etc. The present work involves a comparative study of dielectric properties of selected conducting polymers like Polyaniline, Poly (3, 4-ethylenedioxythiophene), Polythiophene, Polypyrrole, and Polyparaphenylene diazomethine (PPDA) in microwave frequencies (S band). DC conductivity of the polymer samples are also evaluated and compared. The microwave properties like dielectric constant, dielectric loss, absorption coefficient, heating coefficient, skin depth and conductivity in the microwave frequency (S band) and DC fields were compared. PEDOT and Polyaniline were found to exhibit excellent properties in DC field and microwave frequencies, which make them potential materials in many of the aforementioned applications.*

Microwave properties of conductive polymers is crucial because of their wide areas of applications such as coating in reflector antennas, coating in electronic equipments, frequency selective surfaces, EMI materials, satellite communication links, microchip antennas etc[1-3]. Many microwave absorbing materials based on conducting polymers have been developed. Rimili and coworkers have developed

Polyaniline (PANI/DEHEPSA) films of high conductivity (5000-6000 S/m) and permittivity of above 6000 over X and S bands [4]. This confirms the metallic character of PANI films and their efficient use in micro-electronic technology such as microwave integrated circuits (MMIC) and microwave devices.

Many microwave absorbing materials based on conducting polymers have been developed [5, 6]. A comparative study of dielectric properties of selected conducting polymers like Polyaniline, Poly (3, 4-ethylenedioxythiophene), Polythiophene, Polypyrrole, and Polyparaphenylene diazomethine (PPDA) in microwave and DC fields is proposed to be undertaken in this study. The microwave properties like dielectric constant, dielectric loss, absorption coefficient, heating coefficient, skin depth and conductivity in the microwave frequency (S band) and DC fields will be compared.

## **6.1 EXPERIMENTAL METHODS**

Polythiophene was prepared by chemical oxidative polymerisation using  $\text{FeCl}_3$  as oxidant in nitrobenzene solvent [7]. Poly (3, 4-ethylenedioxythiophene) was prepared in aqueous DBSA micellar solution using  $\text{FeCl}_3$  as oxidising agent [8]. Chemical oxidative polymerization of aniline was carried out using  $\text{FeCl}_3$  as oxidising agent in aqueous media [9]. Polyaniline (PANI) was doped with 1M solution of camphor sulfonic acid for 24 hrs. Polypyrrole was prepared by the polymerisation of pyrrole with ferric chloride in methanol solvent [10]. The polymer was then doped in 1M  $\text{FeCl}_3$  solution in nitromethane for 24 hrs. Poly paraphenelyne diazomethine (PPDA) was prepared by solution polycondensation of para phenylene diamine and glyoxal trimeric hydrate in DMF at a molar ratio of 1:1 at 120 °C for 5 hrs. PPDA was doped with 1 M solution of HCl for 24 hrs.

The conductivity measurements were carried out on pellet samples using Keithley 2400 Sourcemeter and a Keithley 2182 Nanovoltmeter having a very low noise of 15 nV at 1s response time. The dielectric properties in microwave frequencies (S band 2-4 GHz) were evaluated by Cavity Perturbation Technique. The transmission type resonator used in this experiment was excited with TE<sub>10P</sub> mode by connecting it to an HP8510 C Network Analyzer. The rectangular wave guide cavity resonator was constructed from a section of standard WR-284 wave guide.

The resonant frequency ' $f_0$ ' and the corresponding quality factor ' $Q_0$ ' of each resonant peak of the empty cavity are first determined. Now after selecting a particular resonant frequency, the dielectric sample is introduced into the cavity and the position is adjusted for maximum perturbation (i.e. maximum shift of resonant frequency towards the low frequency region, with minimum amplitude for the peak) and the corresponding change in the frequency of the resonant peak is observed. The new resonant frequency ' $f_s$ ' the corresponding 3 dB bandwidth and the quality factor ' $Q$ ' are determined. The procedure is repeated for other resonant frequencies and the measurements are carried out for all the samples. Knowing the volumes of the sample and the cavity resonator the dielectric parameters can be evaluated [11-15].

The parameters are calculated using the following formulae (1-7)

$$\epsilon' = 1 + \frac{f_0 - f_s}{2f_s} \left[ \frac{V_c}{V_s} \right] \quad (1)$$

$$\epsilon'' = \frac{V_c}{4V_s} \left[ \frac{Q_0 - Q_s}{Q_0 \cdot Q_s} \right] \quad (2)$$

$$J = \frac{1}{\epsilon \tan \delta} \quad (3)$$

$$\alpha = \frac{\epsilon'' f}{n.c} \quad (4)$$

$$\sigma = 2\pi f \epsilon_0 \epsilon'' \quad (5)$$

$$\tan \delta = \frac{\epsilon''}{\epsilon'} \quad (6)$$

$$d = \frac{1}{\alpha} \quad (7)$$

Where,

$\epsilon'$  = Dielectric constant

$\epsilon''$  = Loss factor

$\epsilon_0$  = Permittivity of free space

$\alpha$  = Absorption Coefficient

$d$  = Penetration depth

$\sigma$  = Conductivity

$J$  = Efficiency of heating

$c$  = Velocity of light

$V_c$  = Volume of cavity

$V_s$  = Volume of sample

## 6.2 RESULTS AND DISCUSSION

### 6.2.1 Microwave properties

#### 6.2.1.1 Dielectric constant ( $\epsilon'$ )

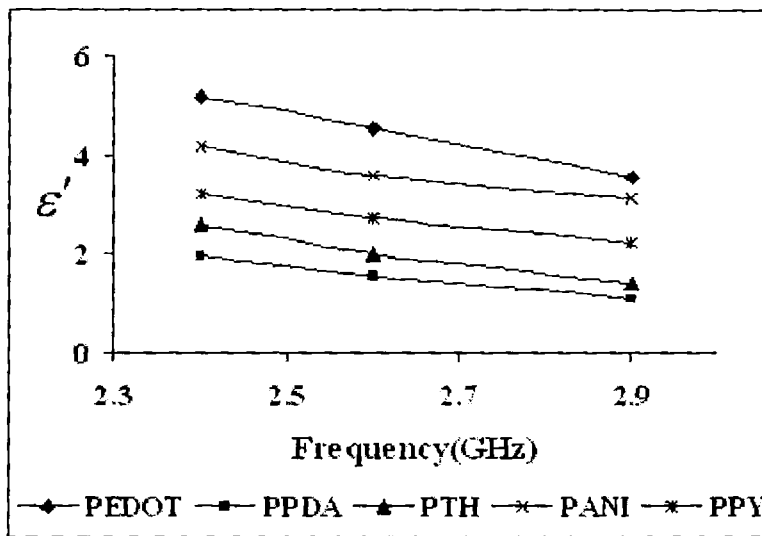
The dielectric constant of different conducting polymers at S band frequency is compared in Figure 6.1. When an electric field is applied to a material, an induced dipole moment connected to the polarizability appears. This dipole moment comes from a non-homogeneous repartition of the electrical charges in the material. That repartition corresponds to several types of polarization

- The electronic cloud displacement around the atom called electronic polarization.
- Electric field can modify the electron repartition and consequently the equilibrium location of the atoms in the molecule, called as the atomic polarization.
- Orientation of permanent dipoles causing dipolar polarization

The higher the polarizability of the material the greater will be the dielectric constant.

Figure 6.1 shows that dielectric constant decrease with increase in frequency. This is due to the orientation polarization in the microwave field. The polarization is caused by the alternating accumulation of charges at interfaces between different phases of the material. This dipole polarization may be related to the frictional losses caused by the rotational displacement of molecular dipoles under the influence of the alternating electrical field. As the frequency of the applied field is increased the polarization has no time to reach its steady field value and the orientation polarization is the first that falls. Due to the orientation polarization of

the dipoles, the possibility of dielectric relaxation (so also dielectric loss) cannot be ruled out at higher frequencies. This might result in the decrease of ' $\epsilon'$ ' with frequency [16-17]. It can be seen that the dielectric constant is highest for PEDOT, and lowest for PPDA.



**Figure 6.1** Variation of dielectric constant ( $\epsilon'$ ) with frequency for various conducting polymers.

In conducting polymers conductivity is not constant along the conducting paths and that several relaxation times may coexist. The distribution of conductivity leads to a dispersion of ' $\epsilon'$ ' and ' $\sigma$ ' without any polarization phenomenon. So the large dielectric constants measured at low frequency in conducting polymers may be linked to the heterogeneity of materials in the form of a conductivity variation along the conducting path. At low frequencies, the different polarizations (electronic, atomic and dipolar polarizations) contribute to a high permittivity ' $\epsilon'$ ' value, beyond that each kind of polarization will create one resonance or one

relaxation process and ' $\epsilon'$ ' decreases. The same trend in variation of dielectric constant with frequency has been reported by Chandrasekhar and Naishadham [18]. The decrease of permittivity with increase in frequency reveals that the systems exhibit strong interfacial polarization at low frequency [19].

### 6.2.1.2 Dielectric loss ( $\epsilon''$ )

The dielectric loss of different conducting polymers at S band frequency is compared in Figure 6.2.

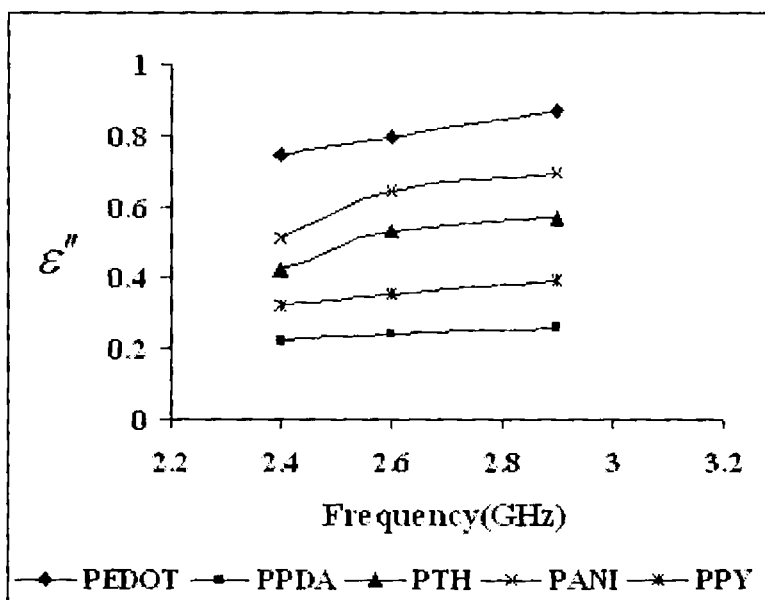


Figure 6.2 Variation of dielectric loss ( $\epsilon''$ ) with frequency for various conducting polymers.

The reorientation of the unassociated groups, because of their high dipole moment, is believed to be a major contributor to the dielectric loss ( $\epsilon''$ ). At higher



frequency, the rotatory motion of the molecules may not be sufficiently rapid for the attainment of equilibrium with the field. The polarization then acquires a component out of phase with the field, and the displacement current acquires a conductance component in phase with the field, resulting in thermal dissipation of energy. When this occurs, dielectric losses will be generated.

Dielectric loss tends to increase with increase in frequency within the range 2.4 to 2.9 GHz. As the frequency is increased the inertia of the molecule and the binding forces become dominant and it is the basis for high dielectric loss at higher frequencies. The dielectric loss factor leads to so called conductivity relaxation. From the Figure 6.2 it is clear that PEDOT is showing higher dielectric loss followed by PANI, PTH, PPY and PPDA.

The loss factor must be regarded as the contribution of three distinct effects, due to DC conductance, interfacial polarization, and dipole orientation or Debye loss factor, i.e. [20]

$$\varepsilon'' = \varepsilon''_{\text{conduction}} + \varepsilon''_{\text{polarization}} + \varepsilon''_{\text{dipolarorientation}}$$

At lower frequencies, the loss factor decreases linearly with the increasing of frequency. This result suggests that dc conductivity process is more significant than interfacial polarization in these materials. The interfacial polarization equation does not follow a linear behavior at lower frequencies. Generally it is believed in dielectric analysis that the high frequency permittivity (dielectric constant) is mainly associated to dipolar relaxation, whereas at lower frequency and higher temperature, the contributions of interfacial polarization and DC conductivity become more significant in both ' $\varepsilon'$ ' and ' $\varepsilon''$ '. Interfacial polarization arises

mainly from the existence of polar and conductive regions dispersed in relatively less polar and insulating matrix. This phenomenon is particularly important in conjugated polymers and may interfere on the relaxation process analysis [21]. The value of  $\varepsilon''$  polarization is related to the molecular polarization phenomena such as dipole rotation (Debye model), space charge relaxation (Maxwell-Wagner model) and hopping of confined charges [22-24].

#### *6.2.1.3 Loss tangent ( $\tan \delta$ )*

The  $\tan \delta$  is commonly employed as a direct measure of the dielectric loss, which in turn provides a measure of the conductivity. Angle ' $\delta$ ' is the angle between the vector for the amplitude of the total current and that for the amplitude of charging current and the tangent of this angle is the loss tangent [25]. Since it is directly related to the dielectric loss, it shows the same behavior as that of dielectric loss. Figure 6.3 shows that the loss tangent of conducting polymers increases with frequency.

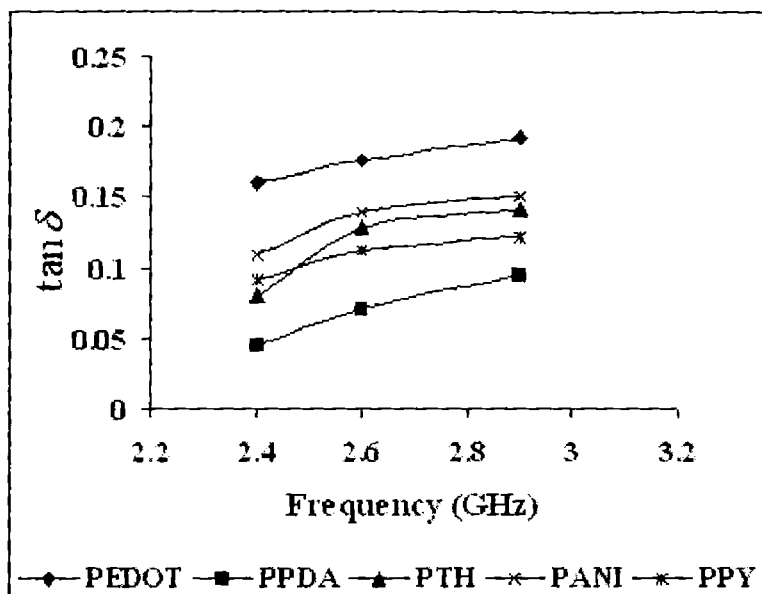


Figure 6.3 Variation of loss tangent ( $\tan\delta$ ) with frequency for various conducting polymers.

#### 6.2.1.4 Absorption coefficient ( $\alpha$ )

Materials can be classified in terms of their transparency of wave through it, which in turn specify the absorption of electromagnetic waves when it passes through the medium [25]. The transparency is defined by the parameter, absorption coefficient. Absorption coefficient is directly related to the dielectric loss factor and therefore it shows the same behavior as dielectric loss. Figure 6.4 shows that PEDOT has highest absorption coefficient followed by PANI, PTH, PPY and PPDA respectively.

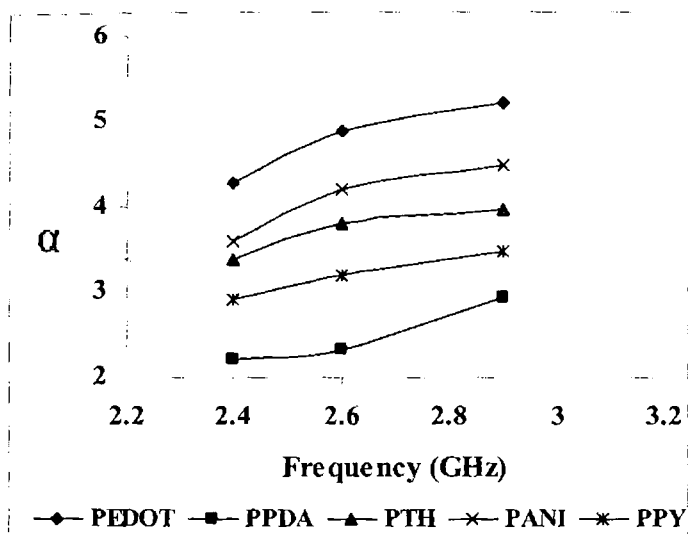
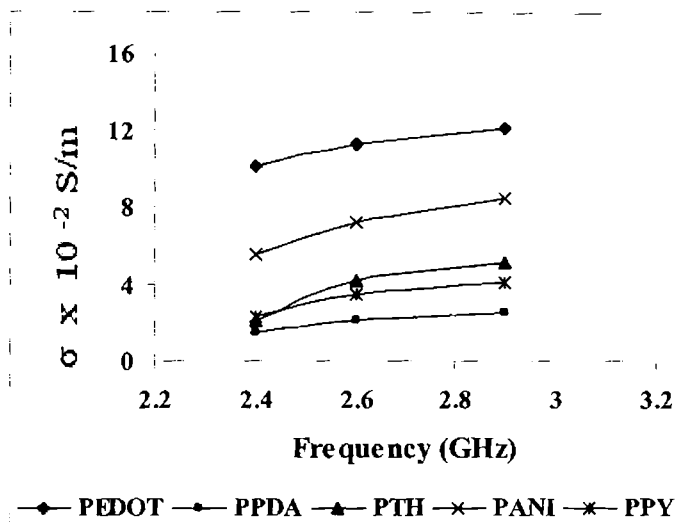


Figure 6.4 Variation of absorption coefficient ( $\alpha$ ) with frequency for various conducting polymers.

#### 6.2.1.5 Conductivity ( $\sigma$ )

The microwave conductivity is a direct function of dielectric loss and so it shows a similar variation with frequency as the dielectric loss factor. Figure 6.5 shows that conductivity increases with frequency. Here also the trend continues with PEDOT showing the best conductivity followed by PANI, PTH, PPY and PPDA successively.



**Figure 6.5** Variation of conductivity ( $\sigma$ ) with frequency for various conducting polymers.

#### 6.2.1.6 Dielectric heating coefficient ( $J$ )

Practically all applications of polymers in electrical and electronic engineering require materials with a low  $\tan \delta$ . However, one application that takes advantage of a high value of loss tangent is high frequency dielectric heating. As the heat generation in polymers is due to relaxation loss, the efficiency of heating of a polymer is compared by means of a heating coefficient [26] ' $J$ '. Higher the ' $J$ ' value, poorer will be the polymer for dielectric heating purposes. Of course, the heat generated in the polymeric material comes from the loss tangent, but that loss may not come entirely from the relaxation loss. Rather, conductivity of the polymeric material may also contribute to the  $\tan \delta$ . This situation may be compared with ohmic heating of metals [13].

The heating coefficient is inversely related to the loss tangent and hence it decreases with increase in frequency.

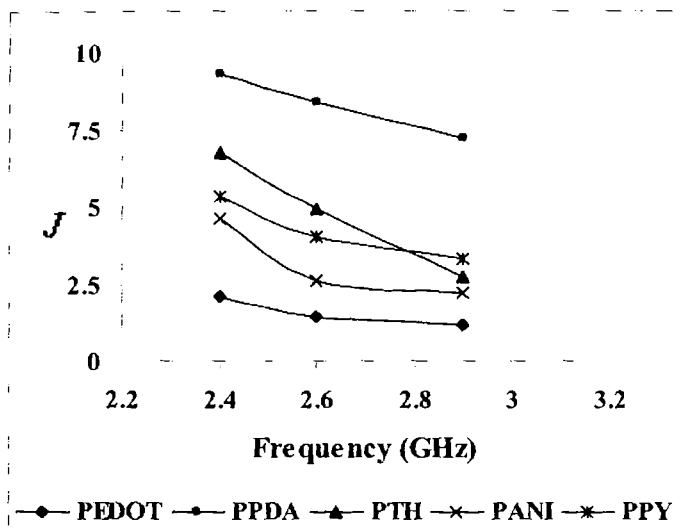
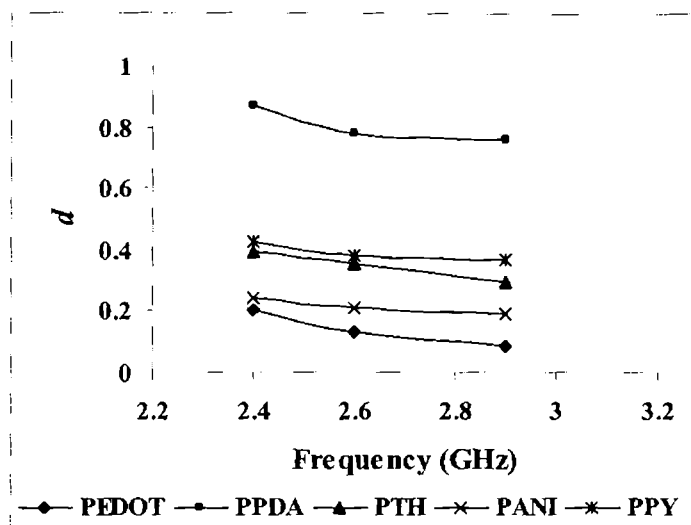


Figure 6.6 Variation of heating coefficient ( $J$ ) with frequency for various conducting polymers.

#### 6.2.1.7 Skin depth ( $d$ )

Figure 6.7 shows that skin depth decreases with increase in frequency. It is the effective distance of penetration of an electromagnetic wave into the material. It can be applied to a conductor carrying high frequency signals. The self inductance of the conductor effectively limits the conduction of the signal to its outer shell and the shell thickness is the skin depth, which decreases with increase in frequency. PPDA shows highest skin depth followed by PPY, PTH, PANI and PEDOT.



**Figure 6.7** Variation of Skin depth ( $d$ ) with frequency for various conducting polymers.

### 6.2.2 DC conductivity

DC conductivity of the polymer samples are tabulated in Table 6.1. From the Table 6.1 it can be seen that the DC conductivity of the conducting polymers follows the order PEDOT > PANI > PTH > PPY > PPDA.

PANI and PEDOT are reported to show very good DC conductivity. In the case of PEDOT synthesized in dodecyl benzene sulfonic acid (DBSA) micellar solutions, DBSA-FeCl<sub>3</sub> complex is expected to be formed. The anchoring efficiency of dodecylbenzene sulfonate anion with iron (III) on the PEDOT particles seems to increase the doping of the bulky anionic surfactant and gives good conductivity [8].

**Table 6.1 DC conductivity of the polymer samples.**

No.	Sample	Dopant	Conductivity (S/m)
1	PEDOT	FeCl <sub>3</sub> &DBSA	26.41
2	PANI	CSA	2.45
3	PTH	FeCl <sub>3</sub>	4.76 x 10 <sup>-1</sup>
4	PPY	FeCl <sub>3</sub>	1.25 x 10 <sup>-1</sup>
5	PPDA	HCl	1.36 x 10 <sup>-4</sup>

### 6.3 CONCLUSIONS

Dielectric constant, dielectric loss, conductivity, absorption coefficient, heating coefficient, loss tangent and skin depth of conducting polymers like PEDOT, PTH, PANI and PPDA were studied and compared at S band frequency. The important conclusions are

- Dielectric constant, Dielectric loss,  $\tan \delta$ , conductivity and absorption coefficient of the conducting polymers are highest for PEDOT and PANI
- Heating coefficient and skin depth are lower for PEDOT and PANI
- Comparing the different polymers, better microwave properties are shown by PEDOT and PANI



- Dielectric constant, heating coefficient and skin depth tends to decrease with increase in frequency and dielectric loss, conductivity, loss tangent and absorption coefficient increases with increase in frequency in S band.
- PEDOT doped with DBSA and  $\text{FeCl}_3$  was found to have very good DC conductivity of 26.41 S/m. PANI also offered very good conductivity, 2.45 S/m.
- DC conductivity of the conducting polymers are in the order  
PEDOT > PANI > PTH > PPY > PPDA

The microwave and electrical properties of some important conducting polymers were successfully evaluated. PANI and PEDOT showed good microwave and electrical properties and hence have potential applications in EMI shielding, microwave absorption etc.

## 6.4 REFERENCES

1. S.K. Dhawan, N.Singh, S. Venkatachalam, *Synthetic Metals*, **129**, Number 3, (2002) 261-267.
2. Narayan Chandra Das et al, *Polymer International*, **54**, Number 2, (2005) 256-259.
3. Mihaela Baibarac, Gómez-Romero, Pedro, *Journal of Nanoscience and Nanotechnology*, **6**, Number 2, (2006) 289-302.
4. H. Rmili, J.L. Miane, H. Zangar and T.E. Olinga, *Eur. Phys. J. Appl. Phys.*, **29**, (2005) 65-72.
5. Roselena Faez, Inácio M. Martin, Marco-A De Paoli, Mirabel C. Rezende, *Journal of Applied Polymer Science*, **83**, Issue 7, (2001) 1568 – 1575.
6. Yuping Duan, Shunhua Liu, Bin Wen, Hongtao Guan and Guiqin Wang, *Journal of Composite Materials*, **40**, No. 20, (2006) 1841-1851.
7. T. Yamamoto et al, *Macromolecules*, **25**, (1992) 1214.
8. Jeong Wan Choi et al, *Synthetic Metals*, **141**, (2004) 293–299.
9. Subramaniam, Radhakrishnan, Deshpande, Shripad Dagadopant, United States Patent 20040198948 (2004).
10. S.Machida, S.Miyata, A.Techagumpuch, *Synthetic Metals*, **31**, (1989) 31.
11. K.Kupfer, A.Kraszewski, and R.Kno"chel, "RF & Microwave Sensing of Moist Materials, Food and other Dielectrics", *Sensors Update*, **7**, Wiley-VCH, Germany, (2000) 186–209.
12. S.B. Kumar et al., *Journal of the European Ceramic Society*, **21**, (2001) 2677–2680.
13. K.T. Mathew et al, *Materials Chemistry and Physics*, **79**, (2003) 187–190.
14. Honey John, Rinku M. Thomas, K. T. Mathew, Rani Joseph, *Journal of Applied Polymer Science*, **92**, Issue 1, (2004) 592 – 598.

15. H.John, S.Bijukumar, K.T.Mathew, Rani Joseph, *Plastics, Rubber and Composites*, **32**, No. 7, (2003) 306-312.
16. E.J. Frommer, R.R. Chance, *Electrical and electronic properties of polymers: state of the art compendium*, Encyclopedia Reprint Series, in: I.J. Kroschwitz (Ed.), Wiley Interscience, New York, (1988) 101-178.
17. T.A. Ezquerra, F. Kremmer, G.Wegner, "AC electrical properties of insulator conductor composites", in: A. Priou (Ed.), *Dielectric Properties of Heterogeneous Materials: Progress in Electromagnetic Research*, **6**, Elsevier, New York, 1992.
18. P. Chandrasekhar and K. Naishadham, *Synthetic Metals*, **105**, (1999) 115-120
19. Legros and A. Fourrier-Lamer, *Mat.Res.Bull.*, **19**, (1984) 1109.
20. C.P.Smyth, *Dielectric behavior and structure*, New York: McGraw-Hill Book Company Inc.; 1955. p. 191.
21. B.G. Soares et al, *European Polymer Journal*, **42**, (2006) 676-686.
22. A.Moliton, J.L.Duroux and G.Froyer, *Ann.Phys., Fr.*, (1988) 261-287.
23. L.Olmedo et al, *Revue des Composites et des Nouveaux Materiaux*, **1**, (1991) 123.
24. I.S.Bradford, M.H. Carpentier, *The Microwave Engineering Handbook*, Chapman and Hall, London (1993).
25. C.Ku Chen, Raimond Liepins, *Electrical Properties of Polymers: Chemical Principles*, Hanser Publishers, Munich, Chapter 3 (1987).

---

# MICROWAVE PROPERTIES OF SELECTED THERMOPLASTIC CONDUCTING COMPOSITES

***Abstract:** To improve the processability of a conducting polymer, various methods to incorporate conducting polymer into processable insulating polymer have been reported. In this study we have prepared thermoplastic conducting composites of selected conducting polymers with PVC and PU. Thermoplastic conducting composites of PPDA, PTH, PEDOT and PANI with PVC and PU were prepared. In the preparation of PTH-PVC, PEDOT-PVC, PANI-PVC, PEDOT-PU and PANI-PU composites, in situ polymerisation of the monomer in thermoplastic polymer solution using  $FeCl_3$  as the oxidising agent was employed. The conditions for preparation of PTH-PVC composites were optimized. The microwave properties of all the composites like dielectric constant, dielectric loss, absorption coefficient, heating coefficient, skin depth and conductivity in the microwave frequency (S band) were studied in the S band and the best composite was selected for further studies.*

Though various novel properties have been observed in conducting polymers, their practical applications have been rather limited, because of poor processability. To improve the processability of a conducting polymer, various methods to incorporate conducting polymer into processable insulating polymer have been reported. Methods of the preparation of insulating polymer - conducting polymer composite in which electrical conductivity can be varied by many orders of

magnitude ranging from insulator to metal by changing the concentration of conducting polymer have been described [1-14].

Conducting polymers show some specific characteristics in microwave frequencies that make them far more interesting than traditional dielectric materials. The intrinsic conductivity of conjugated polymers leads, in the field of their microwave properties, to a dynamic conductivity leading to high levels of dielectric constant [1-4]. One of the inherent problems with conducting polymers is that they are typically intractable. To overcome the problems of processing some of the conducting polymers are made into emulsions and suspensions (PEDOT, PPY etc) ready for coating [5-7]. Formation of composites with thermoplastic materials either by physical blending [8-9] or forming a core-shell type of structures is another method [10-11]. Polypyrrole, has been polymerised on the surface of PVA, PVC and within it to form composites. Textile materials have been used as substrates for a number of materials and have been coated with conducting polymers by soaking them with oxidant and then exposing them to monomer. The use of polypyrrole coated fabrics (including glass fibres) enables the formation of structural Radar Absorbing Material (RAM). The properties of the fabric-coated materials were modelled and made as Salisbury Screens and Jaumann layers [12-14]. It is now possible to design materials possessing permittivities, which have low variation with the frequency ( $\epsilon'' \propto \omega^{-0.3}$ ) or high variation ( $\epsilon'' \propto \omega^{-0.7}$ ) directly correlated to the intrinsic conductivity of the polymer. To obtain the best performance (large bandwidth) these materials have to be associated in multilayer structures. Moreover, the use of structural laminates allows the integration of two functions, stealth and mechanical [1].

It has been shown that PANI can be made compatible with a range of common organic solvents and polymers, with the aid of an appropriate sulfonic acid.

Dodecylbenzene sulfonic acid (DBSA) is particularly important in this regard. This simultaneously renders the PANI conductive and, by acting in a manner analogous to a surfactant [15], presents the possibility of solution blending [16-18] or direct melt-mixing [19] with a range of conventional plastics, to produce blends which show little or no evidence of a percolation threshold [20]. Although similar electrical results obtained from nanoparticle blends of PANI doped with hydrochloric acid [21] imply that the absence of a percolation threshold is not necessarily associated with thermodynamic compatibility, it is evident that conducting polymer blends differ fundamentally from composites containing conducting fillers, in that the two components are intimately mixed on the nanometer scale. Consequently, extensive control of conductivity is theoretically possible, simply by varying the protonating acid, processing conditions, doping level and the amount of PANI within the blend [22].

PVC and PU are among the most versatile thermoplastics widely used alone and as blends with other polymers. They have good processability and are polar in nature making them soluble in many solvents and partially miscible with many polymer matrices. In this study, the preparation of composites of PPDA, PTH, PEDOT and PANI with PVC and PU by in situ polymerisation is proposed to be undertaken. In the preparation of PTH-PVC, PEDOT-PVC, PANI-PVC, PEDOT-PU and PANI-PU composites,  $\text{FeCl}_3$  was used as the oxidising agent. The optimum quantity of  $\text{FeCl}_3$  required for the polymerisation of thiophene in PVC solution has to be determined. For further studies this optimum quantity of  $\text{FeCl}_3$  will be used for the polymerisation of EDOT and aniline in PVC and PU solutions. The microwave properties of all the composites will be studied in the S band and the best combination is proposed to be identified.

## ***PART-I***

### **7.1 OPTIMISATION OF RATIO OF FeCl<sub>3</sub>: THIOPHENE IN PREPARING PTH-PVC COMPOSITES**

One of the easiest routes to prepare polythiophenes is by chemical oxidation of thiophenes using FeCl<sub>3</sub>. The ratio of FeCl<sub>3</sub>: Thiophene for polymerisation used by different research groups was different. [23-25]. Since the PVC- PTH composite is prepared by insitu polymerisation of thiophene in PVC solution, the FeCl<sub>3</sub>: Thiophene ratio is very critical. If the amount of FeCl<sub>3</sub> added is not adequate, it will lead to incomplete polymerisation. If the quantity of FeCl<sub>3</sub> is more than that is required it will affect the properties. So blends with various FeCl<sub>3</sub>: Thiophene ratios were prepared and their microwave properties were studied to find an optimum FeCl<sub>3</sub>: Thiophene ratio.

#### **7.1.1 Experimental methods**

Thiophene was added to the PVC solution in THF to get a 10% 1:1 PVC-Thiophene mixture. FeCl<sub>3</sub> dissolved in THF was then added to this mixture and the reaction is carried out for 24 hrs. Composites were prepared with FeCl<sub>3</sub>: thiophene ratio of 1.5, 2, 2.5 and 3. About 10 ml of the composite solutions were cast in petridish and allowed to dry at room temperature for 24 hrs. Thin strips of the film were cut and the dielectric properties in microwave frequencies (S band 2-4 GHz) were evaluated by Cavity Perturbation Technique. The transmission type resonator used in this experiment was excited with TE<sub>10P</sub> mode by connecting it to an HP8510 C Network Analyzer.

The resonant frequency ' $f_0$ ' and the corresponding quality factor ' $Q_0$ ' of each resonant peak of the empty cavity are first determined. Now, after selecting a

particular resonant frequency, the dielectric sample is introduced into the cavity and the position is adjusted for maximum perturbation (i.e. maximum shift of resonant frequency towards the low frequency region, with minimum amplitude for the peak) and the corresponding change in the frequency of the resonant peak is observed. The new resonant frequency ' $f_s$ ' the corresponding 3 dB bandwidth and the quality factor ' $Q$ ' are determined. The procedure is repeated for other resonant frequencies and the measurements are carried out for all the samples. Knowing the volumes of the sample and the cavity resonator the dielectric parameters can be evaluated. The parameters are calculated using the following formulae (1-7)

$$\varepsilon' = 1 + \frac{f_0 - f_s}{2f_s} \left[ \frac{V_c}{V_s} \right] \quad (1)$$

$$\varepsilon'' = \frac{V_c}{4V_s} \left[ \frac{Q_0 - Q_s}{Q_0 \cdot Q_s} \right] \quad (2)$$

$$J = \frac{1}{\varepsilon \tan \delta} \quad (3)$$

$$\alpha = \frac{\varepsilon'' f}{n.c} \quad (4)$$

$$\sigma = 2\pi f \varepsilon_0 \varepsilon'' \quad (5)$$

$$\tan \delta = \frac{\varepsilon''}{\varepsilon'} \quad (6)$$

$$d = \frac{1}{\alpha} \quad (7)$$

Where,

$\varepsilon'$  = Dielectric constant

$\varepsilon''$  = Loss factor

$\varepsilon_0$  = Permittivity of free space

$\alpha$  = Absorption Coefficient

$d$  = Penetration depth

$\sigma$  = conductivity

$J$  = Efficiency of heating

$c$  = velocity of light

$V_c$  = Volume of cavity

$V_s$  = Volume of sample



## 7.1.2 Results and discussion

### 7.1.2.1 Effect of ferric chloride on dielectric constant ( $\epsilon'$ ) of PTH-PVC composite

Figure 7.1 shows the variation of dielectric constant with FeCl<sub>3</sub>: Thiophene ratio at various frequencies.

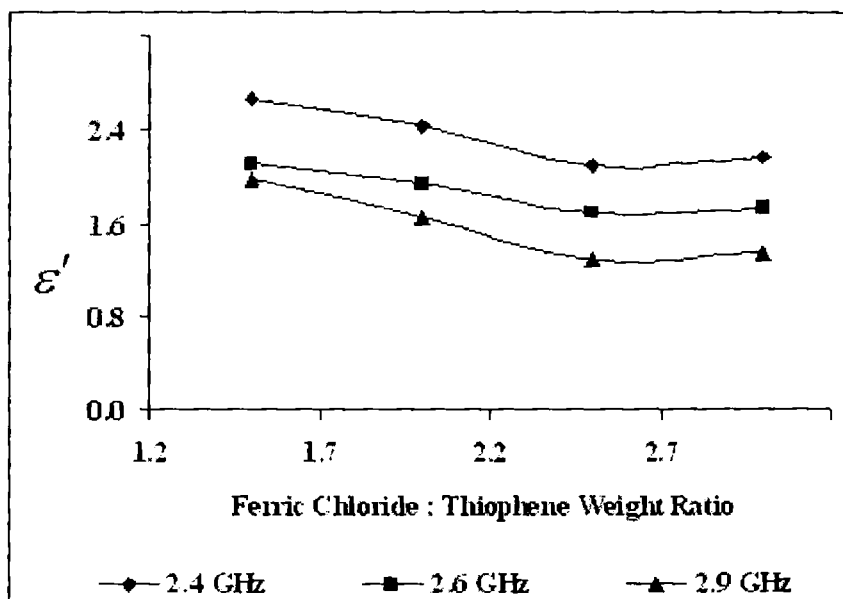


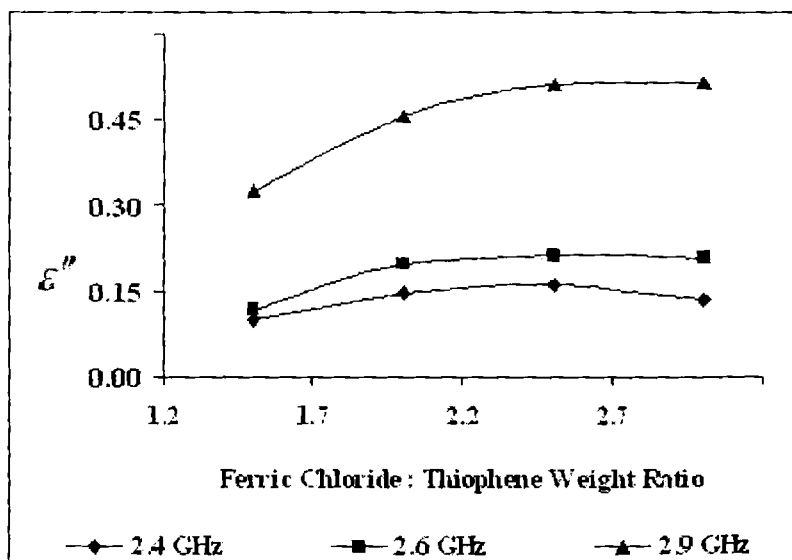
Figure 7.1 Variation of dielectric constant ( $\epsilon'$ ) with FeCl<sub>3</sub>: Thiophene ratio at various frequencies.

Dielectric constant is found to be lower at the ratio 2.5. The values for 1.5 and 2 are higher may be due to the incomplete polymerisation of thiophene. At the ratio 3, there is not much change in the dielectric constant compared to that at 2.5. So we

may infer that the polymerisation would have taken place to a considerable extent at a  $\text{FeCl}_3$ : Thiophene ratio of 2.5 and can be taken as the optimum value. Figure 7.1 also shows that dielectric constant decrease with increase in frequency. As the frequency of the applied field is increased the polarization has no time to reach its steady field value and the orientation polarisation is the first that falls. Due to the orientation polarization of the dipoles, the possibility of dielectric relaxation (so also dielectric loss) cannot be ruled out at higher frequencies. This might result in the decrease of ' $\epsilon'$ ' with frequency [18-19].

*7.1.2.2 Effect of ferric chloride on dielectric loss ( $\epsilon''$ ) of PTH-PVC composite*

Figure 7.2 shows the variation of dielectric loss with  $\text{FeCl}_3$ : Thiophene ratio at various frequencies.



**Figure 7.2** Variation of dielectric loss ( $\epsilon''$ ) with  $\text{FeCl}_3$ : Thiophene ratio at various frequencies.

Dielectric loss is found to be high at the ratio 2.5. The values for 1.5 and 2 are lower may be due to the incomplete polymerisation of thiophene. At the ratio 3, there is not much change in the dielectric loss compared to that at 2.5. So we may infer that the polymerisation would have taken place to a considerable extent at a FeCl<sub>3</sub>: Thiophene ratio of 2.5 and can be taken as the optimum value.

Dielectric loss tends to increase with increase in frequency within the range 2.4 to 2.9 GHz. As the frequency is increased the inertia of the molecule and the binding forces become dominant and it is the basis for high dielectric loss at higher frequencies.

#### *7.1.2.3 Effect of ferric chloride on conductivity ( $\sigma$ ) of PTH-PVC composite*

Figure 7.3 shows the variation of conductivity with FeCl<sub>3</sub>: Thiophene ratio at various frequencies. Conductivity is found to be high at the ratio 2.5. The values for 1.5 and 2 are lower may be due to the incomplete polymerisation of thiophene. At the ratio 3, there is not much change in the conductivity compared to that at 2.5. So we may infer that the polymerisation would have taken place to a considerable extent at a FeCl<sub>3</sub>: Thiophene ratio of 2.5 and can be taken as the optimum value. The microwave conductivity is a direct function of dielectric loss and so it shows a similar variation with frequency as the dielectric loss factor. Figure 7.3 shows that conductivity increases with increasing frequency.

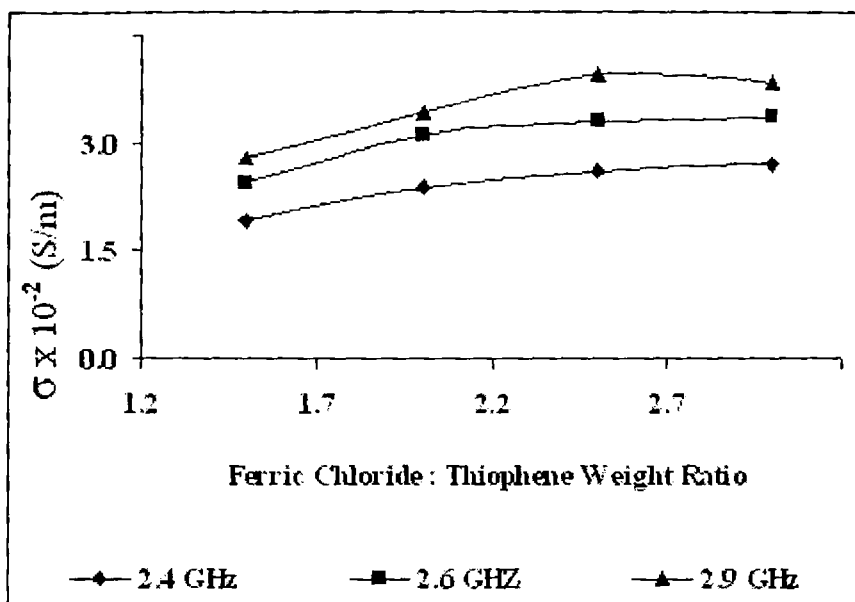


Figure 7.3 Variation of conductivity ( $\sigma$ ) with  $\text{FeCl}_3$ : Thiophene ratio at various frequencies.

From Figure 7.1, 7.2 and 7.3, it is clear that the optimum  $\text{FeCl}_3$ : Thiophene ratio for insitu chemical oxidative polymerization of thiophene in PVC solution is 2.5.

### 7.1.3 Conclusions

PTH-PVC composites were prepared with different  $\text{FeCl}_3$ : Thiophene ratio viz. 1.5, 2, 2.5 and 3. Films were prepared from the samples and the dielectric constant, dielectric loss and conductivity of the samples were evaluated at the microwave frequencies 2-4 GHz using cavity perturbation technique. The major conclusions are:

- Optimum FeCl<sub>3</sub>: Thiophene ratio for insitu chemical oxidative polymerisation of thiophene in PVC solution is 2.5
- Dielectric constant of the PTH-PVC composites decrease with increase in frequency.
- Dielectric Loss and Conductivity of the PTH-PVC composites increases with increase in frequency.

## ***PART-II***

### **7.2 EFFECT OF DRYING CONDITION ON MICROWAVE PROPERTIES OF CONDUCTING POLYMER-PVC COMPOSITES**

The properties of polymer blends are largely dependent on the morphology. The processing method employed has a major impact on the morphology of a blend. Temperature and duration of drying of solution cast blend films are supposed to affect its morphology [20, 21]. In this study an attempt is made to compare the properties of room temperature dried and vacuum dried PVC- conducting polymer composite films. The optimum FeCl<sub>3</sub>: Thiophene ratio for insitu chemical oxidative polymerization of thiophene in PVC solution is to be found. In subsequent studies this ratio will be used for the chemical oxidative polymerizations of thiophene, EDOT and aniline in PVC solutions.

#### **7.2.1 Experimental methods**

Conducting polymer-PVC composites in the ratio of 1:1 were prepared with a FeCl<sub>3</sub>: Monomer ratio of 2.5. Monomer (thiophene, EDOT or aniline) was added to PVC solution in THF to get a 10% 1:1 PVC-Monomer mixture. THF solution of

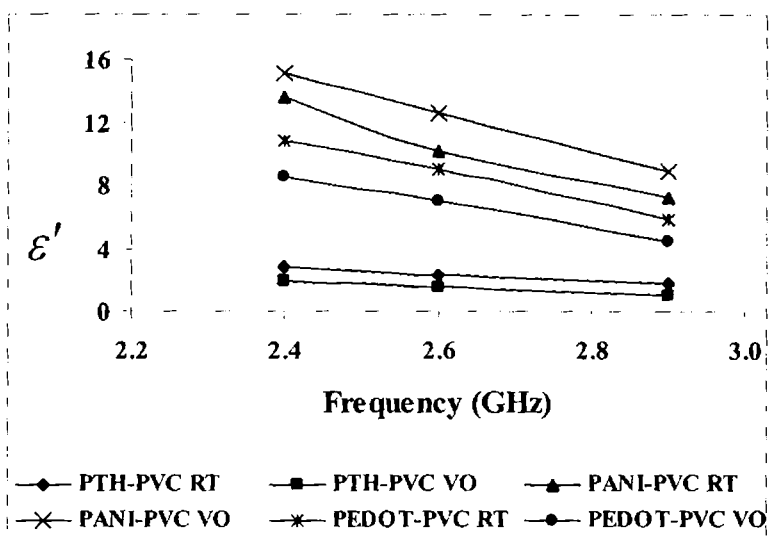
FeCl<sub>3</sub> was added to the solution and the reaction is carried out for 24 hrs. Doping of PVC-PANI was done by adding camphor sulfonic acid to the blend solution in the ratio aniline: CSA (1: 0.5). PTH and PEDOT gets insitu doped with FeCl<sub>3</sub>.

About 10 ml of the composite solutions were cast in petridish and allowed to dry at room temperature for 24 hrs and in vacuum oven at 40 °C for 2 hrs. Thin strips of the films were cut and the dielectric properties in microwave frequencies (S band 2-4 GHz) were evaluated by Cavity Perturbation Technique. The transmission type resonator used in this experiment was excited with TE<sub>10p</sub> mode by connecting it to an HP8510 C Network Analyzer.

## **7.2.2 Results and discussion**

### *7.2.2.1 Variation of dielectric constant ( $\epsilon'$ ) for vacuum dried and room temperature dried conducting polymer- PVC composites*

Figure 7.4 shows variation of dielectric constant for vacuum dried and room temperature dried Conducting polymer-PVC composite with frequency. It can be seen that the dielectric constant is higher for room temperature dried samples of all the compositions. This may be due to more extent of phase separation and heterogeneous structure in room temperature dried samples. In room temperature drying, the rate of drying is low and hence the molecules get more time for diffusion into domains. This may lead to isolation of certain conducting polymer domains and hence conducting path may be interrupted. So it can be inferred that vacuum oven drying is more suitable for casting this type of composite films. PANI-PVC composites are showing highest dielectric constant followed by PEDOT-PVC composites and lowest by PTH-PVC.



**Figure 7.4** Variation of dielectric constant ( $\epsilon'$ ) for vacuum dried and room temperature dried conducting polymer- PVC composites with frequency.

Figure 7.4 shows that dielectric constant decrease with increase in frequency. As the frequency of the applied field is increased the polarization has no time to reach its steady field value and the orientation polarisation is the first that falls. Due to the orientation polarization of the dipoles, the possibility of dielectric relaxation (so also dielectric loss) cannot be ruled out at higher frequencies. This might result in the decrease of ' $\epsilon'$ ' with frequency [18-19].

7.2.2.2. Variation of dielectric loss ( $\epsilon''$ ) for vacuum dried and room temperature dried conducting polymer- PVC composites

Figure 7.5 shows variation of dielectric loss for vacuum dried and room temperature dried conducting polymer –PVC composites with frequency.

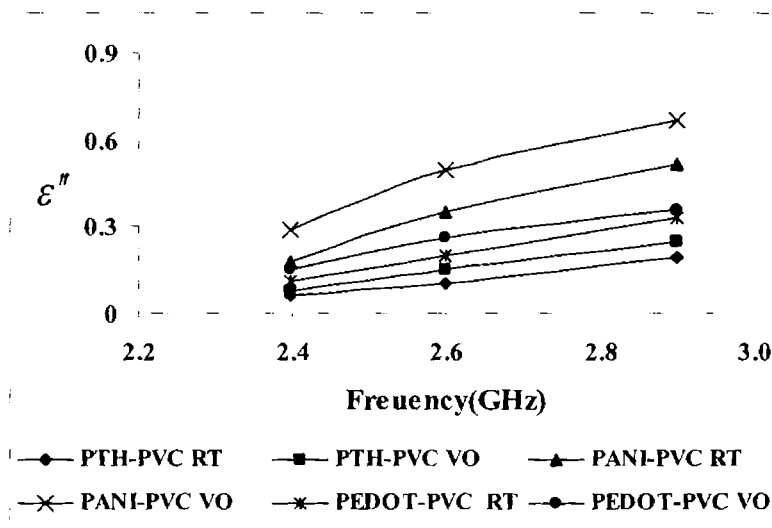


Figure 7.5 Variation of dielectric loss ( $\epsilon''$ ) for vacuum dried and room temperature dried conducting polymer- PVC composites with frequency.

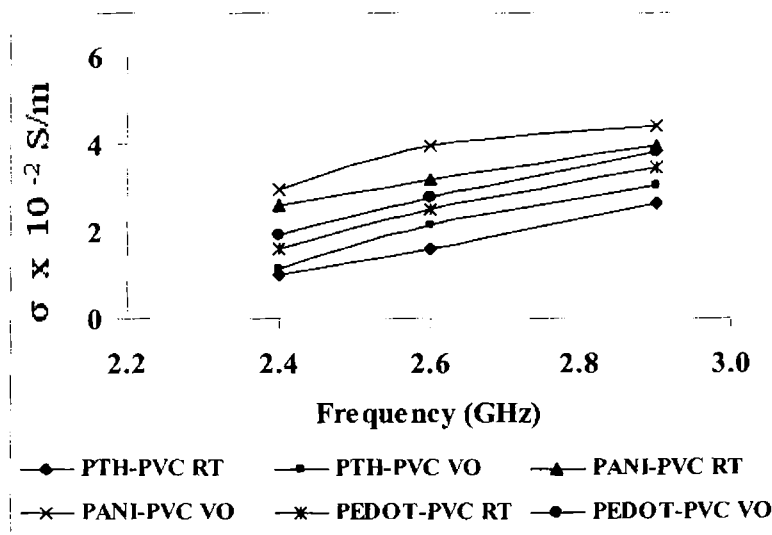
From the Figure 7.5 it can be observed that dielectric loss is higher for vacuum oven dried samples for all the composites. This may be due to more extent of phase separation and heterogeneous structure in room temperature dried samples. In room temperature drying, the rate of drying is low and hence the molecules get more time for diffusion into domains. This may lead to isolation of certain conducting polymer domains and hence conducting path may be interrupted. So it



can be inferred that vacuum oven drying is more suitable for casting this type of composite films. Dielectric loss tends to increase with increase in frequency within the range 2.4 to 2.9 GHz. As the frequency is increased the inertia of the molecule and the binding forces become dominant and it is the basis for high dielectric loss at higher frequencies.

### 7.2.2.3. Variation of conductivity ( $\sigma$ ) for vacuum dried and room temperature dried conducting polymer- PVC composites

Figure 7.6 shows variation of conductivity for vacuum dried and room temperature dried conducting polymer-PVC composites with frequency.

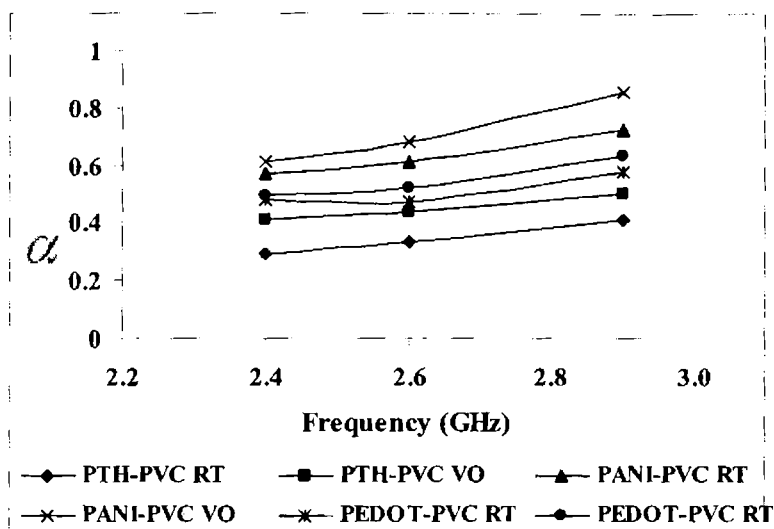


**Figure 7.6** Variation of conductivity ( $\sigma$ ) for vacuum dried and room temperature dried conducting polymer- PVC composites with frequency.

From the Figure 7.6 it can be observed that conductivity is higher for vacuum oven dried samples for all the composites. This may be due to more extent of phase separation and heterogeneous structure in room temperature dried samples. In room temperature drying, the rate of drying is low and hence the molecules get more time for diffusion into domains. This may lead to isolation of certain conducting polymer domains and hence conducting path may be interrupted. So it can be inferred that vacuum oven drying is more suitable for casting this type of composite films. The microwave conductivity is a direct function of dielectric loss and so it shows a similar variation with frequency as the dielectric loss factor. Figure.7.6 also shows that conductivity of all composites increases with frequency.

#### *7.2.2.4 Variation of absorption coefficient ( $\alpha$ ) for vacuum dried and room temperature dried conducting polymer- PVC composites*

Figure 7.7 shows variation of absorption coefficient for vacuum dried and room temperature dried conducting polymer-PVC composites with frequency. From the Figure 7.7 it can be observed that absorption coefficient is higher for vacuum oven dried samples for all the composites. This may be due to more extent of phase separation and heterogeneous structure in room temperature dried samples. In room temperature drying, the rate of drying is low and hence the molecules get more time for diffusion into domains. This may lead to isolation of certain conducting polymer domains and hence conducting path may be interrupted. So it can be inferred that vacuum oven drying is more suitable for preparing films. Absorption coefficient is directly related to the dielectric loss factor and therefore it shows the same behaviour as that of dielectric loss.



**Figure 7.7** Variation of absorption coefficient ( $\alpha$ ) for vacuum dried and room temperature dried conducting polymer-PVC composites with frequency.

### 7.2.3 Conclusions

1:1 composites of polythiophene, PEDOT and polyaniline with PVC were prepared by casting the composite solution both at room temperature and vacuum oven. The dielectric constant, dielectric loss, absorption coefficient and conductivity of the samples were evaluated at the microwave frequencies 2-4 GHz using cavity perturbation technique. The major conclusions are.

- Vacuum oven drying is more suitable for casting Conducting polymer-PVC composite films.
- Dielectric constant of the PTH-PVC composite decreases with increase in frequency

- Dielectric Loss, Conductivity and absorption coefficient of the PTH-PVC composites increases with frequency.

## ***PART-III***

### **7.3 COMPARISON OF MICROWAVE PROPERTIES OF THERMOPLASTIC CONDUCTING COMPOSITES**

Blending of conducting polymers with other insulating polymer matrices have been done to improve processability, obtaining graded conductivity and tuned microwave absorption characteristics, EMI shielding etc [2,22-24]. Blends formed by conducting polymer as the guest and an insulating polymer as the host matrix, constitute a novel class of conducting materials, which present attractive mechanical and processing performance imparted by the insulating polymer matrix with controlled levels of electrical conductivity. These blends are normally obtained by in situ polymerization of the monomer in the presence of the insulating polymer or blending of soluble or processable conducting polymer with an insulating polymer in solution or melts [25, 26]. PANI blends with EVA [27], nylon-6, polyacrylamide, polyoxymethylene [25], PET [28], PMMA [29] etc are reported. Polythiophene blends with polybutadiene [30], PMMA, PS, PVC etc[31] have been studied.

In a heterogeneous system, an interfacial polarisation is created due to the space charges. This polarisation corresponds to the electron motion inside conductive charges, dispersed in an insulated matrix (Maxwell-Wagner Model). This phenomenon will appear as soon as two materials 1 and 2 are mixed so that

$$\sigma_1 / \epsilon_1 \neq \sigma_2 / \epsilon_2$$

where ' $\sigma$ ' is the conductivity and ' $\epsilon$ ' is the dielectric constant at zero frequency [32].

In this study dielectric constant, dielectric loss, conductivity, loss tangent, absorption coefficient, heating coefficient and skin depth of PEDOT-PVC, PTH-PVC, PPDA-PVC and PANI-PVC composites are proposed to be compared in order to identify the most suitable composition.

### **7.3.1 Experimental methods**

1:1 composites of conducting polymer with PVC and PU were prepared with a  $\text{FeCl}_3$ : Monomer ratio of 2.5. Monomer (Thiophene, EDOT or Aniline) was added to the PVC or PU solution in THF to get a 10% 1:1 Thermoplastic-Monomer mixture. THF solution of  $\text{FeCl}_3$  was added to the solution and the reaction was carried out for 24 hrs. Doping of PANI composites were done by adding camphor sulfonic acid to the composite solution in the ratio aniline: CSA (1: 0.5) after the polymerisation is over. PTH and PEDOT gets insitu doped with  $\text{FeCl}_3$ . 1:1 PPDA-PVC composite solution was prepared by mixing PPDA powder in PVC solution to get a 10% solution.

About 10 ml of the composite solutions were cast in petridish and allowed to dry in vacuum oven at 40 °C for 2 hrs. Thin strips of the films were cut and the dielectric properties in microwave frequencies (S band 2-4 GHz) were evaluated by Cavity Perturbation Technique. The transmission type resonator used in this experiment was excited with  $\text{TE}_{10P}$  mode by connecting it to an HP8510 C Network Analyzer.

### 7.3.2 Results and discussion

#### 7.3.2.1 Comparison of dielectric constant ( $\epsilon'$ ) of thermoplastic conducting composites

The variation of dielectric constant of conducting polymer - thermoplastic composites at S band frequency is given in Figure 7.8.

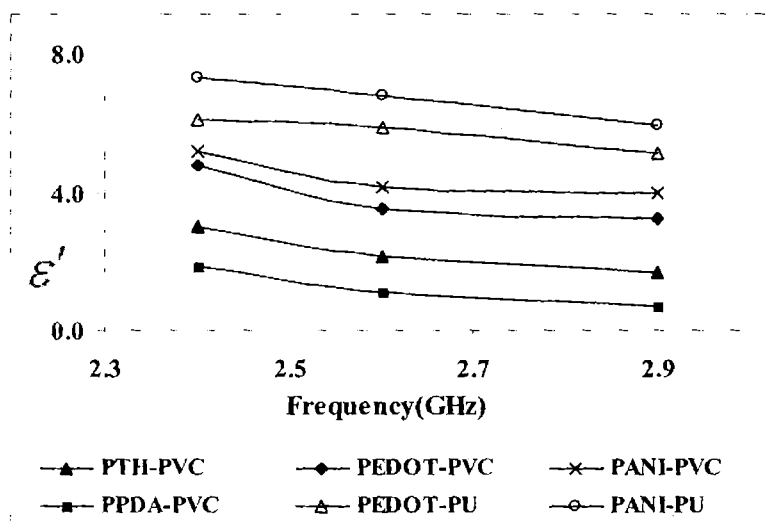


Figure 7.8 Variation of dielectric constant ( $\epsilon'$ ) of conducting polymer - thermoplastic composites with frequency.

It can be observed from the Figure 7.8 that the dielectric constant decreases with frequency for all the composites. This is due to the orientation polarisation in the microwave field. The polarization is caused by the alternating accumulation of charges at the interfaces between different phases of the material. This dipole polarization may be related to the frictional losses caused by the rotational displacement of molecular dipoles under the influence of the alternating electrical

field. As the frequency of the applied field is increased the polarization has no time to reach its steady field value and the orientation polarisation is the first that falls. Due to the orientation polarization of the dipoles, the possibility of dielectric relaxation (so also dielectric loss) cannot be ruled out at higher frequencies. This might result in the decrease of ' $\epsilon'$ ' with frequency [18-19]. PANI-PU composite has highest dielectric constant followed by PEDOT-PU, PANI-PVC, PEDOT-PVC, PTH-PVC and PPDA-PVC respectively.

### 7.3.2.2 Comparison of dielectric loss ( $\epsilon''$ ) of conducting polymer - thermoplastic composites

The variation of Dielectric Loss of conducting polymer - thermoplastic composites at S band frequency is given in Figure 7.9.

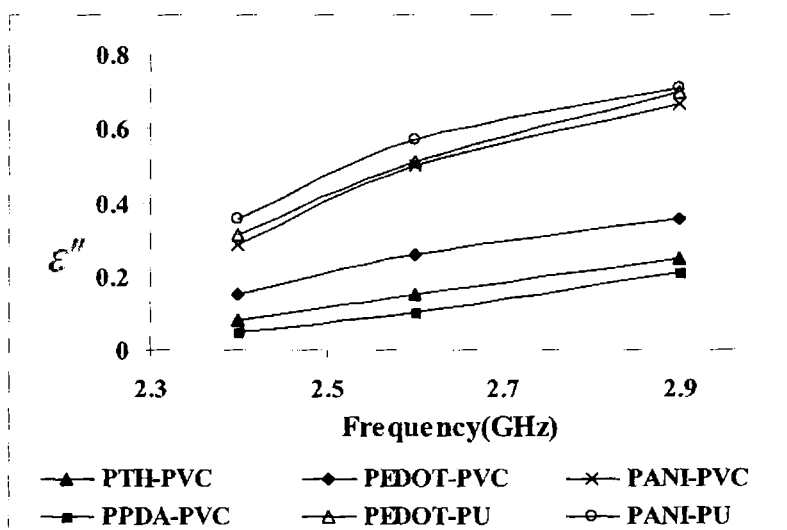
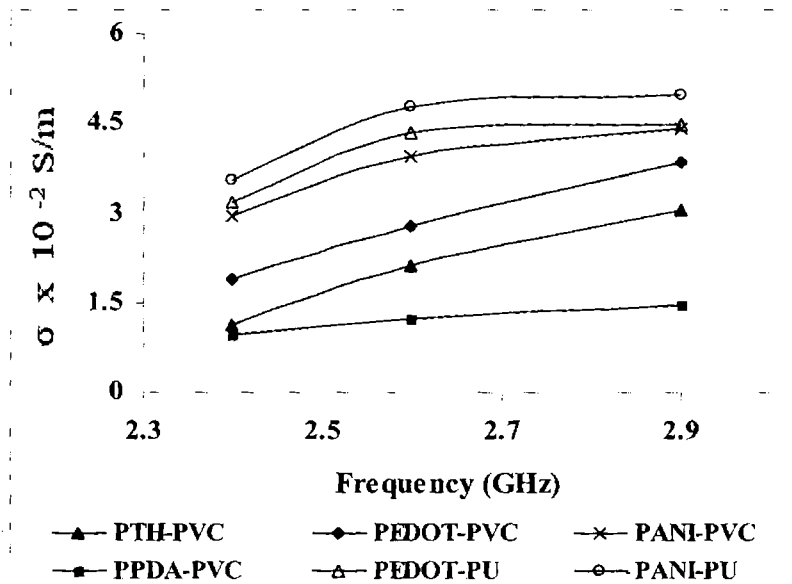


Figure 7.9 Variation of dielectric loss ( $\epsilon''$ ) of conducting polymer - thermoplastic composites at S band frequency.

It can be observed from the Figure 7.9 that the dielectric loss decreases with frequency for all the composites. PANI-PU composite has highest dielectric loss followed by PEDOT-PU, PANI-PVC, PEDOT-PVC, PTH-PVC and PPDA-PVC composite have the lowest dielectric loss.

*7.3.2.3 Comparison of conductivity ( $\sigma$ ) of conducting polymer - thermoplastic composites*

The variation of conductivity of c conducting polymer - thermoplastic composites at S band frequency is given in Figure 7.10.



**Figure 7.10** Variation of conductivity ( $\sigma$ ) of conducting polymer - thermoplastic composites at S band frequency.

It can be observed from the Figure 7.10 that the conductivity increases with frequency for all the composites. The microwave conductivity is a direct function



of dielectric loss and so it shows a similar variation with frequency as the dielectric loss factor. PANI-PU composite has highest conductivity followed by PEDOT-PU, PANI-PVC, PEDOT-PVC, PTH-PVC and PPDA-PVC composite have the lowest conductivity.

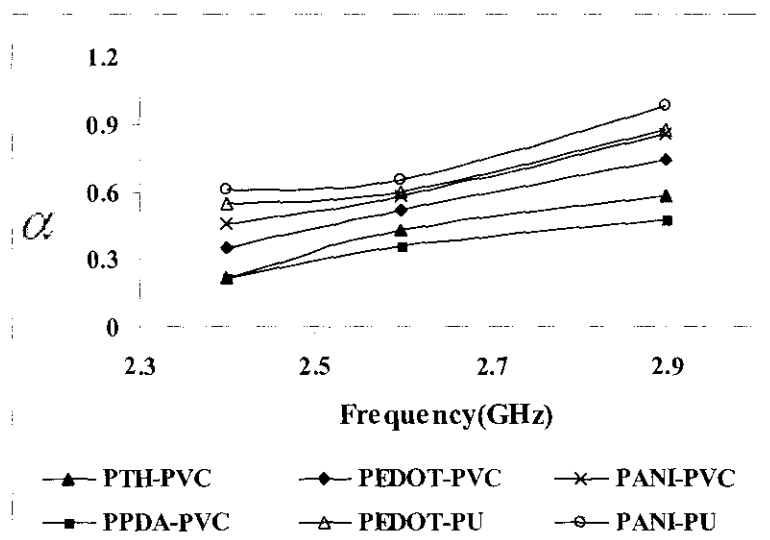
In the low frequency range, ' $\sigma$ ' is constant and equal to ' $\sigma_{dc}$ ' and beyond a frequency called relaxation frequency,  $f_r$ , the ac conductivity appears. From the experimental results it was found that  $f_r \approx \sigma_{dc} \times 10^{10}$ . In heterogeneous systems, the relaxation frequency is given by

$$f_r = \frac{\sigma_2}{2\pi\epsilon_0(2\epsilon_1 + \epsilon_2)}$$

where ' $\epsilon_1$ ' represents the dielectric constant of the matrix and ' $\epsilon_2$ ' represents that of the inclusion [33]. This model predicts that the conductivity is proportional to ' $\omega^2$ ' from low frequencies until the relaxation frequency and that beyond this frequency conductivity is constant [34, 35]. So it seems that the relaxation frequencies of these blends are above 2.9 GHz.

#### *7.3.2.4 Comparison of absorption coefficient ( $\alpha$ ) of conducting polymer - thermoplastic composites*

The variation of absorption coefficient of conducting polymer - thermoplastic composites at S band frequency is given in Figure 7.11.

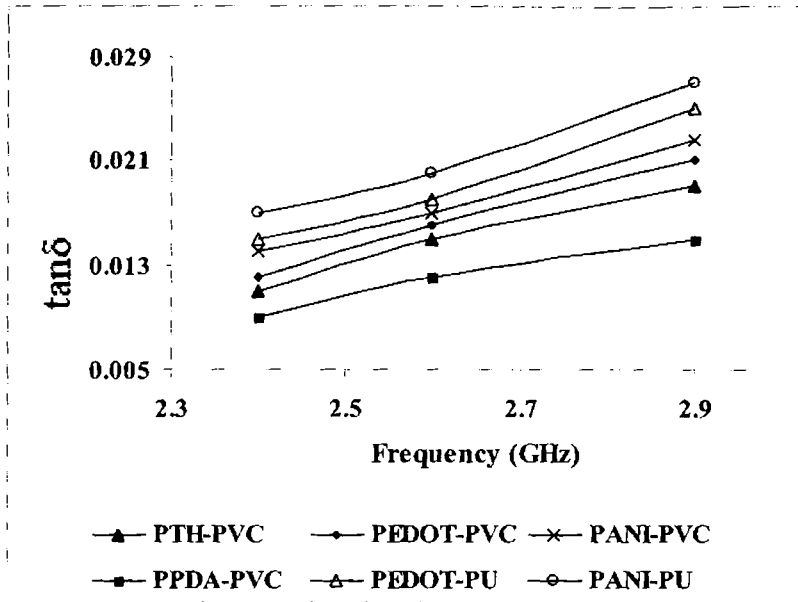


**Figure 7.11** Variation of absorption coefficient ( $\alpha$ ) of conducting polymer - thermoplastic composites at S band frequency.

It can be observed from the Figure 7.11 that the absorption coefficient increases with frequency for all the composites. Absorption coefficient is directly related to the dielectric loss factor and therefore it shows the same behaviour as dielectric loss. PANI-PU composite has highest absorption coefficient followed by PEDOT-PU, PANI-PVC, PEDOT-PVC, PTH-PVC and PPDA-PVC composites respectively.

### 7.3.2.5 Comparison of loss tangent ( $\tan\delta$ ) of conducting polymer - thermoplastic composites

The variation of loss tangent of conducting polymer - thermoplastic composites at S band frequency is given in Figure 7.12.

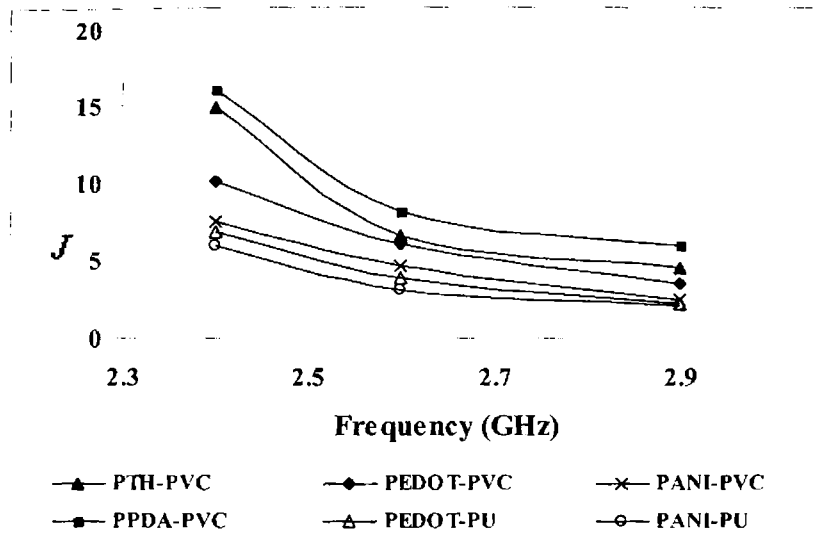


**Figure 7.12 Variation of loss tangent ( $\tan \delta$ ) of conducting polymer - thermoplastic composites at S band with frequency**

It can be observed from the Figure 7.12 that the loss tangent increases with frequency for all the composites. Since it is directly related to the dielectric loss it shows the same behaviour as that of dielectric loss. PANI-PU composite has highest loss tangent followed by PEDOT-PU, PANI-PVC, PEDOT-PVC, PTH-PVC and PPDA-PVC composites respectively.

#### *7.3.2.6 Comparison of heating coefficient (J) of conducting polymer - thermoplastic composites*

The variation of heating coefficient of conducting polymer - thermoplastic composites at S band frequency is given in Figure 7.13.



**Figure 7.13** Variation of heating coefficient ( $J$ ) of conducting polymer - thermoplastic composites at S band with frequency.

It can be observed from the Figure 7.13 that the heating coefficient decreases with frequency for all the blends. The heating coefficient is inversely related to the loss tangent and hence it decreases with increase in frequency. PANI-PU composite has lowest heating coefficient followed by PEDOT-PU, PANI-PVC, PEDOT-PVC, PTH-PVC and PPDA-PVC composites in the ascending order. Higher the  $J$  value, poorer will be the polymer for dielectric heating purposes. The heat generated in the polymeric material comes from the loss tangent, but that loss may not come entirely from the relaxation loss. Rather, conductivity of the polymeric material may also contribute to the  $\tan \delta$ . This situation may be compared with ohmic heating of metals [36].

Practically all applications of polymers in electrical and electronic engineering require materials with a low  $\tan \delta$ . However, one application that takes advantage of a high value of loss tangent is high frequency dielectric heating.

7.3.2.7 Comparison of skin depth ( $d$ ) of conducting polymer - thermoplastic composites

The variation of skin depth of conducting polymer - thermoplastic composites at S band frequency is given in Figure 7.14.

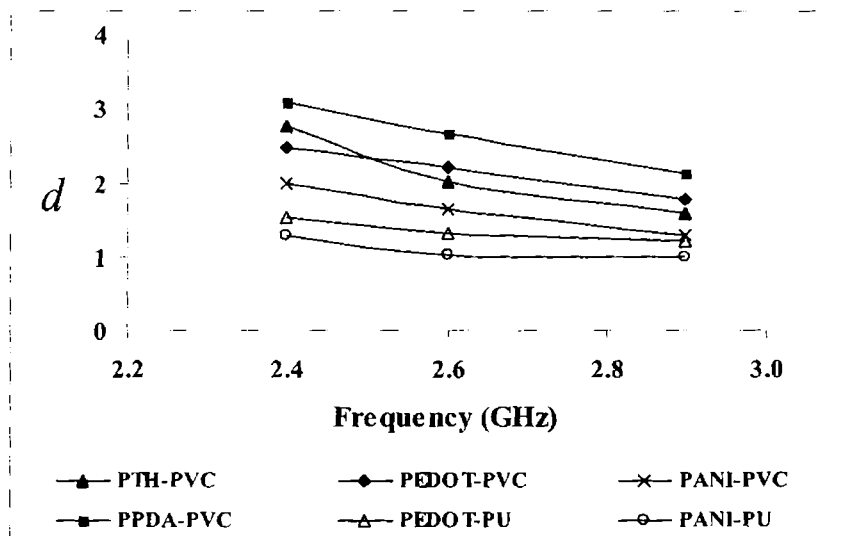


Figure 7.14 Variation of skin depth ( $d$ ) of conducting polymer - thermoplastic composites at S band with frequency.

It can be observed from the Figure 7.14 that the skin depth decreases with frequency for all the composites. The self inductance of the conductor effectively limits the conduction of the signal to its outer shell and the shell thickness is the

skin depth, which decreases with increase in frequency. PANI-PU composite has lowest skin depth followed by PEDOT-PU, PANI-PVC, PEDOT-PVC, PTH-PVC and PPDA-PVC composites in the ascending order.

## 7.4 CONCLUSIONS

In this chapter the microwave properties of PEDOT-PU, PANI-PU, PEDOT-PVC, PTH-PVC, PANI-PVC, and PPDA-PVC composites were studied. The major conclusions are

- The optimum ratio of FeCl<sub>3</sub>: Thiophene in preparing insitu PTH-PVC composites is found to be 2.5.
- Vacuum oven drying is more suited for film preparation as it gives better microwave properties compared to room temperature dried film.
- Comparing the different blends, better microwave properties are shown by PANI-PU and PEDOT-PU composites.
- For all the composites, dielectric constant, heating coefficient and skin depth tend to decrease with increase in frequency and dielectric loss, conductivity, loss tangent and absorption coefficient increases with frequency in S band.

## 7.5 REFERENCES

1. Hari Singh Nalwa, Handbook of Organic Conductive Molecules and Polymers, Vol.3, (Ed), John Wiley & Sons (1997).
2. P.Saville, Review of Radar Absorbing Materials. DRDC Atlantic TM 2005-003, DRDC Atlantic (2005).
3. J.Unsworth et al., *J.Intell.Mater. Syst. Struct.*, **5**, (1994) 595.

4. M.W.Rupich, Y.P.Liu and A.B.Kon, *Mater. Res.Soc. Symp. Proc.*, **293**, (1993) 163-168.
5. Jeong Wan Choi, Moon Gyu Han, Sook Young Kim, Seong Geun Oh, Seung Soon Im., *Synthetic Metals*, **141**, (2004) 293–299.
6. F.Henry, D.Broussoux, J.C.Dubois, US Patent 5104580 (1992).
7. S.P.Armes, M.Aldissi, *Polymer*, **31**, (1990)569.
8. A. B. H Mohamed, J. L.Miane, H.Zangar, *Polymer International*, **50**, Number **169**, (2001) 773.
9. L.Olmedo, P.Hourquebie, F.Jousse, *Adv. Mat.*, **3**, Number **5**, (1993) 373.
10. Z.Qi, P.G.Pickup, *Chem. Mater.*, **9**, (1997) 2934.
11. M.A.Khan, S.P.Armes, *Adv. Mater.*, **12**, (2000) 671.
12. T. C. P.Wong, B.Chambers, A.P.Anderson, P.V.Wright, *Elect. Lett.*, **28**, (1992)1651.
13. T. C. P.Wong, B.Chambers, A.P.Anderson, P.V.Wright, *Proc. 3rd Int Conf. on Electromagnetics in Aerospace Applications, 14-17 Sept 1993, Turin, Italy.* (1993).
14. T.C. P.Wong, B.Chambers, A.P.Anderson, P.V.Wright, Ninth International Conference on Antennas and Propagation, (1995).
15. Y. Cao, P Smith and A. J. Heeger, “Counter-ion Induced Processability of Conducting PANI”, *Synthetic Metals*, **55-57**, (1993) 3514-3519.
16. Y. Cao, J. Qiu and P. Smith, “Effect of Solvents and Co-solvents on the Processability of PANI: Solubility and Conductivity Studies”, *Synthetic Metals*, **69**, (1995)187-190.
17. Y Cao, G. M. Treacy, P. Smith and A. J. Heeger, “Optical-quality Transparent Conductive PANI Films” , *Synthetic Metals*, **55-57**, (1993) 3526-3531.

18. Y. Cao, P. Smith and A. J. Heeger, "Counter-ion Induced Processability of Conducting PANI and of Conducting Polyblends of PANI in Bulk Polymers", *Synthetic Metals*, **48**, (1992) 91-97.
19. T. Ikkala, J. Laakso, K. Vakiparta, E. Virtanen, H. Ruohonen, H. Jirvinen, T. Taka, P. Passiniemi, Y. Cao, A. Andreatta, P. Smith and A. J. Heeger, "Counter-ion Induced Processability of PANI: Conducting Melt Processable Polymer Blends", *Synthetic Metals*, **69**, (1995) 97-100.
20. S. J. Davies, T. G. Ryan, C. J. Wilde and G. Beyer, "Processable Forms of Conducting PANI", *Synthetic Metals*, **69**, (1995) 209-210.
21. P. Banerjee and B. M. Mandal, "Conducting PANI Nanoparticle Blends with Extremely Low Percolation Thresholds", *Macromolecules*, **28**, (1995) 3940-3943.
22. Hosier et al, "Morphology and Electrical Conductivity in Polyaniline Polyolefin Blends", *IEEE Transactions on Dielectrics and Electrical Insulation*, **8**, No.4, (2001) 698-704.
23. R. D. McCullough, *Adv. Mater.*, **10**, (1998) 93-116.
24. K. Y. Jen, R. Oboodi, R. L. Elsenbaumer, *Polym. Mater. Sci. Eng.*, **53**, (1985) 79.
25. R. Sugimoto, S. Takeda, H. B. Gu, K. Yoshino, *Chem. Express*, **1**, (1986) 635.
26. E.J. Frommer, R.R. Chance, *Electrical and electronic properties of polymers: state of the art compendium*, Encyclopedia Reprint Series, in: I.J. Kroschwitz (Ed.), Wiley Interscience, New York, (1988) 101-178.
27. T.A. Ezquerra, F. Kremmer, G. Wegner, AC electrical properties of insulator conductor composites, in: A. Priou (Ed.), *Dielectric Properties of Heterogeneous Materials: Progress in Electromagnetic Research*, Vol. **6**, Elsevier, New York (1992).



28. L. A. Utracki, "Polymer Alloys and Blends", Hanser Verlag, Munich, New York (1989).
29. Charef Harrats, Sabu Thomas, and Gabriel Groeninckx, (Eds.), *Micro- and Nanostructured Multiphase Polymer Blend Systems: Phase Morphology and Interfaces*, CRC Press, (2006).
30. P.E.Schoen, US Patent Navy Case No. 79423 (2001).
31. R.R.Price, J.M.Schnur, P.E.Schoen, D.Zabetakis, M.Spector, U.S Patent 6013206 (2000).
32. C. Y Lee, D.E. Lee, J. Joo, M.S.Kim, J.Y.Lee, S.H.Jeong, S.W.Byun, *Synth. Met.*, **119**, (2001) 429.
33. Jayashree Anand, Srinivasan Palaniappan, and D. N. Sathyanarayana, *Prog. Polym. Sci.*, **23**, (1998) 993–1018.
34. M.A. De Paoli, *Conductive polymer blends and composites*, in: H.S. Nalwa (Ed.), *Handbook of Organic Conductive Molecules and Polymers*, Vol. 2, Chapter 18, Wiley, New York, (1997).
35. G.M.O. Barra et al., *Synthetic Metals*, **130**, (2002) 239–245.
36. H.Zhang and C.Li, *Synth. Met.*, **44**, (1991) 143.
37. L.Terlemezyan, M.Mihailov and B.Ivanova, *Polym. Bull.*, **29**, (1992) 283.
38. S. Kiralp, et al., *Turk. J. Chem.*, **27** (2003) , 417 - 422.
39. Jean Roncali, *Chemical Reviews*, **92**, No. 4, (1992) 711-738.
40. C.J.F. Bottcher and P.Bordewijk, in *Theory of Electric Polarisation*, Vol. 2, Elsevier (1978) 486.
41. R. J. Meakins, in *Progress in Dielectrics*, (Ed) J.B.Briks, **3**, Heywood, London (1961) 161.
42. J. O. Israd, *Proc IEEE*, (1996).
43. R. Singh and R.P.Tandon, *Thin Solid Films*, **196**, L 15 (1991).
44. K. T. Mathew et al, *Materials Chemistry and Physics*, **79**, (2003) 187–190.

---

### **APPLICATION STUDY: MICROWAVE ABSORPTION, REFLECTION, EMI SHIELDING AND MECHANICAL PROPERTIES OF PANI-PU COMPOSITE**

***Abstract:** In order to allow the coexistence of all electronic components without harmful electromagnetic interferences, it is necessary to develop new shielding and absorbing materials with high performance and a large operating frequency band. Conducting polymer composites were found suitable for EMI shielding and for the dissipation of electrostatic charge. In the present study PANI-PU composite was considered for these applications. The microwave absorption, microwave reflection and EMI shielding properties of PANI-PU composite are evaluated both at S band and X band frequencies. The material is found to have good microwave absorption and is a potential candidate for EMI shielding applications. The mechanical properties of the composite film are found to be satisfactory for normal service conditions. The composite shows change in conductivity with load and hence can be applied in load and pressure sensing applications.*

The continuous growth of the telecommunication market has led to the emergence of a huge number of Radio Frequency (RF) systems. In order to allow the coexistence of all of those various instruments without harmful electromagnetic interferences, it is necessary to develop new shielding and absorbing materials with high performance and a large operating frequency band. Conducting polymers are

characterized by attractive features like high anticorrosion property, controlled conductivity, high temperature resistance, low cost and ease of bulk preparation. These properties make conducting polymers as good shielding materials for electromagnetic interference (EMI) [1, 2]. EMI can be defined as spurious voltages and currents induced in electronic circuitry by external sources. In recent years, electromagnetic pollution has received wide attention because of the malfunctioning of the electronic equipments from the radiations generated from the source or those emanating from other electronic equipments. So far conducting composites were made by adding metallic fillers, C-black or metallic powders. Because of certain disadvantages like labour intensity, relatively high cost and time consumption, and the galvanic corrosion observed in metal composites, conducting polymer composites were found suitable for EMI shielding and for the dissipation of electrostatic charge.

Great interest has been focused on polyaniline (PANI), within the conducting polymers field due to its important characteristics, such as, its easy synthesis route, low cost, high-yield, high levels of electrical conductivity, excellent chemical stability etc. Moreover, these properties can be well controlled and are reproducible. The microwave properties of PANI are considerably influenced by their structural parameters, which are dependent on the synthesis routes, doping methods and dopant natures [3]. Because of the poor mechanical properties of conducting polymers it is necessary to blend them with a matrix, usually based on polymeric systems. One of the methods to process PANI, without altering the structure of the polymer, is by blending it with conventional polymers. These blends may combine the desired properties of the two components, the electrical conductivity of PANI with the physical and mechanical properties of the polymeric matrix [4, 5]. Poly aniline and polypyrrole with different proportion of PVC were

prepared and studied at the S-band microwave frequencies. These materials were found to exhibit good EMI shielding behaviour [1].

The research and development of RAM (Radar absorbing Materials) has attracted considerable interests in recent years to eliminate or reduce spurious electromagnetic radiations present in the environment, caused as a consequence of technological advances in telecommunication area and the proliferation of wide variety artefacts that employ high frequencies [6]. The first reported use of RAM was made during World War II, when the Germans applied a mixture of polymeric foam and carbon black on the submarine periscopes to avoid radar detection [7].

The purpose of the widely broadcasted 'Stealth technology' is the reduction of the aircraft RCS (Radar Cross Section). The Radar Cross Section is a measure of reflective behaviour of a target. It is defined as  $4 \pi$  times the ratio of the scattered power per solid angle unit in a specific direction to the power, per unit area in a incident wave plane on the scatterer from a specified direction. More precisely, it is the limit of that ratio as the distance from scatterer to the point where the scattered power is measured approaches infinity [8].

It is absolutely essential for the preparation of RAM, based upon conducting polymers, that the material allows electrical conductivity variation [9]. Therefore, this parameter determines the characteristics of radiation absorption of the conducting polymer, supporting the exchange of incident electromagnetic energy on material by thermal energy. The control of the electrical conductivity is directly related to the efficiency of the processed absorber under the influence of polymer chain size, doping level, dopant type and the conducting polymer syntheses methods [9]. It is well-known that these parameters can cause changes in molecular structures, modifying consequently the electromagnetic properties of radar

absorbing material. These unique characteristics of the conducting polymers make them a set of modulating absorbing centers, allowing to make some changes on final characteristics of the radar absorbing material [10]. Therefore, the domain of the radiation absorbing centers ensures the acquisition of broadband or resonant absorbing materials with previously established absorption frequency range. Indeed, the wide conductivity range and the differences in molecular structures due to the use of different dopants, helps to achieve very efficient absorbers [11].

In general, considering the use of absorbing center in X-band, the following operational requirements are needed, attenuation of the incident radiation at a minimum of 50% (-3 dB), in the operational broadband frequency range, minimum attenuation of 99% (-20dB) in narrow band range (resonant absorber) reduced thickness (smaller than 3mm) and low density [9, 12].

PANI-PU composite was found to have good microwave absorption and EMI shielding. In this study, the microwave absorption, microwave reflection and EMI shielding properties of PANI-PU composite is proposed to be investigated at a larger span of frequencies both at S band and X band. For any product moderate mechanical properties are essential and hence the mechanical properties are also proposed to be studied.

When  $\text{FeCl}_3$  was used as the oxidant in preparing the composites, the films tend to adsorb moisture on long storage. This may be due to the hygroscopic nature of  $\text{FeCl}_3$ . To overcome this problem benzoyl peroxide is proposed to be used as the oxidant in the following studies.

## 8.1 EXPERIMENTAL METHODS

PANI-PU composite was prepared with a  $\text{FeCl}_3$ : Monomer ratio of 2.5. Aniline was added to PU solution in THF to get a 10% 1:1 PU-aniline mixture. 0.5 M benzoyl peroxide was added to the solution and the reaction was carried out for 24 hrs. Doping of composites was done by adding camphor sulfonic acid (CSA) to the composite solution in the ratio aniline: CSA (1: 0.5).

### 8.1.1 Absorption coefficient, reflection coefficient and EMI shielding

From the measurement of S-parameters, absorption coefficient and the shielding efficiency of the material could be calculated. The sample sheet was kept between two coaxial to wave guide adapters and tightened. Using the Agilent E8362B PNA series network analyzer, the S-parameters, ' $S_{11}$ ' and ' $S_{21}$ ' were measured. Reflection coefficient ' $R$ ' and transmission coefficient ' $T$ ' are given as  $R = |S_{11}|^2$  and  $T = |S_{21}|^2$ . The absorption coefficient ' $A$ ' can be obtained from the simple relation  $A+R+T = 1$ . The EMI shielding efficiency ' $SE$ ' is defined (Equation.1) as the ratio of the power of the incident wave ' $P_I$ ' to that of the transmitted wave ' $P_T$ ' [1]

$$SE = 10 \log (P_I/P_T) \text{ dB} \quad (1)$$

### 8.1.2 Mechanical properties

The mechanical properties of the composite were evaluated in Shimadzu Autograph AG-1 series UTM of 10 kN load capacity. Dumbbell specimens were

cut from cast films from different area and they were subjected to tensile tests at a rate of 15 mm/sec.

### **8.1.3 Load sensitivity**

The conductivity of the samples at various loads were carried out by a two-probe technique recorded by a Keithley 2400 Sourcemeter and a Keithley 2182 Nanovoltmeter. Conductivity measurements were done using cast films. The specific resistivity was calculated as:

$$\rho = (R * A) / t$$

Where,  $\rho$  is the resistivity, R is the resistance measured, A is the area of the electrode used and t is the thickness of the sample and,

$$\sigma = 1 / \rho$$

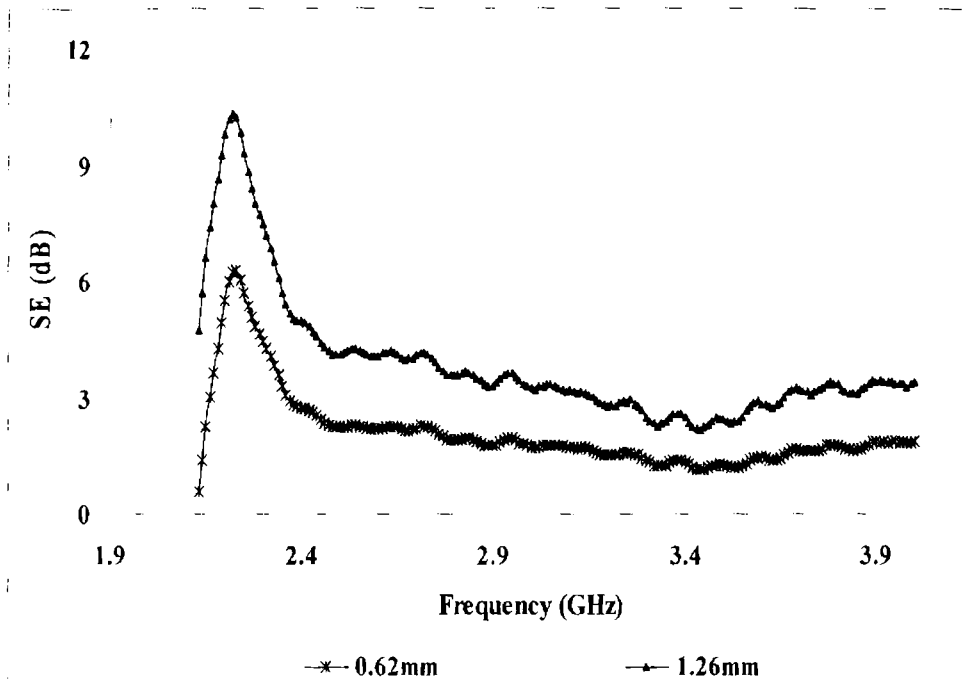
where,  $\sigma$  is the conductivity of the material. The conductivity was measures at various standard loads.

## **8.2 RESULTS AND DISCUSSION**

In this section the microwave absorption, microwave reflection, EMI shielding and mechanical properties of PANI-PU composite are analyzed.

### **8.2.1 EMI shielding**

Variation of EMI shielding of the PANI-PU composite for different thickness at S band frequencies is given in Figure 8.1



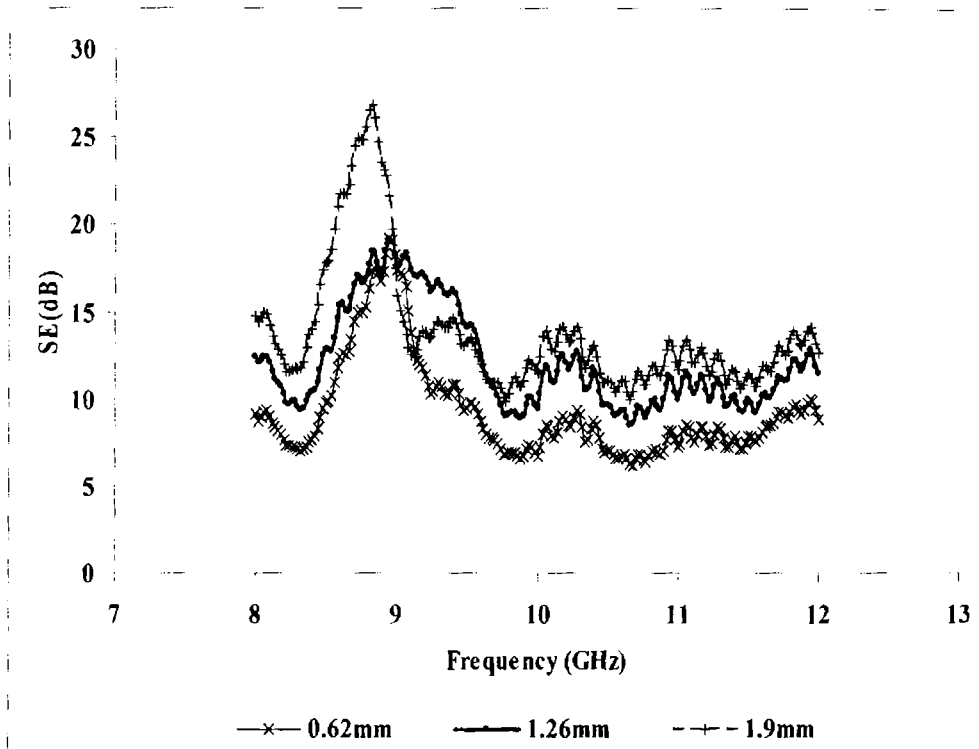
**Figure 8.1** Variation of EMI shielding (SE) of the PANI-PU composite for different thickness at S band frequencies.

The higher the SE value in decibel (dB), lesser the energy passing through the sample. All measured SE is the combination of the electro magnetic (EM) radiation, i.e. reflection from the material's surface, absorption of the EM energy and multiple internal reflections of the EM radiation [13].

From the Figure 8.1 it can be seen that shielding efficiency increases with the thickness of the sample but the trend remains the same. Maximum shielding efficiency in S band frequencies occurs at 2.23 GHz. The shielding efficiency for a thickness of 0.62 mm is 6.3 dB and that at 1.26 mm is 10.2 dB. So it can be inferred that this material is ideal for shielding at 2.23 GHz.



Variation of EMI shielding of the PANI-PU composite for different thickness at X band frequencies is given in Figure 8.2



**Figure 8.2** Variation of EMI shielding (SE) of the PANI-PU composite for different thickness at X band frequencies.

From the figure it can be seen that shielding efficiency increases with the thickness of the sample but the trend remains the same. Maximum shielding efficiency in X band frequencies occurs at 8.82 GHz. The shielding efficiency for a thickness of 0.62 mm is 18.2 dB, at 1.26 mm is 20 dB and that at 1.9 mm is 26.7 dB. The next

peak occurs at 10.18 GHz. The shielding efficiency for a thickness of 0.62 mm is 10.3 dB, at 1.26 mm is 13 dB and that at 1.9 mm is 15.5 dB. So it can be inferred that this material is ideal for shielding at 8.82GHz.

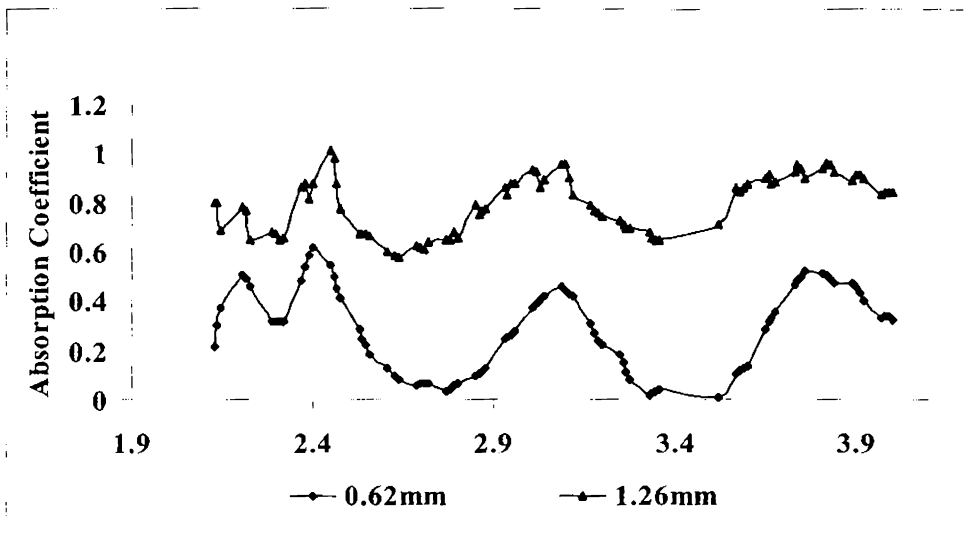
Minimal reflection of the microwave power or matching condition occurs when the sample's thickness, 't' of the absorber approximates to a quarter of the propagating wavelength multiplied by an odd number, that is  $t = n\lambda/4$  ( $n=1, 3, 5, 7, 9, \dots$ ), where  $n=1$  corresponds to the first dip at low frequency. The propagating wavelength in the material ( $\lambda$ ) is given by:

$$\lambda = \lambda_0 / \left( \left| \mu_r^* \right| / \left| \varepsilon_r^* \right| \right)^{1/2} \quad (2)$$

where,  $\lambda_0$  is the free space wavelength and  $|\mu_r^*|$  and  $|\varepsilon_r^*|$  are the moduli of  $\mu_r^*$  and  $\varepsilon_r^*$  respectively. The matching condition can be explained by the cancellation of the incident and reflected waves at the surface of the absorber [14]. Similar peaks and dips have been reported by Phang et al. for polymers. The minimum reflection loss or the dip is due to the minimal reflection or maximal absorption of the microwave power for the particular thickness of the sample. The position and intensity of dip are sensitive to the thickness [15].

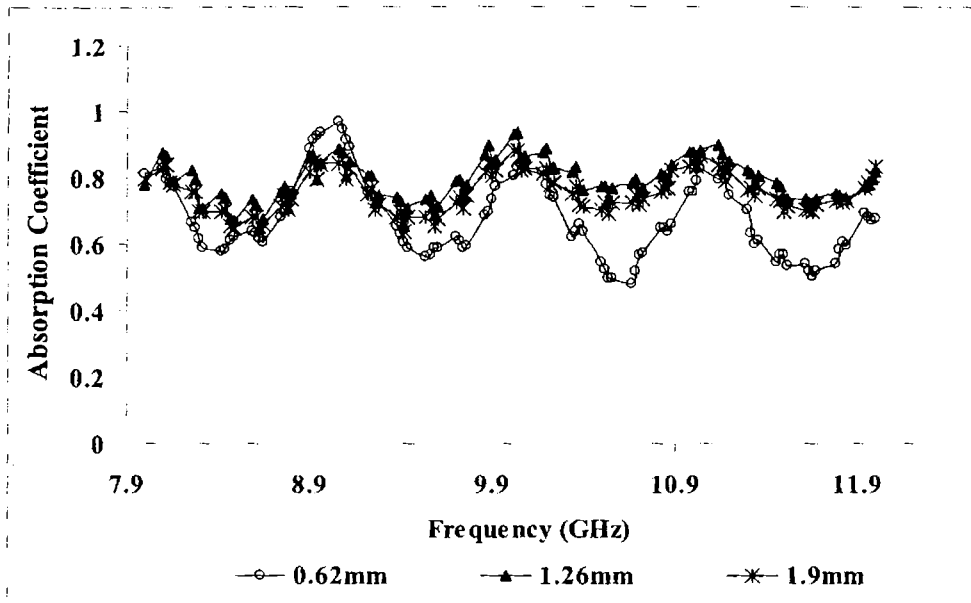
### 8.2.2 Absorption coefficient

Variation of absorption coefficient of the PANI-PU composite for different thickness at S band frequencies is given in Figure 8.3



**Figure 8.3** Variation of absorption coefficient of the PANI-PU composite for different thickness at S band frequencies.

From the figure it can be seen that absorption coefficient increases with the thickness of the sample but the trend remains the same. Variation of absorption coefficient of the PANI-PU composite for different thickness at X band frequencies is given in Figure 8.4.



**Figure 8.4** Variation of absorption coefficient of the PANI-PU composite for different thickness at X band frequencies.

From the figure it can be seen that absorption coefficient increases with the thickness of the sample but the trend remains the same. The peak tends to straighten as the thickness increases which show that after a certain thickness the frequency dependency may not exist.

The behaviour of electromagnetic absorption will critically depend on dielectric and magnetic properties of the materials that are represented by the complex permittivity and complex permeability [16]. PANI-PU composite is organic in nature without any addition of magnetic fillers like carbonyl iron and ferrite, thus the microwave absorbing property of is solely attributed to the dielectric constant,  $\epsilon'$  of the composite.

The frequency dependence of the microwave properties can be attributed to various relaxation processes. At very low frequencies Debye type of relaxation processes occur. Another possibility is the interfacial polarization relaxation effects and dipolar reorientation processes in polymers [17]. The dispersion of conductive regions in a less or non conducting medium is known to lead to Maxwell–Wagner–Sillars (MWS) effect [17-19]. The exact mechanisms can be known from the calculation of relaxation times, activation energies and analysis of dielectric relaxation spectra of the composite. The nature of the polymer matrix is found to influence the relaxations by frequency shift, change in relaxation strength and activation energy [19].

### **8.2.3 Reflection coefficient**

The variation of reflection coefficient of the PANI-PU composite for different thickness at S band frequencies is given in Figure 8.5

The reflection behaviour of microwaves from the samples is seen to be frequency dependent. As the thickness increases the reflection increases but the trend remains the same. Phang et al. have reported a sharp increase in reflection of microwaves from PDPV samples above 2 mm thickness below 5 GHz [15].

The variation of reflection coefficient of the PANI-PU composite for different thickness at X band frequencies is given in Figure 8.6.

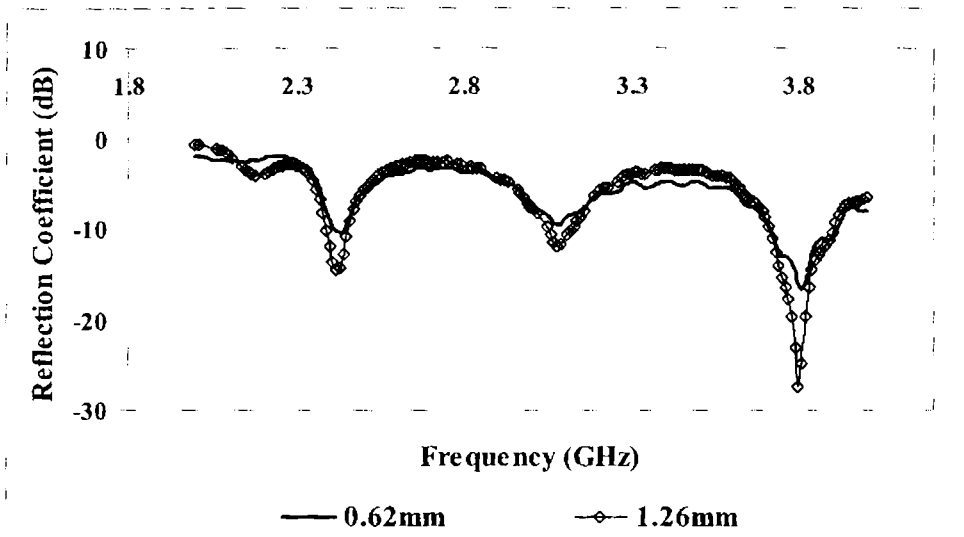


Figure 8.5 Variation of reflection coefficient of the PANI-PU composite for different thickness at S band frequencies.

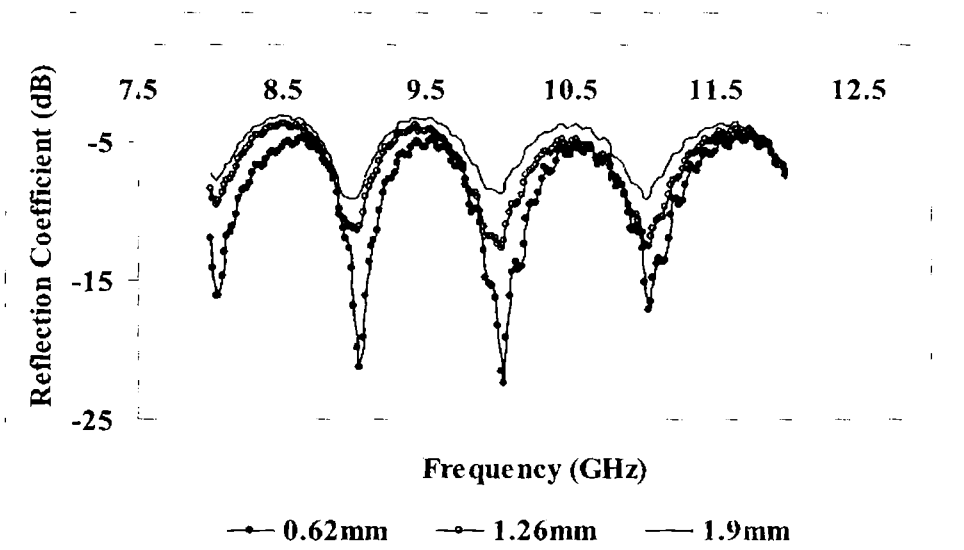


Figure 8.6 Variation of reflection coefficient of the PANI-PU composite for different thickness at X band frequencies.

Comparing Figure 8.5 and 8.6 we can see that the reflection is comparatively low at X band compared to that at S band. The variations of reflection coefficient with frequency at S band and X band show similar behaviour. Reflection seems to be very frequency specific. As the thickness increases the reflection increases but the trend is maintained up to a thickness of 2 mm.

Minimal reflection of the microwave power or matching condition occurs when the sample's thickness,  $t$  of the absorber approximates a quarter of the propagating wavelength multiplied by an odd number, that is  $t = n\lambda / 4$  ( $n=1, 3, 5, 7, 9, \dots$ ), where  $n=1$  corresponds to the first dip at low frequency. The propagating wavelength in the material ( $\lambda$ ) is given by equation (2).

The matching condition can be explained by the cancellation of the incident and reflected waves at the surface of the absorber [14]. Similar peaks and dips have been reported by Phang et al. for polymers [15].

#### **8.2.4 Mechanical properties**

The samples were subjected to tensile tests in Shimadzu Autograph AG-1 series UTM and the modulus and elongation values for the PANI-PU composite is given below.

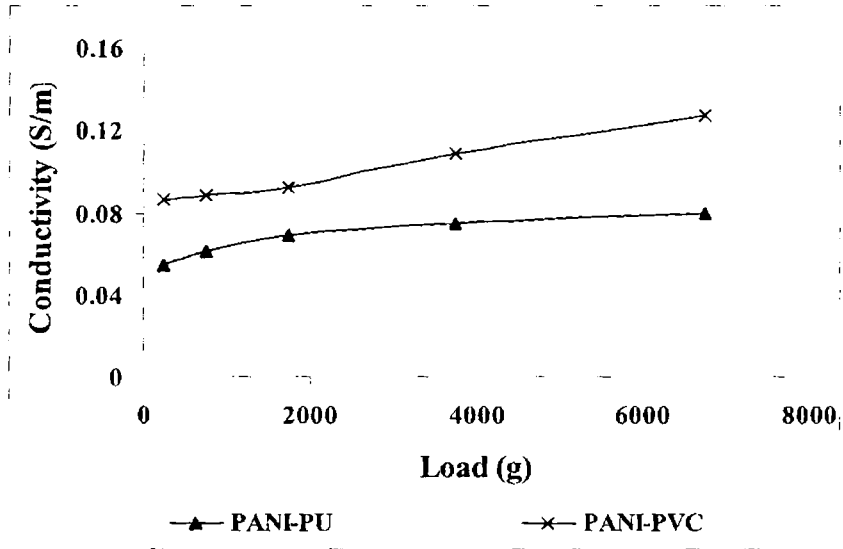
Modulus = 3 N/mm<sup>2</sup>

Elongation at break = 650%

The mechanical properties of the composite are found to be satisfactory for normal service conditions to be use as EMI shielding or microwave absorbers.

### 8.2.5 Load sensitivity

The variation of conductivity for the PANI-PU and PANI-PVC composite with load is given in Figure 8.7.



**Figure 8.7** Variation of conductivity for the PANI-PU and PANI-PVC composite with load

From the figure it can be seen that the conductivity varies with load for both the composites and hence can find application in load and pressure sensors.



### 8.3 CONCLUSIONS

The microwave absorption, microwave reflection, EMI shielding and mechanical properties of PANI-PU composite were analyzed. The shielding efficiency of the composite increases with the thickness of the sample and this material is ideal for shielding at 2.23 GHz and at 8.82 GHz. The variations of reflection coefficient with frequency at S band and X band show similar behaviour. Reflection of microwaves from the PANI-PU films is very frequency specific. As the thickness increases the reflection increases. Minimal reflection of the microwave power or matching condition occurs when the sample's length approximates a quarter of the propagating wavelength multiplied by an odd number. This is interpreted as due to the cancellation of the incident and reflected waves at the surface of the absorber. The position, intensity and number of dips are dependent on the thickness of the sample [14, 15].

The material is found to show good microwave absorption and EMI shielding characteristics. The mechanical properties are found to be satisfactory for normal service conditions. The conductivity of the PANI-PU and PVC-PANI composites vary with load and hence can find application in load and pressure sensors.

## 8.4 REFERENCES

1. K.T. Mathew, A.V. Praveen Kumar and Honey John, "Polyaniline and Polypyrrole with PVC content for effective EMI shielding", *IEEE, International Symposium on Electromagnetic Compatibility, USA*, Aug 14-18, (2006) 443-445.
2. Aimad Saib et al., *IEEE Transactions on Microwave Theory and Techniques*, **54**, No. 6, June (2006).
3. P. Hourquebie, L. Omedo, "Influence of structural parameters of conducting polymers on their microwave properties", *Synthetic Metals*, **65**, (1994)19-26.
4. M. Zilberman, G.I.Titelman, A.Siepann, Y.Wba, M. Narkis and D. Alperstein, "Conductive Blends of Thermally Dodecylbenzene Sulfonic Acid-Doped Polyaniline with Thermoplastic Polymers", *J. Appl. Pol.Science*, **66**, (1997) 243-253.
5. M.A. De Paoli, in *Handbook of Organic Conductive Molecules and Polymers*, **2**, John Wiley & Sons, New York, 1997.
6. P. T. C. Wong, B. Chambers, A. P. Anderson and P. V. Wright, *Electronic Letters*, **28**, No.17, (1992)11651-1653.
7. R. S. Biscaro, E. L. Nohara, G. G. Peixoto, R. Faez, M. C. Rezende, *Proceedings SBMO, IEEE MTT-S IMOC*, (2003) 355-358.
8. *IEEE dictionary of Electrical and Electronics*, John Wiley & Sons; 3<sup>rd</sup> Edition, September 1984.
9. L. Olmedo, P. Houquerbie, F. Jousse, *Handbook of Organic Conductive Molecules and Polymers*, **3**, H.S. Nalwa (Ed.), John Wiley, New York, 1997.

10. K. Facc., M. C. Ruzendc, M. Manin. M. A. De Paoli, *Polimcros. Y*, **10**, No.3, (2000) 130-137.
11. K. Faez, M. A. Ik Paoli, M. Manin, M. C. Rezendz, *J. Appl. Polym. Sci.*, **83**, (2002) 1568-1575.
12. E.F. Knot, J.F. Shaeffer and M.T. Tulcy, *Radar Cross Section Handbook*: Artech House: New York 1993.
13. L.X. Cheng, D.D.L. Chung, *Compos. Part B: Eng.*, **30**, (1999) 3.
14. A.N. Yusoff, M.H. Abdullah, S.H. Ahmad, S.F. Jusof, A.A. Mansor, S.A.A. Hamid, *J. Appl. Phys.*, **876-882**, (2002) 92.
15. S.W. Phang et al., *Thin Solid Films*, **477**, (2005) 125–130.
16. V.T. Truong, S.Z. Riddell, R.F. Muscat, *J. Mater. Sci.*, **4971-4976**, (1998) 33.
17. B.K.P. Scaife, *Principles of Dielectrics*, Clarendon, Oxford, 1989.
18. E. Tuncer, *J. Phys. D: Appl. Phys.*, **37**, (2004) 334.
19. M. Tabellout et al., *Journal of Non-Crystalline Solids*, **351**, (2005) 2835–2841.

### ***SUMMARY AND CONCLUSIONS***

Conducting polymers show very interesting electrical and microwave properties that make them far more attractive than traditional dielectric materials. Wide and diversified areas of potential applications of conducting polymers like diodes, battery electrodes, energy storage and conversion devices, electroluminescence devices, non-linear optical materials, radar absorbers, oscillators, amplifiers, frequency converters, sensors etc. have been reported. Microwave absorbing materials open up a new vista to various technological applications like EMI shielding, frequency selective surfaces, beam steering antennas, anti static coatings, satellite communication links, diathermy and dielectric heating applications.

The microwave and electrical applications of conducting polymers like poly para phenylene diazomethine, polythiophene, polyaniline and that of Poly (3, 4-ethylenedioxythiophene) (PEDOT) are analyzed in this investigation. One of the major drawbacks of conducting polymers is their poor processability, and a solution to overcome this is sought in this investigation. Conducting polymer/thermoplastic composites were prepared by the insitu polymerization method to improve the extent of miscibility probably to a semi IPN level. An important outcome of the work is the development of a processable conducting composite with very good electrical, mechanical and microwave properties and which can be easily cast or coated on various surfaces.

*The attractive features of the conducting composite developed are excellent processability, good microwave and electrical conductivity, good microwave absorption, load sensitivity and satisfactory mechanical properties. The composite shows typical frequency selective microwave absorption and reflection behaviours.*

The vast areas of applications of conducting polymers have been covered and the need for exploring more and more number of conducting polymers in DC and microwave frequencies have been emphasized. Mechanisms and equation governing DC and microwave conductivity in polymers have been discussed thoroughly. The microwave properties and the different methods of evaluating these properties have been explained. The theory and equations governing the cavity perturbation technique, which is the method of evaluation of microwave properties adopted in this work is discussed for the better understanding of the technique.

A detailed literature survey on the methods of preparation and applications of class of polymers selected for the study viz., polyazomethines, polythiophenes, poly(ethylene dioxy thiophene) and polyaniline is given which substantiates the choice of materials for the present work. The importance of following design of experiments in formulating experiments has been emphasized. The Taguchi method which was used in the preparation of PPDA is explained in detail. The scope and objectives of the work are explained. The methodology adopted to achieve these objectives is briefly explained.

A novel polyazomethine, PPDA was prepared by the condensation of para phenylene diammine and glyoxal trimeric dihydrate. The optimum reaction

conditions were determined by design of experiments. Polythiophene was prepared by chemical oxidative polymerization of thiophene with  $\text{FeCl}_3$ . Poly (3, 4-ethylenedioxythiophene) was prepared in DBSA micellar solution using  $\text{FeCl}_3$  as the oxidant. The prepared polymers were characterized by DSC, TGA and FTIR methods. Microwave and electrical properties of the conducting polymers like PANI, PEDOT, PTH, PPY and PPDA were evaluated and compared to select the most suitable polymer for microwave and electrical applications.

The conditions for the preparation of PVC-PTH composite was optimized based on optimum microwave properties. The ratio of  $\text{FeCl}_3$ : Thiophene ratio for the insitu polymerization and the optimum casting conditions were determined. Thermoplastic conducting composites like PTH-PVC, PEDOT-PVC, PANI-PVC, PPDA-PVC, PANI-PU and PEDOT-PU were prepared by in situ polymerization technique. The microwave and electrical properties of the various conducting composites were evaluated and compared. PANI-PU composite was found to show the most suitable microwave and electrical properties. The EMI shielding, microwave reflection and microwave absorption property of PANI-PU composite was studied at S and X bands of microwave frequency and potential applications are discussed. The mechanical properties and load sensitivity of the composites were evaluated and discussed.

## **CONCLUSIONS**

The major conclusions and findings of the work are summarized here.

Design of Experiments can be effectively used in the polycondensation of para phenylene diammine and glyoxal trimeric hydrate to give a novel conducting polymer, polyparaphenylene diazomethine (PPDA). From the analysis of

experiments, it was predicted that optimum yield and conductivity would be obtained by condensation polymerization of PPD and GTD at 1:1 molar ratio at 120 °C for 5 hrs. Validation experiment proved that the predicted levels of reaction conditions do give an optimum yield and conductivity for the polymer. The polymer was found to have good thermal stability. The polymer can be doped with acidic dopants to increase conductivity. It has been observed that metal complexation has not been so effective in this type of polyazomethine for enhancing conductivity though these types of complexations have given good results with other types of polyazomethines.

Polythiophene was successfully prepared by chemical oxidative polymerization of thiophene using  $\text{FeCl}_3$  as oxidant in nitrobenzene solvent. From the FTIR spectra and Dc conductivity studies it can be inferred that  $\text{FeCl}_3$  is a good dopant for polythiophene. Polythiophene was found to be thermally stable upto 280°C. Breakdown of the polythiophene backbone occurs at around 300 °C.

A very promising conducting polymer, PEDOT doped with  $\text{FeCl}_3$  and DBSA, was successfully prepared. The polymer is found to be stable up to the temperature of 300 °C. The  $T_g$  of PEDOT is found to be 102 °C.

Dielectric constant, dielectric loss, conductivity, absorption coefficient, heating coefficient, loss tangent and skin depth of conducting polymers like PEDOT, PTH, PANI and PPDA were studied and compared at S band frequency. Dielectric constant, Dielectric loss,  $\tan \delta$ , conductivity and absorption coefficient of the conducting polymers are comparatively higher for PEDOT and PANI. Heating coefficient and skin depth are comparatively lower for PEDOT and PANI. Comparing the different conducting polymers, better microwave properties are offered by PEDOT and PANI. Dielectric constant, heating coefficient and skin

depth tends to decrease with increase in frequency and dielectric loss, conductivity, loss tangent and absorption coefficient increases with frequency in S band.

PEDOT doped with DBSA and  $\text{FeCl}_3$  was found to have very good conductivity of 26.41 S/m. PANI also offered very good DC conductivity, 2.45 S/m.

DC conductivity of the conducting polymers is in the order

$$\text{PEDOT} > \text{PANI} > \text{PTH} > \text{PPY} > \text{PPDA}$$

PANI and PEDOT showed good microwave and electrical properties and hence have potential applications in EMI shielding, microwave absorption etc.

One of the major limitations for the conducting polymers is their poor processability. To improve the processability the conducting polymers were made in composite form with processable thermoplastics. Insitu polymerization has been effectively used in this work to improve homogeneity in the composite.

Thermoplastic conducting composites of PPDA, PTH, PEDOT and PANI with PVC and PU were prepared. In the preparation of PTH-PVC, PEDOT-PVC, PANI-PVC, PEDOT-PU and PANI-PU composites, in situ polymerisation of the monomer in thermoplastic polymer solution using  $\text{FeCl}_3$  as the oxidising agent was employed.

The conditions for preparation of PTH-PVC composites were optimized. The optimum ratio of  $\text{FeCl}_3$ , Thiophene in preparing insitu PTH-PVC composites was found to be 2.5. It was observed that vacuum oven drying is more suited for solution casting of composite film as it gives better properties.



The microwave properties of all the composites like dielectric constant, dielectric loss, absorption coefficient, heating coefficient, skin depth and conductivity in the microwave frequency (S band) were studied in the S band and the most suitable composite was selected. Comparing the different blends, better microwave properties were shown by PANI-PU followed by PEDOT-PU composites. For all the composites, dielectric constant, heating coefficient and skin depth tends to decrease with increase in frequency and dielectric loss, conductivity, loss tangent and absorption coefficient increases with frequency in S band.

In order to allow the coexistence of all electronic components without harmful electromagnetic interferences, it is necessary to develop new shielding and absorbing materials with high performance and a large operating frequency band. Conducting polymer composites were found suitable for EMI shielding, microwave absorption and for the dissipation of electrostatic charge. Electrical properties in DC field are considered for load sensitivity applications which can be used in sensors. In the present study PANI-PU composite was considered for these applications. The microwave absorption, microwave reflection, EMI shielding, load sensitivity and mechanical properties of PANI-PU composite were evaluated. Microwave properties were evaluated both at S band and X band frequencies.

The shielding efficiency of the PANI-PU composite increases with the thickness of the sample and this material is ideal for shielding at 2.23 GHz and at 8.82GHz. The reflection is comparatively very low at X band compared to that at S band. The variations of reflection coefficient with frequency at S band and X band show similar behaviour. Reflection of microwaves from the PANI-PU films is very frequency specific. As the thickness increases the reflection increases. The material was found to show good microwave absorption and EMI shielding characteristics. The mechanical properties are found to be satisfactory for normal service

conditions. The conductivity of the PANI-PU and PANI-PVC composites was found to vary with load and hence can find application in load and pressure sensors.

## **FUTURE OUTLOOK**

The prepared composite has a lot of potential applications and to explore these further characterisation of the material is necessary.

The prepared conducting polymer based composites have been found to possess good processability. The conductivity and absorption of the composites can be improved further. This can be done by fine tuning the polymerisation of aniline to get highly ordered and crystalline polyaniline which will increase the properties drastically. This can be done by adjusting the polymerisation conditions and by using various in situ dopants that are reported to give polyaniline nanotubes in the system offering very high conductivity. Another way of improving the absorption is by incorporating carbon nanotubes in the matrix. Dispersion of carbon nanotubes should not pose great difficulty in this system because carbon nanotubes can be added at the polymerisation stage itself.

The composition of polyurethane and polyaniline can be varied to get a most suitable proportion of the composites. The thickness required to get optimum absorption and shielding efficiency has to be evaluated.

## LIST OF ABBREVIATIONS AND SYMBOLS

### Symbols used in the thesis

Symbol	Meaning	Symbol	Meaning
$\rho$	Resistivity	$R$	Resistance
$A$	Area of the electrode used	$t$	Thickness
$\epsilon'$	Dielectric constant	$\epsilon''$	Loss factor
$\epsilon_0$	Permittivity of free space	$\alpha$	Absorption Coefficient
$d$	Penetration depth	$\sigma$	Conductivity
$J$	Efficiency of heating	$c$	Velocity of light
$V_c$	Volume of cavity	$V_s$	Volume of sample
$h$	Planck's constant	$e$	Electron charge
$m$	Electron mass	$\mu$	Carrier mobility
$\tau$	Relaxation time	$\mu_0$	Permeability of free space
$\eta$	Free space impedance	$Q$	Quality factor
$f$	Centre frequency	$Q_0$	Quality factor of the cavity without sample
$f_0$	Resonance frequency	$Q_s$	Quality factor of the cavity with sample
$f_s$	Resonance frequency of the cavity with sample	$f_c$	Relaxation Frequency
$T$	Temperature	$H$	Magnetic field
$E$	Electric field	$R$	Reflection Coefficient
$\lambda$	Wave Length		

## Abbreviations used in the thesis

CP	Conducting Polymer
DMF	N,N Di Methyl Formamide
THF	Tetra Hydro Furan
PPD	Para Phenylene Diammine
EDOT	3,4-thylenedioxythiophene
CSA	10-Camphor Sulfonic Acid
PTH	Polythiophene
PPY	Polypyrrole
PVC	Poly vinyl Chloride
DSC	Differential Scanning Calorimetry
TGA	Thermo Gravimetic Analysis
ICP	Intrinsically Conducting Polymer
DMSO	Dimethyl Sulfoxide
FeCl <sub>3</sub>	Anhydrous Ferric Chloride
GTD	Glyoxal Trimer Dihydrate
DBSA	Dodecyl benzene sulphonic acid
PANI	Polyaniline
PPDA	Poly Para Phenylene Diazomethine
PEDOT	Poly (3,4 Ethylene Dioxy Thiophene)
PU	Poly Urethane
FTIR	Fourier Transform Infrared Spectrometry
DTA	Differential Thermal analysis

## LIST OF TABLES AND SCHEMES

### List of tables

<b>Tables</b>	<b>Titles</b>	<b>Page Number</b>
1.1	Standard L <sub>4</sub> Orthogonal array	46
2.1	Design parameters of S, C and X band rectangular wave guide cavities.	79
2.2	Resonant frequencies and Q factors of the cavities used.	82
3.1	Yield and Conductivity of PPDA prepared in various solvents.	93
3.2	Standard L <sub>9</sub> orthogonal Array.	95
3.3	Parameters and levels of parameters affecting the polycondensation.	95
3.4.	Properties of polymers as prepared from various trials (Taguchi Design)	96
3.5	Absorption peaks and the assigned vibrations for undoped PPDA	101
3.6.	Absorption peaks and the assigned vibrations for HClO <sub>4</sub> doped PPDA.	104
3.7	Absorption peaks and the assigned vibrations for copper acetate doped PPDA	106
3.8	DC conductivity of doped PPDA samples	106
4.1	Absorption peaks and the assigned vibrations for undoped polythiophene.	118
4.2	Absorption peaks and the assigned vibrations for doped polythiophene.	120
4.3	DC conductivity of polythiophene samples	121
5.1	Absorption peaks and assigned vibrations for doped PEDOT.	131
6.1	DC conductivity of the polymer samples.	151

## LIST OF SCHEMES

<b>Schemes</b>	<b>Titles</b>	<b>Page Number</b>
1.1.	Synthesis of Polyazomethine ether.	32
1.2	Synthesis of polythiophene by polycondensation dehalogenation reaction.	33
1.3	Synthesis of polythiophene by oxidative polymerization reaction.	34
1.4	Poly (alkyl thiophenes) from cross coupling polymerization.	35
1.5	Mechanism of PAT synthesis by FeCl <sub>3</sub> route and the possible regiochemical couplings possible in Polyalkyl thiophenes.	36
1.6	Chemical polymerization of EDOT.	39
3.1	Polycondensation of paraphenylene Diammine and Glyoxal to form PPDA	102
4.1	Polymerisation of thiophene	118

## LIST OF FIGURES

No.	Titles	Page Number
1.1	Structural formulae of various conjugated polymers.	4
1.2	Schematic representations of Polaron and Bipolaron.	8
1.3	Frequency responses of dielectric mechanisms.	9
1.4	Dipole rotations in an electric field.	10
1.5	Cole-Cole diagram of water at 30 °C.	13
1.6	Reflected and transmitted signals from a material under test.	15
1.7	Reflection coefficient Vs. dielectric constant.	16
1.8	Types of radar absorbing materials	19
1.9	Transmission line, wave guide and coaxial line methods	20
1.10	Resonant cavity measurement, cavity perturbation method	26
1.11	Cavity perturbation method: graphs of empty cavity and samples	27
1.12	Summary of measurement techniques	28
1.13	Intermolecular complexation with copper salts in thienylene phenylene polyazomethine.	32
1.14	PEDOT/PSS blend (BAYTRON P).	40
2.1	Schematic diagram of the rectangular cavity resonator.	80
2.2	Block diagram of the experimental set up	81
2.3	Splitting of electromagnetic wave on passing through a shield	85
2.4	Coaxial wave guide adapters between which material is tightened to measure the S parameters.	86

<b>No.</b>	<b>Titles</b>	<b>Page Number</b>
3.1.	Factor plot for yield.	97
3.2.	Factor plot for conductivity	97
3.3	FTIR of PPDA.	101
3.4	FTIR of HClO <sub>4</sub> doped PPDA.	103
3.5	FTIR of copper acetate doped PPDA.	105
3.6	TGA and DTA curves for PPDA.	107
3.7	DSC curve for PPDA.	108
4.1	FTIR of undoped polythiophene.	117
4.2	FTIR of FeCl <sub>3</sub> doped polythiophene.	119
4.3	TGA/DTA curves of undoped polythiophene.	122
4.4	DSC curves of undoped polythiophene	123
5.1	FTIR of doped PEDOT.	130
5.2	TGA/DTA curves of PEDOT	132
5.3	DSC curve of PEDOT	133
6.1	Variation of dielectric constant with frequency for various conducting polymers.	142
6.2	Variation of dielectric loss with frequency for various conducting polymers.	143
6.3	Variation of loss tangent with frequency for various conducting polymers.	146
6.4	Variation of absorption coefficient with frequency for various conducting polymers.	147
6.5	Variation of conductivity with frequency for various conducting polymers.	148



<b>No.</b>	<b>Titles</b>	<b>Page Number</b>
6.6	Variation of heating coefficient with frequency for various conducting polymers	149
6.7	Variation of Skin depth with frequency for various conducting polymers.	150
7.1	Variation of dielectric constant with FeCl <sub>3</sub> : Thiophene ratio at various frequencies.	160
7.2	Variation of dielectric loss with FeCl <sub>3</sub> : Thiophene ratio at various frequencies.	161
7.3	Variation of conductivity with FeCl <sub>3</sub> : Thiophene ratio at various frequencies.	163
7.4	Variation of dielectric constant for vacuum dried and room temperature dried Conducting polymer- PVC composites with frequency	166
7.5	Variation of dielectric loss for vacuum dried and room temperature dried Conducting polymer- PVC composites with frequency.	167
7.6	Variation of conductivity for vacuum dried and room temperature dried Conducting polymer- PVC composites with frequency	168
7.7	Variation of absorption coefficient for vacuum dried and room temperature dried Conducting polymer- PVC composites with frequency	170
7.8	Variation of Dielectric Constant of conducting polymer - thermoplastic composites with frequency	173
7.9	Variation of Dielectric Loss of conducting polymer - thermoplastic composites with frequency	174
7.10	Variation of conductivity of conducting polymer - thermoplastic composites with frequency	175

<b>No.</b>	<b>Titles</b>	<b>Page Number</b>
7.11	Variation of Absorption coefficient of conducting polymer - thermoplastic composites with frequency	177
7.12	Variation of Loss tangent of conducting polymer - thermoplastic composites with frequency	178
7.13	Variation of heating coefficient of conducting polymer - thermoplastic composites with frequency	179
7.14	Variation of Loss tangent of conducting polymer - thermoplastic composites with frequency	180
8.1	Variation of EMI shielding (SE) of the PU-PANI composite for different thickness at S band frequencies.	191
8.2	Variation of EMI shielding (SE) of the PU-PANI composite for different thickness at X band frequencies.	193
8.3	Variation of absorption coefficient of the PU-PANI composite for different thickness at S band frequencies.	194
8.4	Variation of absorption coefficient of the PU-PANI composite for different thickness at X band frequencies.	195
8.5	Variation of reflection coefficient of the PU-PANI composite for different thickness at S band frequencies.	197
8.6	Variation of reflection coefficient of the PU-PANI composite for different thickness at X band frequencies.	197
8.7	Variation of conductivity for the PU-PANI and PVC-PANI composite with load	200

## **LIST OF PUBLICATIONS FROM THIS WORK**

### **Comparison of Microwave and Electrical Properties of Selected Conducting Polymers**

K.Lakshmi, , Honey John, Rani Joseph , K.E.George and K.T.Mathew  
Microwave Optical Technology Letters, Wiley Interscience, Accepted

### **Microwave Properties of Some Important Conducting Polymers**

K.Lakshmi, Honey John, Rani Joseph, K.T.Mathew , K.E.George  
Presented at the International conference on Polymers in Power Engineering  
at CPRI, Bangalore from 4-6 th October 2007.

### **Synthesis and characterisation of a novel conducting polymer**

K.Lakshmi, K.G.Princy, R.prasanth,, Rani Joseph, K.E.George  
(Communicated)

### **Microwave Properties of Selected Thermoplastic Conducting Composites**

K.Lakshmi,Rani Joseph, K.T.Mathew and K.E.George (Communicated)

### **Microwave Properties of Selected Thermoplastic Conducting Composites**

K.Lakshmi,Rani Joseph, K.T.Mathew and K.E.George (Communicated)

# Curriculum Vitae

## Lakshmi.K

Sr.Lecturer, Dept of Chemical Engineering and Material Science,

Amrita Vishwa Vidya Peetham, Ettimadai, Coimbatore

k\_lakshmi@ettimadai.amrita.edu , lakshmikaimal@gmail.com, Ph: 09349132903

## Research Experience

- Co-Investigator for the multidisciplinary research proposal “Evaluation of Multilayer Shear Damped Visco-Elastic treatments for Launch Vehicle Application “from ISRO.
- Indian side Principal Investigator for the **Indo-US (DST-NSF) MWN** project “Synthesis and Characterization of novel C-ICP and C-ICP-metal nanocomposites with unusually high conductivity and processability”-submitted.
- Reverse Engineering on Patient Positioning Sheet for cancer treatment for Amrita Institute of Medical Sciences (AIMS).
- Optimization of Bead Insulation compound using **DOE for Apollo Tyres.**
- Conducting Polymer Composites for EMI shielding Applications.
- Wood flour-PP Composites, PC/PBT Blends
- M.Tech. Project - Solution dipping of butyl rubber compound for gauntlets-for **IGCAR Kalpakkam.**
- B.Tech. Project - Silica-Phenolic composites for rocket nozzle ablator layer for **VSSC Thiruvananthapuram.**

## Membership in Professional Bodies

- Life Member of ISTE
- Life Member of Indian Society for Advancement of Materials and Process Engineering (ISAMPE)
- Professional Member of Indian Plastics Institute (IPI)